INVESTIGATION OF FUNDAMENTAL PROPERTIES OF NANOREFRIGERANTS

MOHAMMED MAHBUBUL ISLAM

FACULTY OF ENGINEERING
UNIVERSITY OF MALAYA
KUALA LUMPUR

2012

INVESTIGATION OF FUNDAMENTAL PROPERTIES OF NANOREFRIGERANTS

MOHAMMED MAHBUBUL ISLAM

**DISSERTATION SUBMITTED TO THE FACULTY OF ENGINEERING
UNIVERSITY OF MALAYA IN FULFILLMENT OF THE REQUREMENTS FOR THE DEGREE OF MASTER OF ENGINEERING SCIENCE (M.Eng.Sc)**

**FACULTY OF ENGINEERING
UNIVERSITY OF MALAYA
KUALA LUMPUR**

2012

Original Literary Work Declaration

Name of the candidate: **Mohammed Mahbubul Islam**

Registration/Matric No: **KGA 100073**

Name of the Degree: **Master of Engineering Science (M.Eng.Sc)**

Title of Project Paper/Research Report/Dissertation/Thesis (This Work):
Investigation of Fundamental Properties of Nanorefrigerants

Field of Study: **Mechanics and Metal Work (Heat Transfer)**

I do solemnly and sincerely declare that:

(1) I am the sole author/writer of this work;

(2) This work is original;

(3) Any use of my work in which copyright exists was done by way of fair dealing and for permitted purposes and any excerpt or extract from, or reference to or reproduction of any copyright work has been disclosed expressly and sufficiently and the title of the work and its authorship have been acknowledged in this work;

(4) I do not have any actual knowledge nor do I ought reasonably to know that the making of this work constitutes an infringement of any copyright work;

(5) I hereby assign all and every rights in the copyright to this work to the University of Malaya ("UM"), who henceforth shall be owner of the copyright in this work and that any reproduction or use in any form or by any means whatsoever is prohibited without the written consent of UM having been first had and obtained;

(6) I am fully aware that if in the course of making these works I have infringe any copyright whether intentionally or otherwise, I may be subject to legal action or any other action as may be determined by UM.

Candidate's Signature Date

Subscribe and solemnly declare before,

Witness Signature Date

Name :

Designation :

Abstract

In the past decade, rapid advancements of nanofluids science in many areas have been observed. In recent years, refrigerant-based nanofluids have been introduced as nanorefrigerants due to their better heat transfer performance. The objectives of this research include preparation, characterization and investigation of the thermophysical and migration properties of nanorefrigerants. Al_2O_3/R141b and TiO_2/R141b nanorefrigerants with various proportions of concentrations have been prepared to investigate their fundamental properties. Nanoparticles size, shape, and elemental proportion have been characterized with Field Emission Scanning Electron Microscope (FESEM) and Transmission Electron Microscope (TEM). Moreover, this study investigated thermal conductivity, viscosity, and density of Al_2O_3/R141b nanorefrigerants for different concentrations and temperatures. In addition, migration properties of Al_2O_3 and TiO_2 nanoparticles with R141b refrigerant along with lubricating oil have been investigated for different heat fluxes, initial liquid level heights, vessel sizes, insulation, nanoparticle sizes, and oil mixture. In this study, the thermal conductivity of Al_2O_3/R141b nanorefrigerant increased with the augmentation of particle concentration and temperature. Besides, viscosity and density of the nanorefrigerant increased with the increase of volume fractions. However, these parameters decreased accordingly with the increment of temperature. Migration of nanoparticles during pool boiling increased with the increase of initial nanoparticle mass fraction, nanoparticle size, heat flux, and insulation. However, migration of nanoparticles decreased with the increase of particle's self-density, boiling vessel size, and initial liquid level height. Therefore, nanoparticle has strong relationship with thermophysical and migration properties of refrigerants.

Abstrak

Dalam dekad yang lalu, kemajuan pesat sains “nanofluids” dalam banyak bidang telah diperhatikan. Dalam tahun-tahun kebelakangan ini, “nanofluids” berasaskan penyejuk telah diperkenalkan sebagai “nanorefrigerants” kerana prestasi pemindahan habanya yang lebih baik. Objektif kajian ini termasuk penyediaan, pencirian dan penyiasatan termofizikal dan sifat penghijrahan “nanorefrigerants”. Al_2O_3/R141b dan TiO_2/R141b “nanorefrigerants” dengan pelbagai nisbah campuran telah disediakan untuk disiasat sifat-sifat asasnya. Saiz nanopartikel, bentuk dan nisbah unsur-unsur telah dicirikan dengan Pengimbasan Mikroskop Elektron Pancaran Medan (FESEM) dan Mikroskop Transmisi Elektron (TEM). Selain itu, kajian ini telah menyiasat kekonduksian terma, kelikatan dan ketumpatan “nanorefrigerants” Al_2O_3/R141b untuk nisbah campuran dan suhu yang berbeza. Di samping itu, sifat penghijrahan Al_2O_3 dan TiO_2 nanopartikel dengan penyejuk R141b berserta minyak pelincir telah disiasat bagi fluks haba yang berbeza, ketinggian tahap cecair awal, saiz vesel, penebatan, saiz nanopartikel, dan campuran minyak. Dalam kajian ini, kekonduksian haba nanorefrigerant Al_2O_3/R141b meningkat dengan penambahan kepekatan zarah dan suhu. Selain itu, kelikatan dan ketumpatan nanorefrigerant meningkat dengan peningkatan pecahan isi padu. Walau bagaimanapun, parameter ini menurun sewajarnya dengan kenaikan suhu. Penghijrahan nanopartikel semasa pendidihan tenang meningkat dengan peningkatan pecahan jisim nanopartikel awal, saiz nanopartikel, fluks haba dan penebat. Walau bagaimanapun, penghijrahan nanopartikel menurun dengan peningkatan ketumpatan diri-zarah, saiz vesel mendidih dan tahap ketinggian cecair awal. Oleh itu, nanopartikel mempunyai hubungan yang kukuh dengan sifat termofizikal dan penghijrahan penyejuk.

Acknowledgements

In the Name of Allah, The Beneficent, The Merciful, I would like to express my utmost gratitude and thanks to the almighty Allah (s.w.t) for the help and guidance that He has given me through all these years. My deepest appreciation is to my family for their blessings and supports.

I would like to express my sincere gratefulness and gratitude to my supervisors, **Professor Dr. Saidur Rahman** and **Dr. Amalina Binti Muhammad Afifi.** I am grateful to them for their brilliant supervision, guidance, encouragement and supports in carrying out this research work. I am deeply indebted to them.

Finally, thanks to University of Malaya for financial support, privileges, and opportunities to conduct this study. This project was carried out under the Fundamental Research Grant Scheme (FRGS) fund (Project no. FP017/2010B, FRGS) and Postgraduate Research Grant (PPP) (No. PV013/2011A). I gratefully acknowledge to the members of Energy Laboratory in helping me and for suggestion, ideas, discussions, and advices in completing this research work.

Table of Contents

List of Figures

List of Tables

Nomenclatures

Abbreviations

C Alumina constant = 30

CNT's Carbon Nanotubes

C_p Specific heat (J/kg.K)

d_b Bubble departure diameter (m)

d Diameter of nanoparticles (nm)

$\bar{d}$ Average diameter of nanoparticles (m)

DIW Deionized Water

DW Distilled Water

dp Nanoparticle diameter (nm)

EG Ethylene Glycol

g Grams

k Thermal conductivity (W/m.K)

m Number of the particles per unit volume

M Molecular mass (kg/kmol)

ml Millilitre

n Empirical shape factor for Hamilton and Crosser model

m_n Initial mass of nanoparticles (grams)

m_o Initial amount of lubricating oil (grams)

m_r Required amount of refrigerant (ml)

Δm Migrated mass of nanoparticles (grams)

MWCNT's Multi walled Carbon Nanotubes

P Power (W)

PG Propylene Glycol

R Refrigerant

r Particle radius (m)

S Suppression factor

t Interfacial layer thickness (m)

T Temperature (K)

q" Heat flux (W/m^2)

vol. % Volume concentration of particles

V_f Volume of fluid

V_p Volume of particles

W Water

wt. % Weight concentration of particles

X Parameter of Lockhart and Martinelli

Greek letters

Δ Change rate with the system

μ Dynamic viscosity (N.s/m^2)

ρ Density (kg/m^3)

σ Surface tension (N/m)

ϕ Particle volume fraction

ψ Sphericity of nanoparticle

Dimensionless numbers

Nu Nusselt number

Pr Prandlt number

Re	Reynolds number
We	Weber number

Subscripts

bf	Base fluid
eff	Effective
f	Fluid
l	Interfacial layer / nanolayer
L	Liquid
nf	Nanofluid
p	Nanoparticle
$pool$	Pool boiling
r	Pure refrigerant
r,n	Nanorefrigerant
TP	Two-phase

CHAPTER 1: INTRODUCTION

1.1 Background

Optimization of engineering devices, which include heat transfer mechanisms, has been the major focus of many researches since it can substantially affect the efficiency and the performance of those systems. There are various ways to achieve this goal including augmentation of heat transfer area or increasing the heat transfer coefficients of a fluid. The former is usually tried to be avoided due to the fact that it could cause the bulkiness of the device. The latter way, however, has been implemented by changing different parameters. A recently introduced means of increasing the heat transfer rate includes the utilization of nanofluids. Nanofluids are the mixture of solid nanoparticles with a base fluid. This is a special type of heat transfer fluid which has higher thermal conductivity than that of the conventional host fluids (e.g. ethylene glycol, water, propylene glycol, engine oil, and so on). Nanoparticles that used to prepare nanofluids are basically metals (e.g. Cu, Ni, Al, etc.), oxides (e.g. Al_2O_3, TiO_2, CuO, SiO_2, Fe_2O_3, Fe_3O_4, $BaTiO_3$, etc.) and some other compounds (e.g. CNT, SiC, $CaCO_3$, TNT, etc.) with a size of 1-100 nm. Figure 1.1 shows some real life examples of nanometer to millimeter scale substances. For very small size and large specific surface areas of the nanoparticles, nanofluid possess better heat transfer properties like: high thermal conductivity, less clogging in flow passages, long-term stability, and homogeneity (Chandrasekar et al., 2010; Peng et al., 2011c). Extensive studies have done to clarify the performance of these colloidal suspensions unanimously state that the suspension of particles leads to augmentation in the thermal conductivity and diffusivity. Large enhancements in thermal conductivity at even low volume concentrations for metallic particles (Das et al., 2006) and enhancement on the thermal conductivity when augmenting the volume concentration (Xuan & Li, 2000) are among these observations.

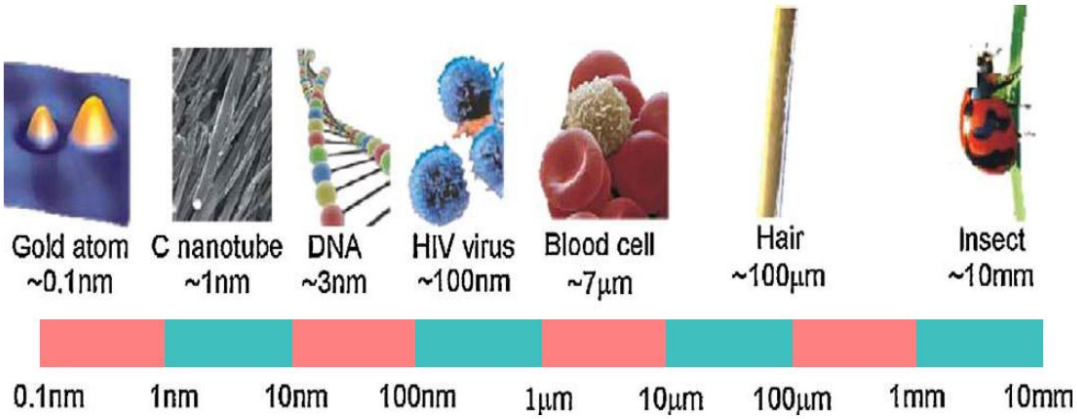

Figure 1.1: Some real life examples of nanometer to millimeter scale substances (Serrano et al., 2009).

Figure 1.2 shows that, at the ambient temperatures, thermal conductivity of metallic solids is an order-of-magnitude greater than that of fluids (e.g. thermal conductivity of copper is about 700 and 3000 times greater than the thermal conductivity of water and engine oil, respectively). Conventional heat transfer fluids like water, propylene glycol, ethylene glycol, and refrigerants have very low thermal conductivity. As a result their heat transfer performance is also very poor. However, some solids (metal, metal oxide and other composites) have very high thermal conductivity. Therefore, thermal conductivity of the solid metallic or non-metallic particles suspended fluids are significantly higher than the thermal conductivity of the traditional heat transfer fluids (Murshed et al., 2008a). Since the heat transfer performance is directly proportional to the thermal conductivity of a substance. Then, the idea came to use the mixture of solid particles with fluid to increase the heat transfer properties. But the problem is clogging on the flow passages. Therefore, the researchers proposed to use nano grade solid particles in the mixture.

Stephen Choi from National Argonne Laboratory (USA) is the pioneer who for the first time demonstrated that the use of nanoparticles enhances the heat transfer performances of liquids in 1995 (Choi, 1995). Since then a lot of research has been going on

tremendously about thermal conductivity, viscosity, density, specific heat, different modes of heat transfer, pressure drop, pumping power, different properties of nanofluids (e.g. fundamental, thermal, physical, optical, magnetic, etc.), etc. Most widely used heat transfer fluids such as water, oil, ethylene glycol (EG), and refrigerants have poor heat transfer properties, however their huge applications in the field of power generation, chemical processes, heating and cooling processes, transportation, electronics, automotive, and other micro-sized applications make the re-processing of these heat transfer fluids to have better heat transfer properties reasonably necessary.

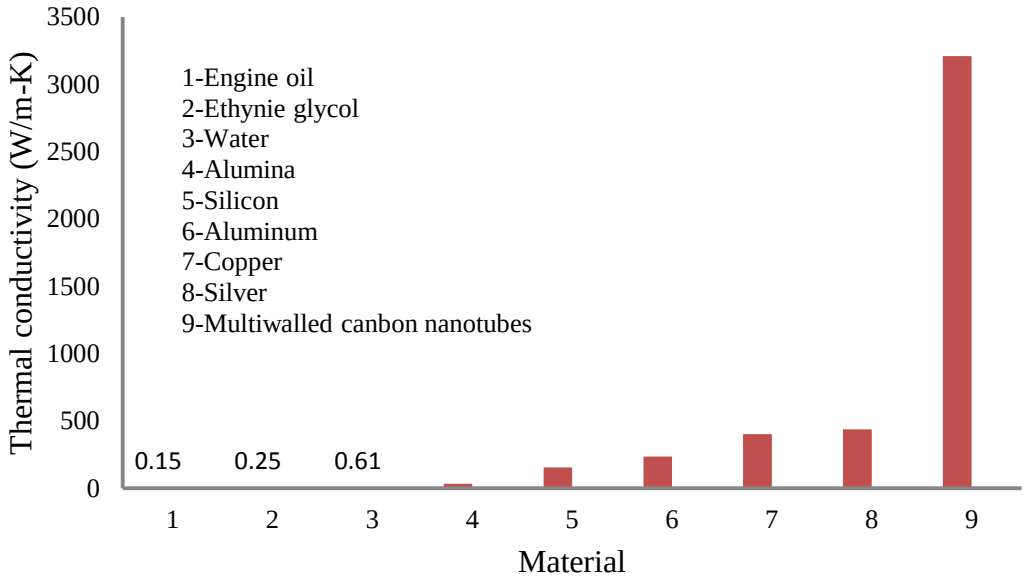

Figure 1.2: Thermal conductivity of solid and liquid materials at 300 K (Choi et al., 2004; Murshed et al., 2008a).

Since the invention of the vapor compression refrigeration system in the middle of the 18th century, the utilization of refrigeration systems have entered in numerous fields. The application includes preservation of food and medicine, air-conditioning for comfort, and industrial processing. During the refrigeration process a heat carrying medium called refrigerant absorb heat from a low temperature system and give off the heat to a higher temperature system (Jones & Stoecker, 1982).

The nanorefrigerant is one kind of nanofluid, with a refrigerant as its host fluid. Recently (since 2005) scientists are trying to work on nanorefrigerant a kind of nanofluids to enhance the heat transfer performance in refrigeration and air-conditioning systems (Bi et al., 2011; Bi & Shi, 2007; Bi et al., 2008). Since then, numerous experiments are going on about nanorefrigerants. Wang et al. (2005) introduced the term "nanorefrigerants" for the first time. Like the rest of the nanofluids, this type of refrigerants have shown enhanced thermal conductivity and heat transfer performance (Jiang et al., 2009a). Since the energy efficiency of air conditioning and refrigerators can be influenced by adding nanoparticles into the refrigerants, recently some research has been done in this area (Bi et al., 2008; Saidur et al., 2011; Wang et al., 2003).

1.2 Importance of nanorefrigerant study

Refrigerants are widely used in refrigeration and air conditioning systems in industry and commercial buildings. About 20-50% of total energy is used by these systems in industry and commercial buildings. Moreover, energy is on the head of "Top Ten" global problems of humanity for the next fifty (50) years (Smalley, 2005). Nanorefrigerants have the potentiality to enhance heat transfer rate thus making heat exchanger of air conditioning and refrigeration systems compact. In addition, they decreases the amount of energy needed to operate those systems. This, consequently, will reduce energy consumption in these sectors along with reduction in emission, global warming potential, and greenhouse gas effect. However, for accurate and reliable performance (e.g. heat transfer, energy, and lubricity) investigation; determination of fundamental characteristics like: thermal conductivity, viscosity, density, surface tensions, and specific heat capacity of nanorefrigerant with varied concentrations need to be carried out.

There are some literatures on the pool boiling, nucleate boiling, convective heat transfer, energy performance, lubricity, and material compatibility of nanorefrigerants. It may be noted that these performance parameters are dependent of different properties of a fluid or refrigerant (Daungthongsuk & Wongwises, 2007; Trisaksri & Wongwises, 2007; Wang & Mujumdar, 2007). At the moment, scientists are using mathematical relationships/models for thermal conductivity (e.g. Maxwell model (1891), Hamilton and Crosser (HC) model (1962), etc.), viscosity (e.g. Einstein model (1906), Brinkman model (1952), etc.) of other fluids applying in nanorefrigerants. As different fluids have different fundamental properties, the model used may not be suitable for another fluid. It is expected that if experimental values of thermophysical properties of nanorefrigerants are obtained, it would be more appropriate for better analysis of heat transfer, energy performance, lubricity, and so on.

1.3 Objectives of the research

Refrigerants are widely used in air conditioning and refrigeration systems. Nanorefrigerants could save energy in these sectors. However, very few researchers work on nanorefrigerants. Moreover, available information about nanorefrigerants is still limited. This study tried to minimize these gaps by preparing, characterizing, and analyzing thermal conductivity, viscosity, density, and migration characteristics of nanorefrigerants.

The objectives of the research are as follows:

- To prepare and characterize nanorefrigerants
- To investigate thermophysical properties (e.g. thermal conductivity, viscosity, and density) of nanorefrigerants
- To analyze migration properties of nanorefrigerants

1.4 Outline of the dissertation

This dissertation comprises five chapters. The contents of the individual chapters have been outlined as follows:

Chapter 1: This chapter starts with some background information about nanorefrigerants as well as describing the importance, aim, objectives, and limitations of the dissertation.

Chapter 2: In this chapter, a review of the literature on preparation, characterization, thermophysical properties (e.g. thermal conductivity, viscosity, and density), and migration properties of nanorefrigerants have been addressed.

Chapter 3: It describes the experimental set up, materials, procedures and equipment that have been used during preparation, characterization, and determination of thermophysical properties (e.g. thermal conductivity, viscosity, and density), and migration properties of nanorefrigerants.

Chapter 4: This chapter analyzes the outcomes of preparation, characterization, thermophysical properties (e.g. thermal conductivity, viscosity, and density), and migration properties of nanorefrigerants.

Chapter 5: This is the last chapter and wraps up the dissertation with some concluding remarks and recommendations for future work.

CHAPTER 2: LITERATURE REVIEW

2.1 Introduction

This chapter contains an overview of other related studies, their approach development and significance to this study in order to set up the objectives of the research. Pertinent literatures in the form of journal articles, reports, conference papers, internet sources, and books collected from different sources are used for this study. It may be mentioned that about 80–90% of the journal papers collected from most relevant and prestigious peer reviewed international referred journals such as International Journal of Refrigeration, International Journal of Heat and Mass Transfer, Applied Thermal Engineering, Journal of Applied Physics, Applied Physics Letters, Renewable and Sustainable Energy Reviews, Journal of Nanoparticle Research, International Journal of Thermal Science, etc. Moreover, the substantial amount of relevant information has been collected through personal communication with the key researchers around the world in this research area.

2.2 An overview on preparation of nanorefrigerants

Preparation of nanofluids with traditional fluids is a little bit different from the preparation of nanorefrigerants. Generally, two techniques have been using to prepare nanofluids: a) single step method and b) two step method.

In a single step method (Eastman et al., 2001; Zhu et al., 2004), both the preparation of nanoparticles as well as mixture of nanofluid are done in a joint process. Some commonly used techniques for single step method of nanofluid preparation includes: physical vapor deposition (PVD) technique (Eastman et al., 2001) or liquid chemical method (Zhu et al., 2004). This single step method has both merits and demerits. One of

the most important advantages is the enhanced stability and minimized agglomeration. One of the important disadvantages of this method is that just the low pressure fluids could be synthesized by this process.

In two step method (Paul et al., 2011; Yu et al., 2011), first nanoparticles are initially prepared. Then homogenize into the fluid by some methods such as: high shear (Pak & Cho, 1998; Wen & Ding, 2005) and ultrasound (Goharshadi et al., 2009). Figure 2.1 shows typical nanoparticle preparation methods. Nowadays, nanoparticles are available from commercial sources. This method has attracted scientists and commercial users. The disadvantage of this method is that the particles quickly agglomerate before dispersion and sometimes nanoparticles disperse partially.

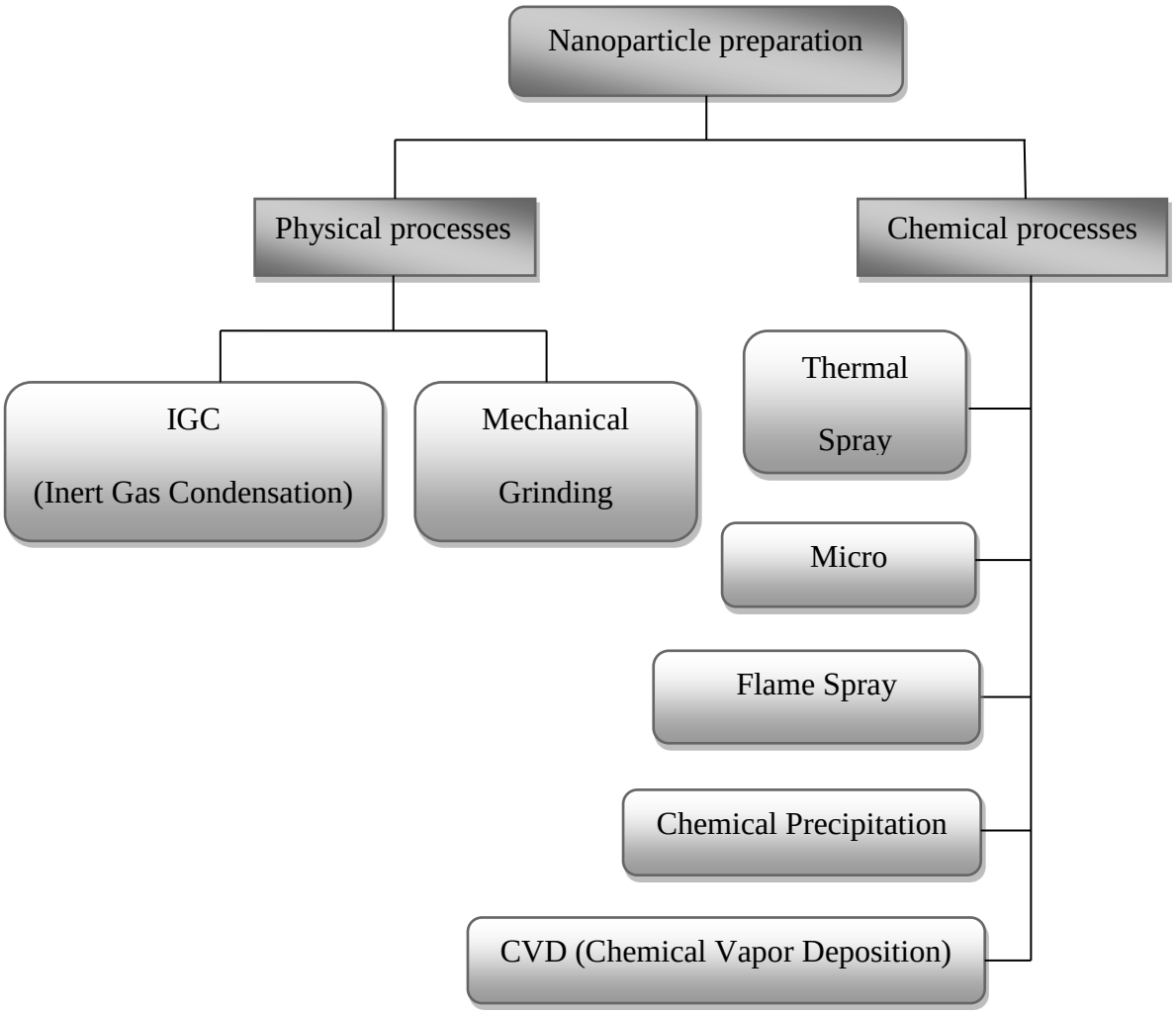

Figure 2.1: Nano particle manufacturing method.

Table 2.1 shows typical synthesis method used by the researchers to prepare nanofluids. From the table it is clear that, most of the researchers used two step method by ultra-sonication process for proper dispersion. Only, Garg et al. (2008) used chemical reduction methods for synthesis of nanofluids. Two step methods have also been used to prepare nanorefrigerants and nanolubricants. Few researchers (Jiang et al., 2009a; Jiang et al., 2009b; Peng et al., 2011a; Peng et al., 2009a) used ultrasonic vibration for 30 minutes to stabilize the nanorefrigerants. Kedzierski (2011) used ultrasonic vibration for 24 hours to stabilize the Al_2O_3/polyolester/R134a (a mixture of nanoparticles with lubricants and refrigerants). However, Henderson et al. (2010) prepared the nanorefrigerants with direct dispersions of nanoparticles in R134a refrigerants. Refrigerants are low temperature fluids and most of the refrigerants are at gaseous state at normal temperature and pressure. Hence, this ultra-sonication process is not a correct method to prepare nanorefrigerants. There are some refrigerants (e.g. R141b, R113, R123, and n-Pentane) are available in liquid form at ambient temperature and pressure. However, during ultra-sonication process these refrigerants will start to evaporate even before their boiling point. This is because; ultrasonic process creates a force to homogenize the solution that causes, refrigerants to start evaporate. Figure 3.1 of section 3.3 showed this phenomenon during ultra-sonication process. This would be harmful for the operator as well as the surroundings. However, in this experiment two step method with ultra-sonication process was used to prepare nanorefrigerant. Furthermore, another new type of two step preparation process has been introduced by using an incubator shaker.

Table 2.1: Summery of different types of synthesis process that have been used by the researchers.

Base fluid	Nanoparticle (diameter in nm)	Particle volume concentration (%)	Synthesis process	Reference
DW, EG	Al_2O_3 (28)	1 to 6	Two-step	(Wang et al., 1999)
Water	Al_2O_3 (37)	0.01 to 0.16	Two-step	(Tseng & Chun, 2002)
Terpineol	Ni (300)	3 to10	Two-step	(Tseng & Chen, 2003)
Water	TiO_2 (7–20)	5 to12	Two-step	(Tseng & Lin, 2003)
EG	CuO (12)	0.002	Two-step	(Kwak & Kim, 2005)
EG	TiO_2 (25)	0 to 8 wt %	Two-step	(Chen et al., 2007a)
EG	TiO_2 (25)	0.1 to 1.86	Two-step	(Chen et al., 2007b)
Ethanol	SiO_2 (35,94 &190)	1.4 to 7	Two-step	(Chevalier et al., 2007)
DW	TiO_2 (20)	0.024 to 1.18	Two-step	(He et al., 2007)
EG-W(60:40)	CuO (29)	0 to 6.12	Two-step	(Namburu et al., 2007a)
EG-W(60:40)	SiO_2 (20,50 & 100)	0 to10	Two-step	(Namburu et al., 2007b)
EG	Cu (200)	0.4 to 2	Single-step	(Garg et al., 2008)
Water, EG	Al_2O_3(10 & above)	5	Two-step	(Lu & Fan, 2008)
DIW, EG	TiO_2 (15), Al_2O_3 (80 & 150)	1 to 5	Two-step	(Murshed et al., 2008a)
Water	Al_2O_3 (45&150)	1 to 6 wt %	Two-step	(Anoop et al., 2009b)
EG	TNT (~10), L=100 nm	0 to 8% mass	Two-step	(Chen et al., 2009a)
Water	MWCNTs (10–20)	1 wt%	Two-step	(Garg et al., 2009)
EG-W(60:40)	CuO (30), Al_2O_3 (45), SiO_2 (50)	0 to 6.12	Two-step	(Kulkarni et al., 2009)
DIW	Fe_2O_3 (20, 40)	0.2 wt %	Two-step	(Phuoc & Massoudi, 2009)
DIW	TiO_2 (21)	0.2 to 3	Two-step	(Turgut et al., 2009)
Water	Al_2O_3 (43)	0.33 to 5	Two-step	(Chandrasekar et al., 2010)
Car engine coolant	Al_2O_3 (<50)	0.1 to 1.5	Two-step	(Kole & Dey, 2010)
DW	CNT	0.1 to 0.5 wt%	Two-step	(Ding et al., 2006)
R113	Cu,Ni,Al,CuO, Al_2O_3	0.1 to 1.2	Two-step	(Jiang et al., 2009b)
R113	CNT's	0.2 to 1.0	Two-step	(Jiang et al., 2009a)
Water	MWCNT's		Single-step	(Madni et al., 2010)
PG-water	CuO (<50)	0.025 to 1.25	Two-step	(Naik et al., 2010)
DW	$CaCO_3$ (20–50)	0.12 to 4.11	Two-step	(Zhu et al., 2010)
Water	CuO (23–37, 11±3)	0.05 to 10 wt%	Single-step, Two-step	(Pastoriza-Gallego et al., 2011)
Water	MWCNTs (20–30), L=10–30 μm	0.24 to 1.43	Two-step	(Phuoc et al., 2011)

2.3 An overview on characterization of nanorefrigerants

Stability of nanofluids is an important phenomenon that needs to be characterized. If nanofluids are not stable, clogging, aggregation and sedimentation would happen that decline the performance of suspensions via decreasing thermal conductivity and increasing viscosity. Literature about characterization of refrigerant based nanofluid is limited however there are some studies have been done based on other fluids. Some apparatus and procedures have introduced in literature that can measure the comparative stability of nano-suspensions. UV-Visible spectrophotometer, Sediment photograph capturing, SEM (Scanning Electron Microscope) and TEM (Transmission Electron Microscope) are some well-known instruments that have been used to measure the relative stability of nanofluids.

2.3.1 UV–Visible spectrophotometer

Generally, UV–Visible spectrophotometer quantitatively illustrates the colloidal stability of nanofluids. A UV–Visible spectrophotometer exploits the fact that the intensity of the light becomes different by absorption and scattering of light passing through a fluid. Normally, nanofluid stability is determined by comparing the sedimentation amount versus the sedimentation time. Nevertheless, this method is not suitable for nanofluids with high concentration of particles. Particularly for the case of nanofluids with CNT nanoparticles, the dispersions are dark enough to distinguish the sediment visibly. For the first time, Jiang et al. (2003) investigated sedimentation estimation for nanofluids using UV-Visible spectrophotometer. This method was used by Kim et al. (2007) and Lee et al. (2009). To the best of author's knowledge, there is no available literature for the evidence of using UV-Visible spectrophotometer to characterize stability of nanorefrigerants. Furthermore, the author had used this method to characterize the nanorefrigerants. Figure 1.3 of section 1.3 is the evidence of difficulties when using this method for refrigerant based nanofluids.

2.3.2 Sediment photograph capturing

This is a basic, easy and cheap method to find out the sedimentation of suspensions. After the preparation of nanofluids, some percentages of the particles will be inside a test tube or bottle (the bottles need to be clear enough so that the fluid inside could easily be captured by camera). Usually, photos can be captured after certain period of time. From the captured photo, sedimentation of suspension can be compared. Peng et al. (2009a) used this method to measure the stability of nanorefrigerants. In this study, this sediment photograph capturing method has been successfully implemented.

2.3.3 SEM and TEM

SEM and TEM are suitable equipment to determine the size, shape, elemental composition, and distribution of nanoparticles. Though, they cannot state the real condition of nanoparticles in nanofluids, especially when the dried samples are measured. There are some specialized electron microscope like Cryogenic electron microscope (Cryo-TEM and Cryo-SEM) that could directly monitor the nanoparticles aggregation state in nanofluids (Wu et al., 2009). Though these equipment are high costly. However, now a days, these methods are widely used to determine the sizes and shape of nanoparticles. Throughout this study, both of these types of equipment have been used to measure the nanoparticles size, shape, and elemental composition.

2.4 An overview on thermophysical properties of nanorefrigerants

This section is divided into three subsections as review of thermal conductivity, viscosity, and density of nanorefrigerants.

2.4.1 Thermal conductivity of nanorefrigerants

Heat transfer performance is directly related to thermal conductivity of a substance. Research is going on tremendously about the thermal conductivity of nanofluids.

According to the author's knowledge, there are two literatures available about thermal conductivity of nanorefrigerants. Jiang et al. (2009a) analyzed the thermal conductivity of four different types of CNT with R113 refrigerants for a volume concentrations of 0.2 to 1 %. They modified the Yu-Choi model (Yu & Choi, 2003) and presented a correlation to determine the thermal conductivity of CNT nanorefrigerants. Jiang et al. (2009b) investigated the thermal conductivity of R113 with Cu, Al, Ni, CuO and Al_2O_3 with a controlled volume concentrations of 0.1 to 1.2 %. The authors proposed a model based on Wang model (Wang, 2003) for measuring thermal conductivity of nanorefrigerants. Furthermore, there are a plenty of literature available about thermal conductivity of nanofluids based on water or ethylene glycol. Available literatures could be divided into two sections as: effect of volume concentrations and effect of temperatures.

2.4.1(a) Effect of volume fractions on thermal conductivity of nanofluids

It is well known that the thermal conductivity is increased with increasing the volume faction of nano particle. Figure 2.2 shows that thermal conductivity increases with the enhancement of particle concentrations.

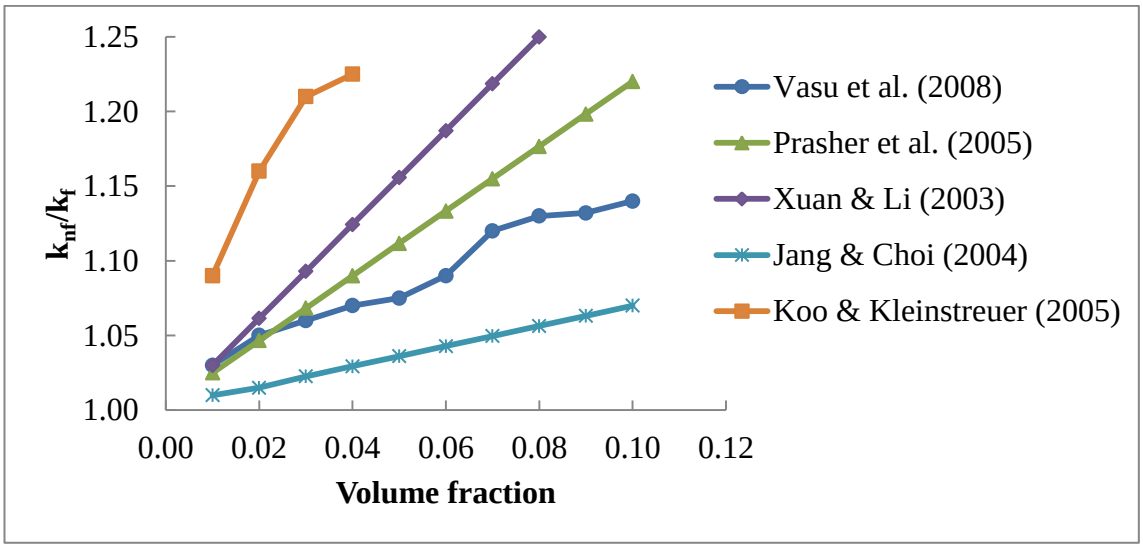

Figure 2.2: Variation of thermal conductivity of nanofluids with different volume concentrations of nanoparticles.

From the figure it is clear that, in most cases thermal conductivity increases linearly (Jang & Choi, 2004; Prasher et al., 2005; Xuan & Li, 2003) and in some cases increases abruptly (Koo & Kleinstreuer, 2005; Vasu et al., 2008).

2.4.1(b) Influence of temperatures on thermal conductivity of nanofluids

Besides, it is found that the thermal conductivity is increased accordingly with the temperature of the nanofluids. This would be a good reason to apply nanofluids in heat exchangers. Figure 2.3 shows that thermal conductivity augmented accordingly with the increase of temperatures. It is clear from the figure that, in most cases thermal conductivity increases linearly. However, the increment rate is different for different researchers; this may be due to various reasons as nanoparticle type, size, and base fluid.

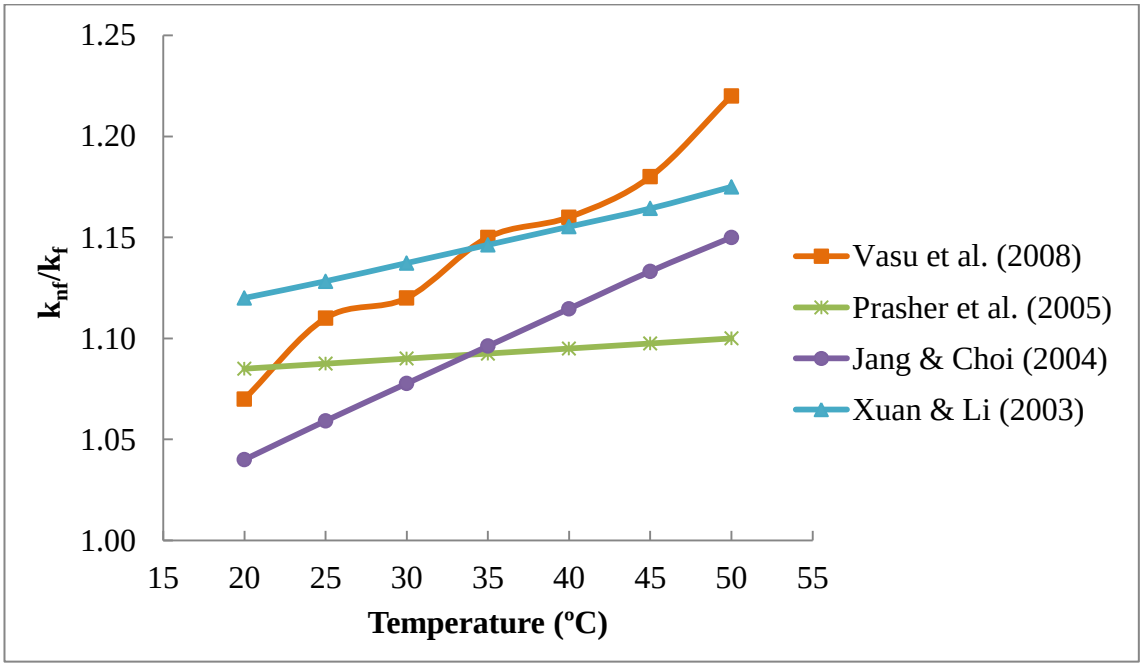

Figure 2.3: Variation of thermal conductivity of nanofluids with different temperatures.

There are some existing theoretical formulae to estimate thermal conductivity of suspensions. First, Maxwell (1891) proposed the model as:

$$k_{eff} / k_f = \frac{k_p + 2k_f + 2\phi(k_p - k_f)}{k_p + 2k_f - \phi(k_p - k_f)} \tag{2.1}$$

Later on considering the effective thermal conductivity of two-phase mixture, Hamilton and Crosser (HC) (1962) proposed a model as:

$$k_{eff} / k_f = \left[\frac{k_p + (n-1)k_f - (n-1)\phi(k_f - k_p)}{k_p + (n-1)k_f + \phi(k_f - k_p)} \right] \tag{2.2}$$

Where, $n = \frac{3}{\psi}$.

For a binary mixture of homogeneous spherical particles, the Bruggeman model (Hui et al., 1999) gives a better estimation compared with other models specially for spherical particles is given by:

$$k_{eff} = \frac{1}{4}\left[(3\phi - 1)k_p + (2 - 3\phi)k_f\right] + \frac{k_f}{4}\sqrt{\Delta} \tag{2.3}$$

$$\text{Where } k_{eff} = \left[(3\phi - 1)^2 \left(\frac{k_p}{k_f} \right)^2 + (2 - 3\phi)^2 + 2\left(2 + 9\phi - 9\phi^2\right)\frac{k_p}{k_f} \right] \tag{2.4}$$

A modified version of , Hamilton and Crosser (HC) is Wasp model (Wasp et al., 1977)

$$k_{eff} / k_f = \frac{k_p + 2k_f - 2\phi(k_f - k_p)}{k_p + 2k_f + \phi(k_f - k_p)} \tag{2.5}$$

Where, ϕ is the particle concentrations and is measured by

$$\phi = \frac{V_p}{V_f + V_p} = m\frac{\pi}{6}\bar{d}_p^3 \tag{2.6}$$

The difference between Equations (2.2) and (2.5) is that Wasp's model is limited with the sphericity 1.0 of the Hamilton and Crosser's model.

Yu and Choi (2003) amended the Maxwell correlation to predict the effective thermal conductivity of solid and liquid mixtures.

$$k_{eff} / k_f = \frac{k_{pe} + 2k_f + 2\phi(k_{pe} - k_f)(1+\beta)^3}{k_{pe} + 2k_f - \phi(k_p - k_f)(1+\beta)} \quad (2.7)$$

This modification was based on interfacial layer of nanofluids that enhances the thermal conductivity. But, this renewed Maxwell model is limited to predict the thermal conductivity of nanofluids with spherical nanoparticles. After that, the authors extended the Hamilton–Crosser model for nanofluids of non-spherical particles to assume the effect of a solid/liquid interface of nanofluids. The extended Hamilton–Crosser model (Yu & Choi, 2004) is:

$$k_{eff} / k_f = 1 + \frac{n\phi_{eff} A}{1 - \phi_{eff} A} \quad (2.8)$$

Where, $A = \frac{1}{3}\sum_{j=a,b,c} \frac{k_{pj} - k_f}{k_{pj} + (n-1)k_f}$ (2.9)

Xuan et al. (2003) proposed a model considering the physical properties of the base fluid and the nanoparticles, and the structure of the nanoparticles and aggregation. The model is:

$$k_{eff} / k_f = \frac{k_p + 2k_f - 2\phi(k_f - k_p)}{k_p + 2k_f + \phi(k_f - k_p)} + \frac{\phi\rho_P c_P}{2k_f}\sqrt{\frac{K_B T}{3\pi r_c \eta}} \quad (2.10)$$

Where, K_B is the Boltzmann constant = 1.381x10^{-23} JK^{-1} and η is the viscosity in Kg/(s.m).

Considering the role of Brownian motion Jang and Choi (2004) developed a correlation to determine the thermal conductivity of nanofluids including the effect of volume fraction, temperature and particle size. The correlation is expressed as:

$$k_{eff} / k_f = 1 + c \frac{d_f}{d_p} k_f \phi \mathrm{Re}_{d_p}^2 \mathrm{Pr} \tag{2.11}$$

Prasher et al. (2005) proposed a semi-empirical Brownian model to measure the thermal conductivity of nanofluids as:

$$k_{eff} / k_f = \left(1 + A\phi \mathrm{Re}^m \mathrm{Pr}^{0.333}\right) \frac{(1+2\alpha) + 2\phi(1-\alpha)}{(1+2\alpha) - \phi(1-\alpha)} Where \alpha_f = 2R_b k_f / d_p$$

(2.12)

Koo and Kleinstreuer (2005) proposed a correlation to measure the thermal conductivity of suspensions. This model can consider the effects of particle size, volume concentrations and temperature also the properties of base liquid. This model is stated as:

$$k_{eff} / k_f = \frac{k_{MG}}{k_f} + \frac{1}{k_f} 5 \times 10^4 \beta \phi \rho_P c_P \sqrt{\frac{K_B T}{\rho_P D}} f(T, \phi) \tag{2.13}$$

Leong et al (2006) proposed a new equation to determine the effective thermal conductivity of nanofluids based on the interfacial layer effect at the solid particle/liquid interface. This new presented model can interpret the effects of particle sizes, interfacial layer thicknesses, and volume concentration of nanoparticles on thermal conductivity of nanofluids.

$$k_{eff} = \frac{\left(k_p - k_{lr}\right)\phi k_{lr}\left[2\beta_1^3 - \beta^3 + 1\right] + \left(k_p + 2k_{lr}\right)\beta_1^3\left[\phi\beta^3\left(k_{lr} - k_f\right) + k_f\right]}{\beta_1^3\left(k_p + 2k_{lr}\right) - \left(k_p - k_{lr}\right)\phi\left[\beta_1^3 + \beta^3 - 1\right]} \tag{2.14}$$

Where, $\beta = 1 + \frac{t}{r_p}$ and, $\beta_1 = 1 + \frac{t}{2r_p}$

Sitprasert et al. (2009) extended Leong et al.'s model and proposed that, the thickness of interfacial layer, t depends on temperature where $t = 0.01(T - 273) r_p^{0.35}$, and the

thermal conductivity of the interfacial layer can be found from $k_{lr} = C\frac{t}{r_p}k_r$ where C = 30, a constant for Al_2O_3 nanoparticles.

More investigation is needed to justify the application of these theories for refrigerant based nanofluids as most of this theory developed based on water and ethylene glycol based nanofluids.

Table 2.2 shows the available literatures about thermal conductivity of nanorefrigerants. To make a comparison the entire thermal conductivity enhancement ratio has been selected for 0.2 volume fraction of nanoparticles concentrations (%).

Table 2.2: Summery of available literatures about thermal conductivity of nanorefrigerants.

Refrigerant	Nanoparticle (size)	Volume fraction (%)	Thermal conductivity enhancement ratio, k_{nf}/k_f for 0.2 vol.%	Reference
R113	CNT's (L=1.5µm, d=15nm)	0.2 to 1.0	1.35	(Jiang et al., 2009a)
R113	CNT's (L=10µm, d=15nm)	0.2 to 1.0	1.46	(Jiang et al., 2009a)
R113	CNT's (L=1.5µm, d=8 nm)	0.2 to 1.0	1.06	(Jiang et al., 2009a)
R113	CNT's (L=10µm, d=80nm)	0.2 to 1.0	1.06	(Jiang et al., 2009a)
R113	Cu (Avg. d=25 nm)	0.1 to 1.2	1.05	(Jiang et al., 2009b)
R113	Al. (Avg. d=18 nm)	0.1 to 1.2	1.03	(Jiang et al., 2009b)
R113	Ni (Avg. d=20 nm)	0.1 to 1.2	1.04	(Jiang et al., 2009b)
R113	CuO (Avg. d=40 nm)	0.1 to 1.2	1.03	(Jiang et al., 2009b)
R113	Al_2O_3 (Avg. d=20 nm)	0.1 to 1.2	1.04	(Jiang et al., 2009b)

From the table it is obvious that, almost all the available literatures about nanorefrigerants are based on R113 refrigerants. This refrigerant is mostly used for manufacturing soft PU foam. It is a CFC gas and it will be phased out within 2030. This

research will enrich the scientific contents and try to fill some gaps of the study about thermal conductivity of nanorefrigerants.

2.4.2 Viscosity of nanorefrigerants

Viscosity is an important phenomenon like thermal conductivity. Pumping power and pressure drop is proportional to viscosity of any liquid, especially in laminar flow (Mahbubul et al., 2012). To the best of author's knowledge there is no literature available about viscosity of nanorefrigerants. However, literatures are available on viscosity of nanofluids based on water, ethylene glycol, etc. Most of the available literatures about viscosity of nanofluids are based on the volume concentrations effect over viscosity. Moreover, some literatures are also available on temperatures and particle sizes effects over viscosity of nanofluids.

2.4.2(a) Viscosity of nanofluids as a function of volume fraction

Most of the available literatures about viscosity of nanofluids show that viscosity of nanofluids enhances accordingly with the augmentation of the volume concentrations. Das et al. (2003) and Putra et al. (2003) showed that viscosity of nanofluid increases accordingly with the enhancement of nanoparticle concentration for Al_2O_3/water nanofluid, for the concentrations between 1 % and 4 % particle (volume) fractions. Prasher et al. (2006) presented that viscosity of nanofluids enlarges around 10 X (ten times) as the volume fraction enhances.

Some researchers stated that, viscosity of liquids increases tremendously after the addition of nanoparticles. For example, for 12 volume concentration (%) of Al_2O_3/water, viscosity enhances 5.3 times (Nguyen et al., 2008), and for 12 volume concentration (%) of TiO_2 with water viscosity increased 1200 times (Tseng & Lin, 2003). Seemingly, viscosities of metal oxide based nanofluids have been broadly

investigated and Al_2O_3 and TiO_2 related literatures are foremost among the accessible literatures on viscosity of nanofluids. Hence, graphical representations of viscosity of nanofluids with Al_2O_3 and TiO_2 nanoparticles have been presented in Figure 2.4.

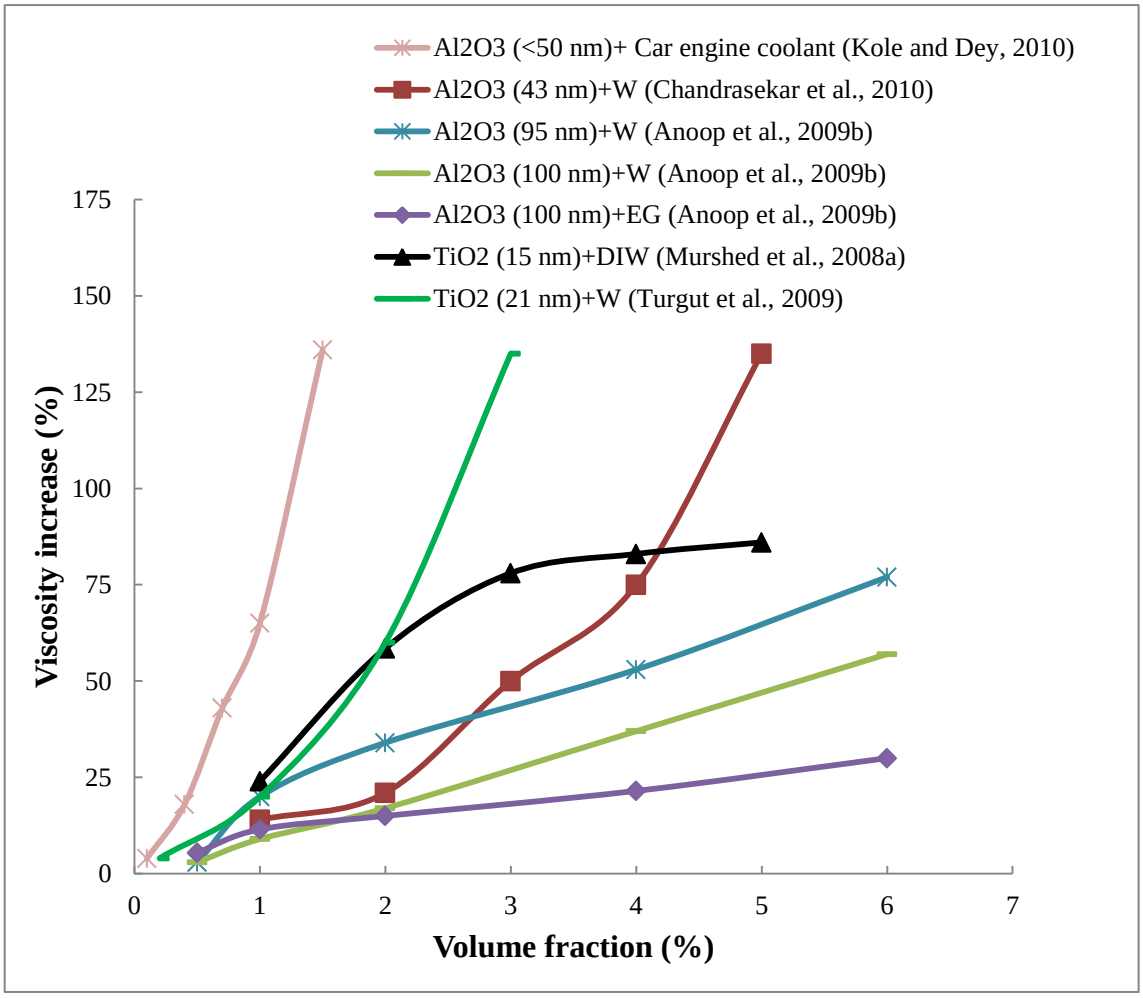

Figure 2.4: Viscosity of nanofluids increases accordingly with the intensification of volume fraction.

2.4.2(b) Effects of temperatures on viscosity of nanofluids

There are some literatures available on the effects of temperatures over viscosity of nanofluids. Available literatures show, the researchers' agreement over the fact that, viscosity of nanofluid augmented with the intensification of volume fraction. On the other hand, there are debates about the effects of temperatures over viscosity of nanofluids. Most of the researchers showed that, viscosity of nanofluids decreases with the enhancement of temperatures like the viscosity of most of the base fluids decreases

with the intensification of temperatures. However, some of the researchers argued that, viscosity of nanofluids is not related to temperature (Prasher et al., 2006).

Yang et al. (2005) measured the effects of temperature for viscosity of nanofluids with four different temperatures (35, 43, 50, and 70^{o}C) and for four different nanofluids mixtures having graphite as the common nanoparticles. The authors demonstrated that kinematic viscosity declines with the augmentation of temperatures. Chen et al. (2008b) measured the effects of temperature for multi walled carbon nanotubes with distilled water for a temperatures ranges of 5^{o}C to 65^{o}C and stated that comparative viscosity rises considerably after the temperature of 55^{o}C. Turgut et al. (2009) showed that, viscosity of TiO_2 with deionized water for a temperature range of 13^{o}C to 55^{o}C and for volume concentration of 0.2 to 3 % decreases with the rise of temperatures but in very less amount of deterioration. Figure 2.5 shows viscosity of nanofluids deteriorates with the rise of temperature.

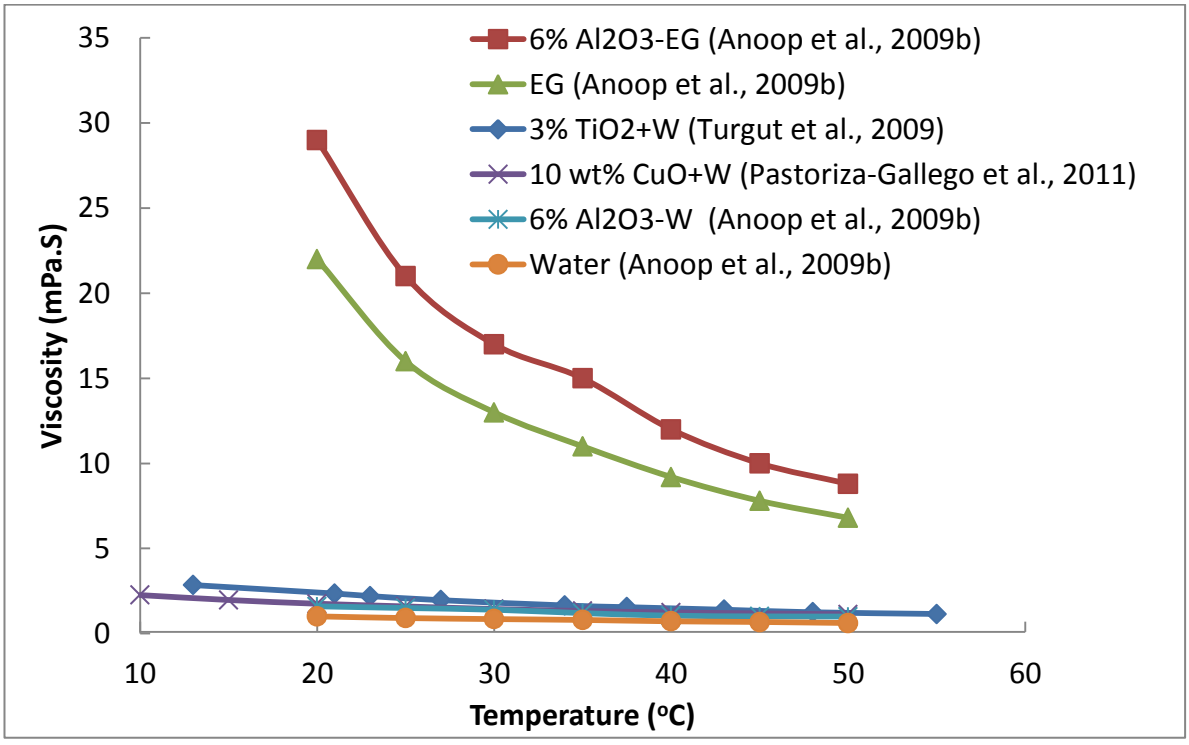

Figure 2.5: Viscosity of fluids decreases with the increase of temperature.

From the figure it is obvious that, the viscosity of ethylene glycol and Al_2O_3/ethylene glycol deteriorates tremendously with the increase of temperature compared with water based nanofluids. This is because of the viscosity of the base fluids (viscosity of pure ethylene glycol is higher than that of water).

There are some theoretical formulas (model or correlations) available in literature to calculate the viscosity of nanofluids (in general these formulas are for particle suspension viscosity). Among these theories, Einstein (1906) is the pioneer and some other researchers derived relations basically from this equation. The assumptions made for this theory is linearly viscous fluid having dilute, suspended, and spherical particles for a low particle volume concentration $(\phi < 0.02)$. The model is stated as:

$$\mu_{nf} = \mu_{bf}(1 + 2.5\phi) \tag{2.15}$$

In 1952, Brinkman (1952) has modified Einstein's model to be used with reasonable particle volume fraction, as bellow:

$$\mu_{nf} = \mu_{bf} / (1 - \phi)^{2.5} \tag{2.16}$$

Lundgren (1972) proposed the bellow correlation to predict the suspension viscosity. This equation is the form of a Taylor series in terms of ϕ:

$$\mu_{nf} = \mu_{bf}\left(1 + 2.5\phi + \frac{25}{4}\phi^2 + f(\phi^3)\right) \tag{2.17}$$

Batchelor (1977) proposed the below model with the consideration of the effect of Brownian motion of particles on suspension of rigid and spherical particles;

$$\mu_{nf} = \mu_{bf}(1 + 2.5\phi + 6.5\phi^2) \tag{2.18}$$

It is clear from Equations 2.17 and 2.18 that, if second or higher order of ϕ are discounted, then these formula will be the same as Einstein's formula.

Murshed et al. (2008b) recommended that the popular models such as (Einstein, 1906), (Krieger, 1959), (Batchelor, 1977), and (Nielsen, 1970) could not calculate the viscosity of nanofluids accurately. Truly, there is no model that could assume the viscosity of nanofluids accurately considering the wide range of nanoparticle volume concentrations, temperature and particle size. Table 2.3 shows the available literatures on the viscosity of nanofluids. Here in this table, particle size and volume concentrations have been considered.

Table 2.3: Some literatures about enhancement of viscosity of nanofluids with the increase of volume fractions.

Researchers	Base fluid	Nano-particle	Particle size (nm)	Volume fraction (%)	Viscosity enhancement (%)
Chandrasekar et al. (2010)	Water	Al_2O_3	43	1 to 5	14 to 136
Nguyen et al. (2008; 2007)	Water	Al_2O_3	47	1 to 13	12 to 430
Wang et al. (1999)	EG	Al_2O_3	28	1.2 to 3.5	7 to 39
Prasher et al. (2006)	PG	Al_2O_3	27	0.5 to 3	7 to 29
Murshed et al. (2008a)	DIW	Al_2O_3	80	1 to 5	4 to 82
Anoop et al. (2009b)	Water	Al_2O_3	45	2 to 8 wt %	1 to 6
Anoop et al. (2009a)	Water	Al_2O_3	95	0.5 to 6	3 to 77
Masuda et al. (1993)	Water	TiO_2	27	1 to 4.3	11 to 60
Murshed et al. (2008a)	DIW	TiO_2	15	1 to 5	24 to 86
Chen et al. (2007a; 2007b; 2009b)	EG	TiO_2	25	0.1 to 1.86	0.5 to 23
He et al. (2007)	DW	TiO_2	95,145, 210	0.024 to1.18	4 to 11
Chen et al. (2009b)	Water	TiO_2	25	0.25 to 1.2	3 to 11
Duangthongsuk and Wongwises (2009)	Water	TiO_2	21	0.2 to 2	4 to 15
Turgut et al. (2009)	DIW	TiO_2	21	0.2 to 3	4 to 135
Pastoriza-Gallego et al. (2011)	Water	CuO	11±3	1–10 wt %	2.5 to 73
Chevalier et al. (2007)	Ethanol	SiO_2	35	1.2 to 5	15 to 95
Chevalier et al. (2007)	Ethanol	SiO_2	94	1.4 to 7	12 to 85
Chen et al. (2009a; 2009b)	EG	TNT	~10,L= 100 nm	0.1 to 1.86	3.3 to 70.96
Chen et al. (2009b; 2008a)	Water	TNT	~10, L= 100 nm	0.12 to 0.6	3.5 to 82
Garg et al. (2008)	EG	Cu	200	0.4 to 2	5 to 24
Zhu et al. (2010)	DW	$CaCO_3$	20–50	0.12 to 4.11	1 to 69
Lee et al. (2011)	DW	SiC	<100	0.001 to 3	1 to 102

Table 2.3 shows that, viscosity of nanofluids increases accordingly with the enhancement of volume concentrations. However, the increment rate is not similar from one researcher to another. Even for the same authors, variations exist among the different studies. So, it is needed to study the viscosity of different types of nanofluids for different parameters. Furthermore, there is no literature available about the viscosity of nanorefrigerants. This study will help the scientific community by introducing experimentation about viscosity of nanorefrigerants.

2.4.3 Density of nanorefrigerants

Density of fluid is an important thermophysical property. Like viscosity, density of any fluid also has direct impact over pressure drop and pumping power. There are some literatures available about density of nanofluids. Still, there is no literature available on density of nanorefrigerants. However, Kedzierski (2009) measured the density of copper (II) oxide (CuO) nanoparticles with synthetic polyolester lubricant. The author reported that, density of nanolubricant increases with the increase of volume concentration of nanoparticles. Furthermore, density of nanolubricant decreases with the increase of temperature.

There are some equations used to calculate the density of mixture. The most widely used Mixture equation for suspensions by Wasp et al. (1977) is:

$$\frac{1}{\rho_m} = \frac{x_m}{\rho_s} + \frac{1 - x_m}{\rho_L} \tag{2.19}$$

Where the density of solid nanoparticles is ρ_s, ρ_L is the density values of pure liquid, ρ_m is the measured liquid density of the mixture and x_m is the particle mass fraction.

Pak and Cho (1998) suggested a correlation to measure the density of nanofluid as:

$$\rho_{nf} = (1-\phi)\rho_{bf} + \phi\rho_s \tag{2.20}$$

Where, density of solid nanoparticles is ρ_s , ρ_{bf} is the density values of base fluid, ρ_{nf} is the density of the suspension.

In this study, density of Al_2O_3/R141b nanorefrigerants has been measured for different concentration of nanoparticles. In addition, the available correlations to measure the mixture density of fluids has been used to compare with the experimental data.

2.5 An overview on migration properties of nanorefrigerants

Migration properties of nanoparticles during the pool boiling of nanorefrigerants are essential information for the application of nanorefrigerants in a refrigeration system. When implementing nanorefrigerants in the refrigeration systems, one important issue is to be considered and that is the migration of nanoparticles during the boiling process. This knowledge will help to identify, how the distribution of nanoparticles affect the cycle behavior of a refrigeration system (Peng et al., 2011b).

Regarding the migration properties of nanoparticles during boiling of a nanorefrigerant very few literatures exists up to the present and more research seems to be helpful in this area. Ding et al. (2009) for the first time investigated the major factors influencing the migration characteristics of nanoparticles during pool boiling. A comparison was made between pure nanofluid and nanofluid/oil mixture. The original mass of the nanoparticles and the mass of nanorefrigerant were stated to be effective on the migration rate. While investigating the both mentioned effects, the nanorefrigerant showed higher migrated mass of nanoparticles compared to the nanorefrigerant/oil mixture (17.5 % and 8.7% respectively). In another experimental study by- Peng et al. (2011b) other parameters including nanoparticle type and size, refrigeration type heat

flux and initial liquid-level height where analyzed. It was expressed that migration of nanoparticles inversely changes with nanoparticle size as it was said to be higher for Cu particles with 20 nm diameter compared with that for particles with 50 nm diameter. The authors outlined that due to the exclusion of parameters considering nanofluid composition as well as heating conditions, the model presented by Ding et al. (2009) would not be able to predict the migration characteristics. A more inclusive model were developed in the study by Peng et al. (2011c) which was claimed to be 90 % in accordance with the experimental data. Another literature is also available on the migration characteristics of Carbon Nanotube (CNT's) on the pool boiling of R113, R141b, and n-pentane refrigerants (Peng et al., 2011d). The available literatures about migration properties of nanorefrigerants are tabulated in Table 2.4.

Table 2.4: Summery of available literatures about migration properties of nanorefrigerants.

Objective	Refrigerant	Nanoparticle (size, nm)	Reference
Effect of nanoparticles and refrigerant weight	R113	CuO (40 nm)	(Ding et al., 2009)
Influence of nanoparticle type	R113	Cu (20 nm), Al (20 nm), Al_2O_3 (20 nm)	(Peng et al., 2011b, 2011c)
Influence of nanoparticle size	R113	Cu (20 nm), Cu (50 nm), Cu (80 nm)	(Peng et al., 2011b, 2011c)
Influence of refrigerant type	R113, R141b, n-pentane	CuO (40 nm)	(Peng et al., 2011b, 2011c)
Influence of mass fraction of lubricating oil	R113	CuO (40 nm)	(Peng et al., 2011b, 2011c)
Influence of heat flux	R113	CuO (40 nm)	(Peng et al., 2011b, 2011c)
Influence of initial liquid level height	R113	CuO (40 nm)	(Peng et al., 2011b, 2011c)
Influence of CNT's physical dimensions	R113	Different types of CNT's	(Peng et al., 2011d)
Influence of refrigerant type	R113, R141b, n-pentane	CNT (d_{out}=15 nm, d_{in}=10 nm, L=10 µm)	(Peng et al., 2011d)
Influence of oil concentration	R113	CNT (d_{out}=15 nm, d_{in}=10 nm, L=10 µm)	(Peng et al., 2011d)
Influence of heat flux	R113	CNT (d_{out}=15 nm, d_{in}=10 nm, L=10 µm)	(Peng et al., 2011d)
Influence of initial liquid level height	R113	CNT (d_{out}=15 nm, d_{in}=10 nm, L=10 µm)	(Peng et al., 2011d)

From the Table 2.4, it is clear that, most of the available literatures are based on refrigerant R113 and with nanoparticles CuO and CNT's. There is no literature available on the most widely used TiO_2 nanoparticle. This experiment have introduced the migration characteristics of TiO_2 and Al_2O_3 nanoparticles with R141b refrigerant for different parameters including nanoparticle type, size, initial liquid level height, boiling vessel size, heat flux, insulation, and oil. Two nanoparticles types have been chosen to see the effect of density of particles to predict the sedimentation inside the compressor of refrigeration system. Size has been considered to check the effect of particle size. It has been considered that if the nanoparticle size is smaller and spherical shaped it would be better for refrigeration system. The level of refrigerant inside the compressor varies time to time. So, the effect of liquid level size has been characterized. Different refrigeration systems have different size of compressors, evaporators, and piping systems. Therefore, the effect of boiling vessel size has been analyzed. Refrigerant are used in refrigeration system as they are too much heat sensitive and very low heat transfer fluids. Therefore, the effects of heat flux on migration of nanoparticles have been studied. Some air conditioning system use insulation on piping. Therefore, the effects of insulation during pool boiling of nanorefrigerants have also been analyzed. Some researchers used nanoparticles with refrigeration oil to study the performance of refrigeration system. Hence, the effects of refrigeration oil on migration of nanorefrigerants have been investigated.

2.6 Summary

The available literatures about nanorefrigerants have been summarized in Table 2.5.

Table 2.5: Summery of the available literatures about nanorefrigerants.

Investigator	Nanorefrigerant	Investigation
Kedzierski et al. (2007)	R134a -CuO	Heat transfer coefficient enhanced from 50% to 275% for 0.5% nanolubricant.
Park & Jung (2007)	(R123, R134a)-CNT's	Heat transfer coefficient enhanced up to 36.6%.
Shengshan & Lin (2007)	R134a -TiO_2	Energy savings 7.43%.
Bi et al. (2008)	Mineral oil -TiO_2	26.1% less energy consumption.
Ding et al. (2009)	R113-CuO	Migration of nanoparticles increased with the intensification of initial mass of nanoparticles.
Jiang et al. (2009a)	R113-CNT's	Thermal conductivity of CNT's nanorefrigerants increased with the intensification of CNT's volume concentrations.
Jiang et al. (2009b)	R113-Cu,Al,Ni,CuO, Al_2O_3	Thermal conductivity of nanorefrigerants increased with the intensification of nanoparticle volume concentrations.
Peng et al. (2009a)	R113-CuO	Highest heat transfer coefficient enhanced 29.7%.
Peng et al. (2009b)	R113-CuO	Highest enhancement of frictional pressure drop was 20.8%.
Trisaksti & Wongwises (2009)	R141b -TiO_2	Nucleate pool boiling heat transfer decreased with increase of particle concentrations.
Peng et al. (2010)	R113/VG68-Diamond	About 63.4% nucleate pool boiling heat transfer coefficient increased.
Bi et al. (2011)	R600a-TiO_2	9.6% less energy used
Peng et al. (2011b)	R113-Cu,Al,CuO,Al_2O_3 R141b,n-pentane-CuO	Migration of nanoparticles increased with the decrease of nanoparticle density and size.
Peng et al. (2011c)	R113-Cu,Al,CuO,Al_2O_3 R141b,n-pentane-CuO	Model development for migration properties of nanoparticles within a deviation of ±20%.
Peng et al. (2011d)	R113,R141b,n-pentane-CNT's	Migration ratio of CNT's increased with the increase of particle size (e.g. outside diameter or length of CNT's).

From the Table 2.5 it is obvious that, most of the available literatures about nanorefrigerants are about heat transfer coefficient and energy performance of refrigerating system. This study could contribute to enrich the analysis about

preparation, characterization, thermal conductivity, viscosity, density, and migration properties of nanorefrigerants.

From the literature- it is evident that, most of the studies about nanorefrigerants and nanofluids have been done with oxide nanoparticles. Moreover, TiO_2 and Al_2O_3 nanoparticles are widely used in nanofluid. These two oxides are comparatively chemically stable. They are cheap and readily available as they are produced industrially in large scale (Chen et al., 2007b). Furthermore, Al_2O_3 has good thermal conductivity compared with TiO_2 and other heat transfer fluids. Therefore, Al_2O_3/R141b nanorefrigerants were prepared to measure the thermal conductivity, viscosity, and density of nanorefrigerants. TiO_2 is safe for human and animals. Therefore, TiO_2 was used to analyze the migration of nanoparticles during the pool boiling of refrigerants.

CHAPTER 3: METHODOLOGY

3.1 Introduction

The aim of this chapter is to describe the materials, equipment, experimental settings and to introduce the various parameters that have been used to conduct the research. Moreover, the related equations used in this research are presented. The subsequent sections start with the description of the materials and their properties and brief information about the equipment that were used. The sections also are followed by the preparation methods along with challenges faced with during the preparation of nanorefrigerants; characterization processes; and the measuring procedure of thermophysical properties (e.g. thermal conductivity, viscosity, and density). Finally, the processes to analyze the migration properties of nanorefrigerants have discussed.

3.2 Experimental set-up

This section is divided into materials and equipment that were used throughout this study.

3.2.1 Materials

TiO_2 and Al_2O_3 nanoparticles have been used in this study. Table 3.1 shows the properties of TiO_2 and Al_2O_3 nanoparticles. Both of these two nanoparticles were purchased readily from the mentioned source. Each of the nanoparticles was purchased with two different sizes. TiO_2 with manufacturer defined average diameter of ~21 nm and two different sizes of Al_2O_3 (manufacturer defined sizes of 13 nm and 50 nm) were purchased from Sigma Aldrich (Malaysia). TiO_2 of 40 nm diameter size has also been purchased from Hefei Kaier Nanometer Energy & Technology Co., Ltd (China) with a manufacturer defined purity of more than 99%. The elemental compositions of the

nanoparticles have been checked by SEM-EDAX analysis and have presented in Appendix B. Nanoparticles sizes and shapes have been checked by SEM and TEM analysis and have been presented in Appendix C.

Table 3.1: Properties of nanoparticles used in this experiment.

Property	Al_2O_3	TiO_2
Molecular mass (g/mol)	101.96	79.87
Average particle diameter (nm)	13 and 50	~21 and 40
Density (kg/m^3)	4000	4260
Thermal conductivity (W/mk)	40	8.4
Specific heat (J/kgK)	773	692

Refrigerant R141b has been used throughout this experiment as its boiling temperature is 32.06°C. Though, this refrigerant is no longer used in refrigeration and air conditioning systems. However, the basic properties of this refrigerant are similar to the most of used ones like- R22, R410a, R134a, etc. Table 3.2 shows the properties of R141b refrigerant at atmospheric pressure. The lubricant used as refrigerant oil for this experiment was manufactured by FOVAC Superior Ind. Inc. USA. This is ester oil with viscosity of 32 cp at 40^oC and density of 880 kg/m^3.

Table 3.2: Properties of R141b refrigerant.

Property	R141b
Chemical formula	CH3CCL2F
Molecular mass (g/mol)	116.95
Normal boiling point (^oC)	32.06
Freezing point (^oC)	-103.5
Critical temperature (^oC)	204.50
Critical Pressure (MPa)	4.25
Liquid phase density (kg/m^3)	1220.30
Liquid phase thermal conductivity (W/m.K)	0.0888
Liquid phase dynamic viscosity (mPas)	0.3780
Liquid phase isobaric specific heat (J/kg.K)	1165
Surface tension (N/m)	0.0174

3.2.2 Equipment

Table 3.3 shows the equipment used in this study. Other than this, some refrigerants properties like thermal conductivity, viscosity, and density for R141b refrigerants have been taken from REFPROP7 software (Lemmon et al., 2002).

Table 3.3: List of equipment used for data collection.

Equipment	Manufacturer	Model	Purpose	Accuracy
Sonics vibra cell	Madell		To prepare nanorefrigerant	
Digital power meter	YOKOGAWA	WT 130	To measure power to calculate heat flux	±0.2%
Precision analytical balance	AND	GR-200	To weigh nanoparticles	±0.1 mg
Orbital shaker incubator	Hottech	718	To prepare nanorefrigerant	
UV-Visible spectrophotometer	SHIMADZU	UV-1601	To characterize nanorefrigerant	
Portable density meter	Kyoto	DA-130	To measure density of nanorefrigerant	±0.001 g/cm^3
Programmable rheometer	Brookfield	LVDV-III	To measure viscosity of nanorefrigerant	±1%
Thermal properties analyzer	DECAGON	KD2-Pro	To measure thermal conductivity of nanorefrigerant	±0.01 W/(m· K)
Hot plate heater	YONGQIAN	YQ-1010A	To evaporate refrigerant	
Digital photo camera	Samsung	ES65	To capture photo of nanorefrigerant	
Field Emission Scanning Electron Microscope (FESEM)	Zeiss	AURIGA	To analyze the particle size, shape, and composition	
Transmission Electron Microscope (TEM)	Zeiss	TEM LIBRA 120	To analyze the particle size, shape, and distribution	
Refrigerated circulator bath	CPT Inc.	C-DRC 8	To maintain constant temperature	±0.02ºC

3.3 Preparation of nanorefrigerants

R-141b was used throughout the experiment as the host fluid because it is in the liquid state in room temperature and normal atmospheric condition. The most widely used refrigerants (such as R-134a and R-410A,) are in the gaseous state under the same

conditions. Therefore, nanorefrigerants based on R-141b refrigerant are easier for preparation compared to the other refrigerants. In this study no surfactant has been used. Acid treatment may be dangerous for the operator and it might be harmful for the refrigeration system as well. Hence, no acid treatment has been applied throughout this study to control the pH of nanorefrigerants. Sonics Vibra Cell ultrasonic vibrator was used for preparation of nanorefrigerants. This device can generate frequency up to 20,000 hertz (Hz). Thirty percent (30 %) amplitude of frequency was used for oscillation. A 2s:2s pulse (that means 2 seconds vibration and 2 seconds rest) was used throughout the preparation.

The experimental procedure for preparation of nanorefrigerants includes the following steps: weighing the desired amount of nanoparticle, m_n and put them into a vessel; in the next step adding the required amount of refrigerant, m_r into that vessel. Finally, the nanorefrigerants have been prepared by vibrating the mixture with ultrasonic processor for 60 minutes.

The equation used to calculate the volume fraction of nanorefrigerants is as follows:

$$\varphi = \frac{m_n / \rho_n}{m_n / \rho_n + m_r / \rho_r} \tag{3.1}$$

Table 3.5 and Table 3.6 show the proportion of R141b refrigerant with TiO_2 and Al_2O_3 nanoparticles, respectively for different volume concentrations.

Calculated amount of TiO_2 nanoparticles (Table 3.4 and Table 3.6) and Al_2O_3 nanoparticles (Table 3.5 and Table 3.7) was measured by “AND” precision analytical balance. The measurement range is between 10.0 mg to 210.0000 g with the highest error of 0.1 mg.

Table 3.4: Amount of TiO_2 nanoparticles and R141b refrigerant required for making 100 ml of desired concentration.

Concentration of TiO_2/R141b	TiO_2 (g)	R141b (ml)
0.2 wt. %	0.20	100.00
0.5 vol. %	2.14	100.00
1.0 vol. %	4.28	99.50

Table 3.5: Amount of Al_2O_3 nanoparticles and R141b refrigerant required for making 100 ml of desired concentration.

Concentration of Al_2O_3/R141b	Al_2O_3 (g)	R141b (ml)
0.1 vol. %	0.40	99.50
0.2 vol. %	0.80	99.50
0.3 vol. %	1.20	99.50
0.4 vol. %	1.61	100.00
0.5 vol. %	2.00	99.50
1.0 vol. %	4.06	100.50
1.5 vol. %	6.09	100.00
2.0 vol. %	8.20	100.50
2.5 vol. %	10.20	99.50
3.0 vol. %	12.31	99.50

Figure 3.1 shows the limitation of preparation of nanorefrigerants by the ultra-sonication method. Figure 3.1 (a) shows when the beaker is filled with 1 volume concentration (%) of TiO_2/R141b nanorefrigerants, just before starting the ultra-sonication process. From the figure it is clear that, the level of liquid and solid mixture is more than 80 ml. Figure 3.1 (b) shows the level of mixture after 30 minutes of ultra-sonication where it is almost 40 ml. Therefore, about half of the refrigerants evaporated with vibration of the ultrasonic amplitude. Figure 3.1 (c) shows that, the amount of nanorefrigerants is about 30 ml after 1 hour of ultra-sonication. The same thing happened for Al_2O_3/R141b nanorefrigerants. Therefore, this ultrasonic vibration method is not suitable for preparation of nanorefrigerants.

(a)

(b)

(c)

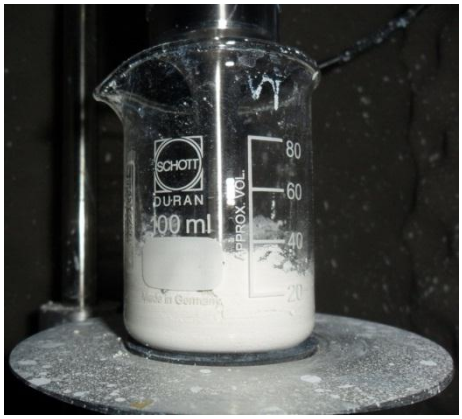

Figure 3.1: Effect of evaporation during ultra-sonication of TiO_2/R141b to prepare 1 volume concentration (%) of nanorefrigerant; (a) before ultrasonication; (b) just after 30 minutes of ultra-sonication; and (c) just after 60 minutes of ultra-sonication.

Then nanorefrigerants were prepared using an orbital incubator shaker. In most cases, the mixture of nanoparticles and refrigerants was continuously shaken at 240 rpm for about 24 hours. But, in some cases the period of shaking lasted about 6 hours. Constant temperature of 15ºC was maintained inside the incubator to avoid evaporation of refrigerants. The refrigerant remained liquid under these conditions.

To validate this method of preparation, two other types of nanofluids as TiO_2/water and Al_2O_3/water was prepared by continuously shaking at 240 rpm for about 24 hours. Then, a sediment photograph capturing method was applied to check the stability of the prepared nanofluids by using an orbital shaker. One volume concentration (%) of nanoparticles was prepared by this method having the nanoparticles and liquid proportion as described in Table 3.6 and Table 3.7 for TiO_2/water and Al_2O_3/water, respectively.

Table 3.6: Amount of TiO_2 nanoparticles and water required for making 100 ml, 1 volume concentration (%) of nanofluids.

Concentration of TiO_2/water	TiO_2 (g)	water (ml)
1 vol. %	4.30	100.00

Table 3.7: Amount of Al_2O_3 nanoparticles and water required for making 100 ml, 1 volume concentration (%) of nanofluids.

Concentration of Al_2O_3/water	Al_2O_3 (g)	water (ml)
1 vol. %	4.04	100.00

3.4 Characterization of nanorefrigerants

The methodology of characterization section is divided into four subsections based on four different methods used for characterization of nanorefrigerants.

3.4.1 UV-Visible spectrophotometer

SHIMADZU (UV-1601) UV-Visible spectrophotometer was used to characterize the sedimentation of nanorefrigerants. The spectrum of UV-Visible spectrophotometer was analyzed for 0.2 weight concentration (%) of TiO_2/R141b nanorefrigerants with pure R141b refrigerant. Initially, the range of wavelength was arbitrarily taken from 200 to 500 nm. From the trial and error of different wave length finally, the spectrum was measured within the range of 190 nm to 350 nm.

3.4.2 Sediment photograph capturing

A Samsung digital camera was used to capture the photograph of nanorefrigerants. Sedimentation photo of Al_2O_3/R141b nanorefrigerants prepared by an orbital incubator shaker was taken just after the preparation, and until seven (7) days after preparation with an interval of 1 day (24 hours). Also, photos of Al_2O_3/water and TiO_2/water nanofluids prepared by an orbital incubator shaker were taken just after the preparation, and until seven (7) days after preparation with an interval of 1 day (24 hours) to check the sedimentation and to validate the preparation method. The prepared nanorefrigerants were kept in closed glass bottle inside normal chamber of the domestic refrigerator at temperature below 15ºC to avoid evaporation.

3.4.3 SEM and TEM

Nanoparticle size and shape of Al_2O_3 (13 nm and 50 nm) and TiO_2 (~21 nm and 40 nm) were measured with the Field Emission Scanning Electron Microscope (FESEM), AURIGA (made by Zeiss, Germany). Moreover, the elemental compositions of these nanoparticles were checked by Energy Dispersive Spectroscopy (EDS) on the FESEM. Furthermore, a LIBRA 120, Transmission Electron Microscope (TEM) made by Zeiss, Germany was used to analyze the particle dispersion. TEM was used to check the particle size, shape, and distribution of 0.5 % particle volume concentration (%) of

four solutions. All the four combinations were based on R141b refrigerant with four different nanoparticles. The four nanorefrigerants include: Al_2O_3/R141b (13 nm), Al_2O_3/R141b (50 nm), TiO_2/R141b (21 nm), and TiO_2/R141b (40 nm). All the samples for TEM were collected, 24 hours after the preparation by 6 hours of mechanical shaker at 240 rpm. A pin point sample of each solution was taken into the fluorescent screen. The solution evaporated naturally during the transfer, i.e. only the particles was in dry form.

3.5 Thermophysical properties of nanorefrigerants

This section is divided into three subsections according to the methodology to measure thermal conductivity, viscosity, and density of nanorefrigerants.

3.5.1 Thermal conductivity of nanorefrigerants

A KD2 Pro thermal properties analyzer (Decagon, USA) was applied to analyze the thermal conductivity of nanorefrigerants. This device could measure thermal conductivity of liquids within the range of 0.02 to 2.00 W/(m· K). The accuracy of the equipment is ± 5 % from 0.2 - 2 W/(m· K) and ±0.01 W/(m· K) from 0.02 - 0.2 W/(m· K). The accuracy of this device was also measured with the standard sample (glycerin) provided by the manufacturer. Figure 3.2 shows the accuracy and precision of the device. The deviations of the measured value with the standards have shown in the figure. The figure indicated that, this equipment could produce very good data since the maximum deviation found to be less than 1.5 %.

Finally, the thermal conductivity of 0.5, 1.0, 1.5, 2.0, 2.5, and 3.0 volume concentration (%) of Al_2O_3/R141b (13 nm) were measured for a temperature range of 1.5 to 20.5ºC with this device. A KS-1 sensor was used to determine the thermal conductivity of suspensions. The details of sensor specifications presented in Table A1 (Appendix A).

Each experiment was conducted three times to get more precise value and the mean value of three data was plotted in the results. Some of the data (about 5 %) was omitted considered as abnormality. Some other models (e.g. Maxwell (1891), Yu-Choi (2003), Koo & Kleinstreuer (2005), Sitprasert et al. (2009), and Leong et al. (2006)) were used to verify the results of nanorefrigerants' thermal conductivity at 20ºC.

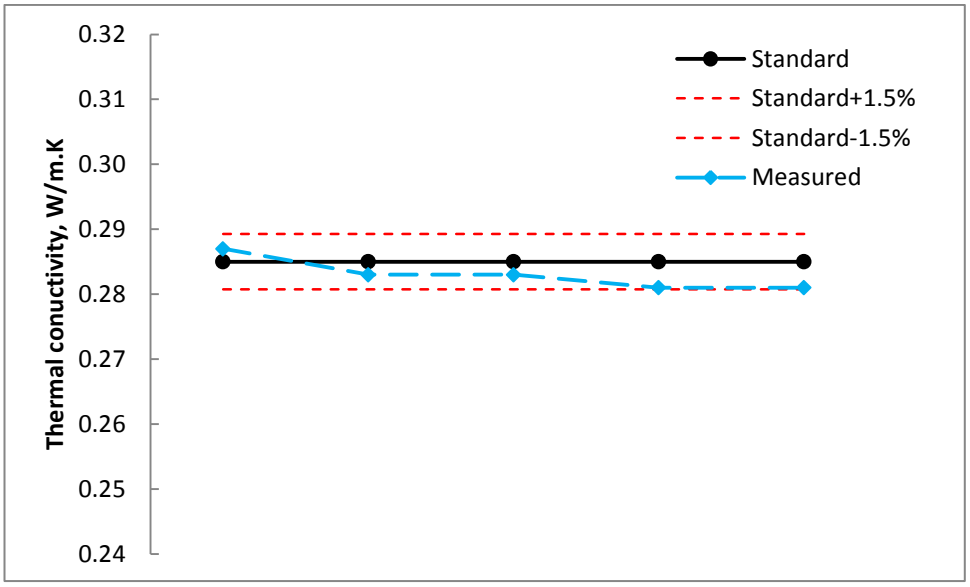

Figure 3.2: Accuracy of the KD2 Pro thermal properties analyzer (Decagon, USA) compared by the sample (glycerine) measured by the manufacturer.

3.5.2 Viscosity of nanorefrigerants

LVDV series (LVDV II, LVDV III, and LVDV III Ultra Programmable) viscometers are most widely used to determine the viscosity of suspensions. These LV series are suitable for measuring the low viscous fluid like water or ethylene glycol based nanofluids. Available literatures show that, most of the viscosity data have been measured by this equipment. LVDV III Ultra Programmable viscometer could measure the viscosity of suspensions within the range of 1.0 to 6,000,000 mPa.s by using the UL Adapter as an accessory with the main machine. As the viscosity of pure R141b refrigerant is less than 1 mPa.s, so the accuracy of this device was measured with the ethylene glycol. Standard viscosity of ethylene glycol (Incropera et al., 2007) was

compared with the measured viscosity for different temperature range. It was found that, the maximum deviation was within ±6 %. Figure 3.3 shows the accuracy of this device.

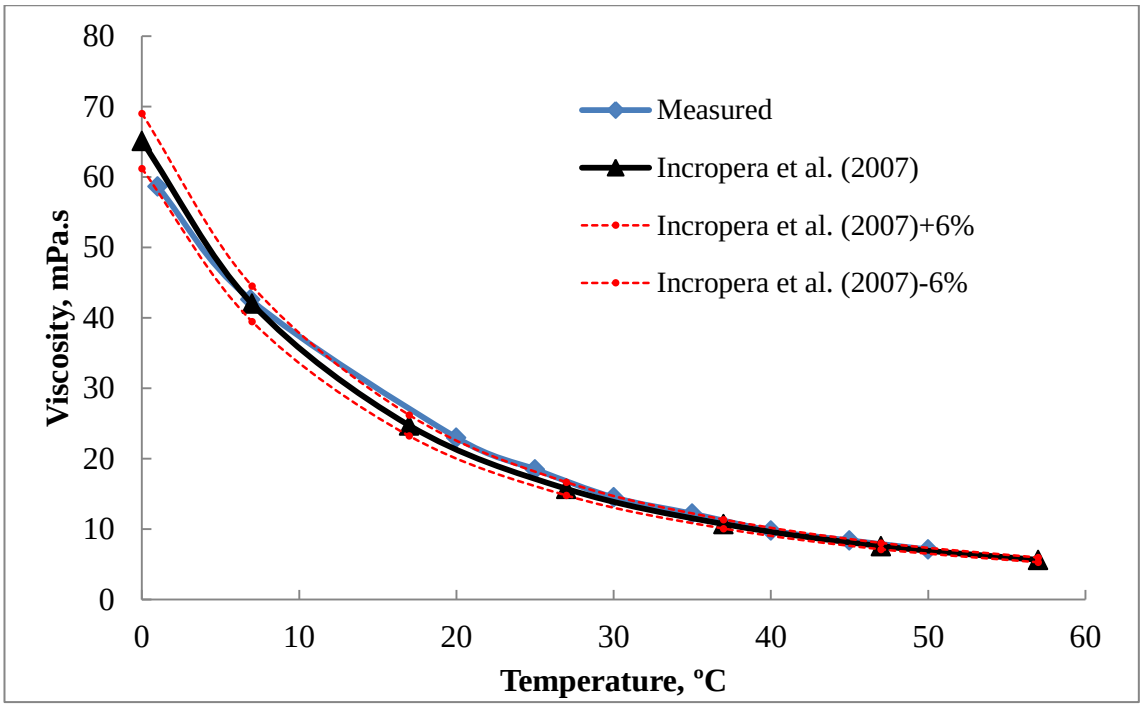

Figure 3.3: Accuracy of the LVDV III Ultra Programmable viscometer (Brookfield Engineering, USA) measured by ethylene glycol.

The viscosity of 0.5, 1.0, 1.5, and 2.0 volume concentration (%) of Al_2O_3/R141b (13 nm) were measured for a temperature range of 3 to 20ºC with this device. LV-2 (code: 62) spindle was used to measure the viscosity of suspensions at 250 rpm. The details of spindle specifications presented in Table A2 (Appendix A). Each experiment was conducted three times to get more precise value. The mean value of the three data was considered for analysis. Most widely used Brinkman model (1952) was implemented to compare the measured values for different nanoparticle concentrations at 20ºC.

3.5.3 Density of nanorefrigerants

The density of nanorefrigerants was measured by KEM-DA130N portable density meter (KYOTO, Japan). It measured the density with resonant frequency method. It could measure the density within a range of 0.0000 to 2.0000 g/cm^3 with a precision of ±0.001

g/cm^3. It has the resolution of 0.0001 g/cm^3 and can measure density within a temperature range of 0 to 40.0°C. Figure 3.4 shows the accuracy of the machine. The comparison of the measured data with REFPROP7 (Lemmon et al., 2002) standard data base shows the maximum deviation to be only about 0.2 %. This device was a small and portable type and the inlet tube was very small capillary. High concentration of nanorefrigerants could not support this device. Therefore, very low concentrations of nanorefrigerants were measured. Density of pure R141b refrigerant and 0.1 to 0.4 volume concentrations (%) of Al_2O_3/R141b were measured for a temperatures range of 5 to 20°C. All the data was taken three times to get more precise values and the mean value of three data was considered for analysis. Some of the data (about 5 %) were omitted as considered abnormality, especially above 20°C. When the refrigerant was evaporated at above 20°C, some of data showed abnormality.

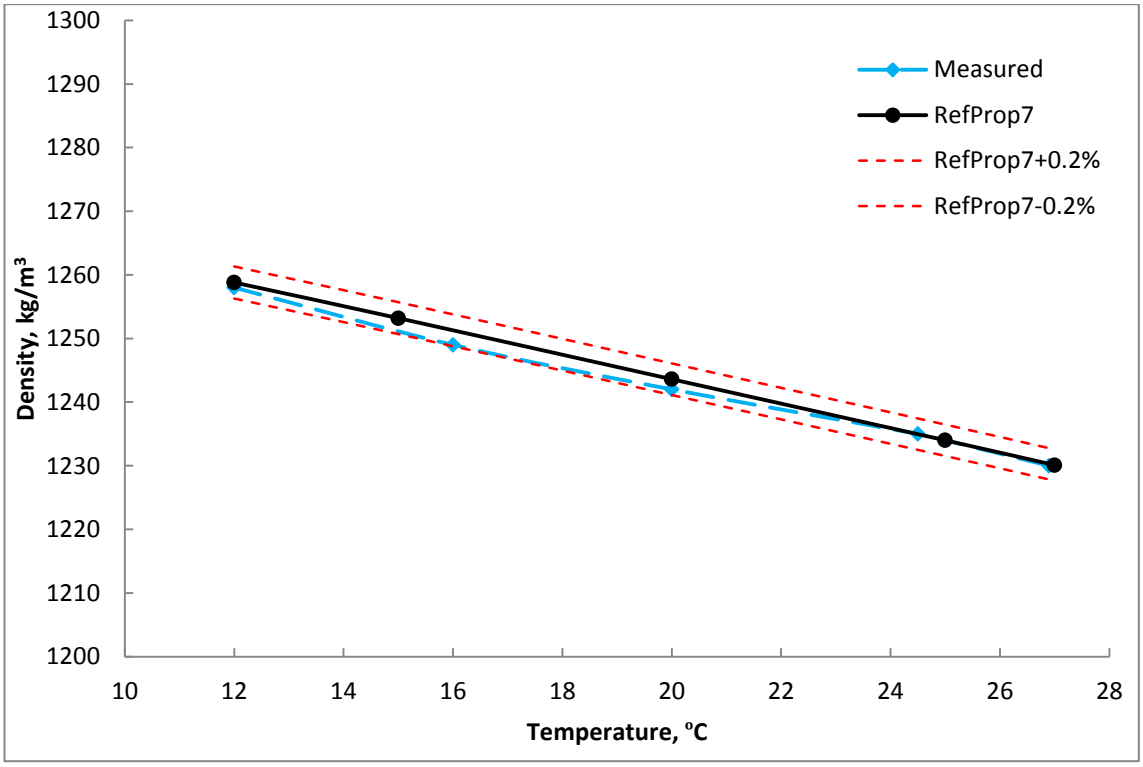

Figure 3.4: Accuracy of the DA 130N portable density meter (KYOTO, Japan) measured by pure R141b.

3.6 Migration properties of nanorefrigerants

In this section more details on the experimental procedures of migration of nanoparticles during the pool boiling process of refrigerants have been presented. Different conditions and set up will be expressed along with the step-by-step description of experimental process.

3.6.1 Materials and test conditions

The nanoparticles used for this experiment were basically Titanium Oxide (TiO_2) as it is safe for human being. Aluminum Oxide (Al_2O_3) was used only to compare the influence of particle types on migration of nanoparticles during the pool boiling of nanorefrigerants. Table 3.1 shows some properties of different nanoparticles used in this experimental investigation.

All of the experiments were conducted at atmospheric pressure (101.3 kpa). The details of materials and their categories were presented in Table 3.8.

Table 3.8: Materials categories and test conditions for migration of nanoparticles.

Objective	Nanoparticle (size, nm)	Mass fraction of lubricating oil, x_o (wt. %)	Heat flux, q (kW/m^2)	Initial liquid level height, L (cm)	Initial refrigerant volume, (ml)	Initial nanoparticle weight, (grams)
Influence of heat flux	TiO_2 (40)	0	10–40	0.9	30	0.50–1.50
Influence of initial liquid level height	TiO_2 (40)	0	20	0.9, 2.7	30,90	0.50–3.01
Influence of size of boiling vessel	TiO_2 (40)	0	20	1.8	30,60	0.50–2.50
Influence of insulation of boiling vessel	TiO_2 (40)	0	20	0.9	30	0.25–1.50
Influence of particle types	TiO_2 (40) and Al_2O_3 (50)	0	20	1.8	60	0.50–2.65
Influence of particle size	TiO_2 (40) and TiO_2 (21)	0	20	1.8	60	0.50–2.65
Influence of mass fraction of lubricating oil	TiO_2 (40)	0–10	20	0.9	30	0.50–2.50

3.6.2 Experimental apparatus

Mainly, three apparatus were used in this experimental work. A digital power meter (WT130, YOKOGAWA) was used to measure the voltage, ampere, and power. A variable electrical hot plate heater (YQ-1010A, YONGQIAN) was used to heat the refrigerant for migration at different heat fluxes. Direct current was supplied for this heater. Heat flux could be set at any point between 0 to 54 kW/m^2 with this hot plate. A precise digital analytical balance (GR200, AND) was used to measure the mass of nanoparticles, lubricant, and refrigerant. The measurement range is between 10.0 mg to 210.0000 g with a maximum error of 0.1 mg. The used boiling vessel was a cylindrical beaker with inside diameter of 67 mm and height of 94 mm. To measure the effect of

boiling vessel size another boiling vessel was used with inside diameter of 47 mm and height of 69 mm. All the experiments were conducted without insulating the beaker. However, the boiling vessel was insulated only when the effect of insulation of boiling vessel during migration was to be analyzed.

3.6.3 Experimental procedure

In this experiment, the same procedure introduced by Ding et al. (2009) was used. The experimental process can be divided into two parts: (1) experiments for migration of nanoparticles without lubricants; and (2) experiments for migration of nanoparticles with lubricants.

Experiments for migration of nanoparticles without lubricants includes the following steps: adding the desired amount of nanoparticle, m_n into the boiling vessel; In the next step weighing the total mass of the nanoparticles and boiling vessel, m_1; Then adding the required amount of refrigerant, m_r into the boiling vessel and switching on and adjusting the heater to control the heat flux afterwards. Next heating the boiling vessel until the refrigerant is fully evaporated; after this, weighing the total mass of the nanoparticles and boiling vessel, m_2 (weighing should be kept on until the mass of the mixture becomes constant after 12 hours); and finally calculating the migrated mass of nanoparticles from the equation $\Delta m = m_1 - m_2$.

Experiments for migration of nanoparticles with lubricants would be followed as: adding the desired amount of nanoparticle, m_n and the required amount of lubricating oil, m_o into the boiling vessel; Next weighing the total mass of the nanoparticles and boiling vessel, m_3; Then adding the required amount of refrigerant, m_{r0} into the boiling

vessel and switching on and adjusting the heater to control the heat flux afterwards. For the next step, heating the boiling vessel until the refrigerant is fully evaporated followed by weighing the total mass of the nanoparticles, lubricant, and boiling vessel, m_4 (weighing should be kept on until the mass of the mixture becomes constant after 12 hours) and lastly calculating the migrated mass of nanoparticles from the equation $\Delta m = m_3 - m_4$. Figure 3.5 shows the experimental setup for migration of nanoparticles during the pool boiling of nanorefrigerant. Here, Figure 3.5 (a) shows weighing the initial mass of nanoparticles and refrigerants or nanoparticles plus the refrigerant and oil, Figure 3.5 (b) shows boiling of nanorefrigerant and Figure 3.5 (c) shows weighing after the complete evaporation.

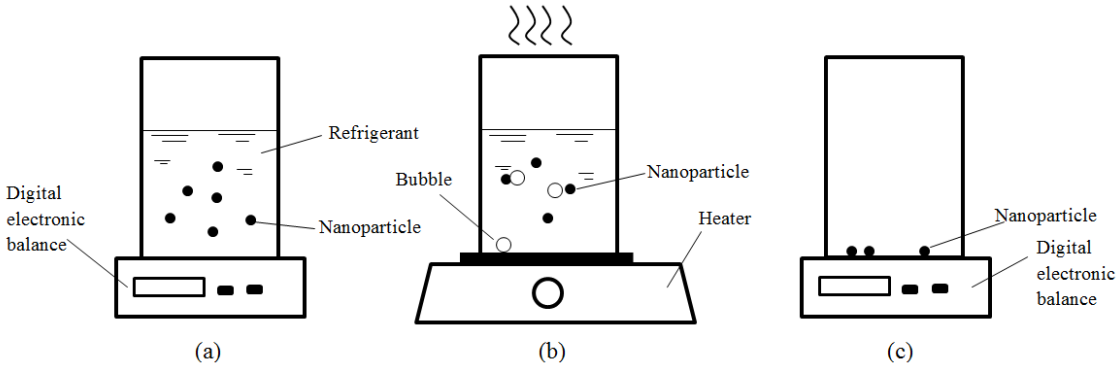

Figure 3.5: Experimental setup for migration properties of nanoparticles; (a) taking weigh of refrigerant, nanoparticles and beaker, (b) heating the refrigerant and nanoparticles for boiling, and (c) taking weigh of beaker and nanoparticles after fully evaporation of refrigerant.

CHAPTER 4: RESULTS AND DISCUSSIONS

4.1 Introduction

The aim of this chapter is to describe the results and discussions of the characterization and investigation of thermophysical and migration properties of nanorefrigerants. The subsequent sections start with the characterization of nanorefrigerants where UV-Visible spectrophotometry, sediment photograph capturing and SEM and TEM have discussed. The sections also are followed by the effect of particle concentration and temperature on thermophysical properties (e.g. thermal conductivity, viscosity, and density) of nanorefrigerants have discussed. Finally, the results of migration of nanoparticles during the pool boiling of nanorefrigerants have been discussed.

4.2 Characterization of nanorefrigerants

The results and discussions about characterization of nanorefrigerants section is divided into three subsections which are presented below.

4.2.1 UV-Visible spectrophotometer

Characterization for stability of nanorefrigerants was analyzed with the UV-Visible spectrophotometer. Figure 4.1 shows the spectrum image of 0.2 weight concentration (%) of TiO_2/R141b nanorefrigerants in UV-Visible spectrophotometer compared to the pure R141b refrigerant. Figure shows the noises on the image and that the graph was not clear to understand. However, it was assumed that the peak point would be within 200 to 300 nm. Figure 4.2 shows the image of 0.2 weight concentration (%) of TiO_2/R141b nanorefrigerants in UV-Visible spectrophotometer compared to the pure R141b refrigerant for more small range of wave length (from 190 nm to 350 nm).

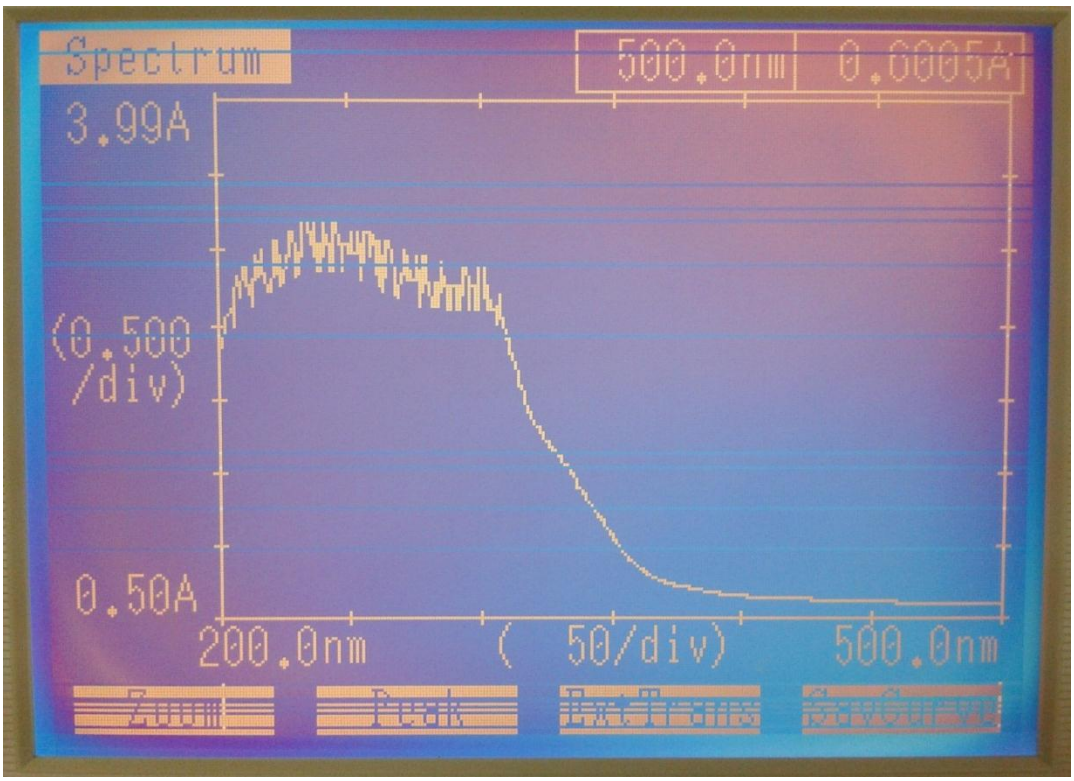

Figure 4.1: UV-Visible spectrophotometer image of 0.2 weight concentration (%) of TiO_2/R141b comparing with the pure R141b.

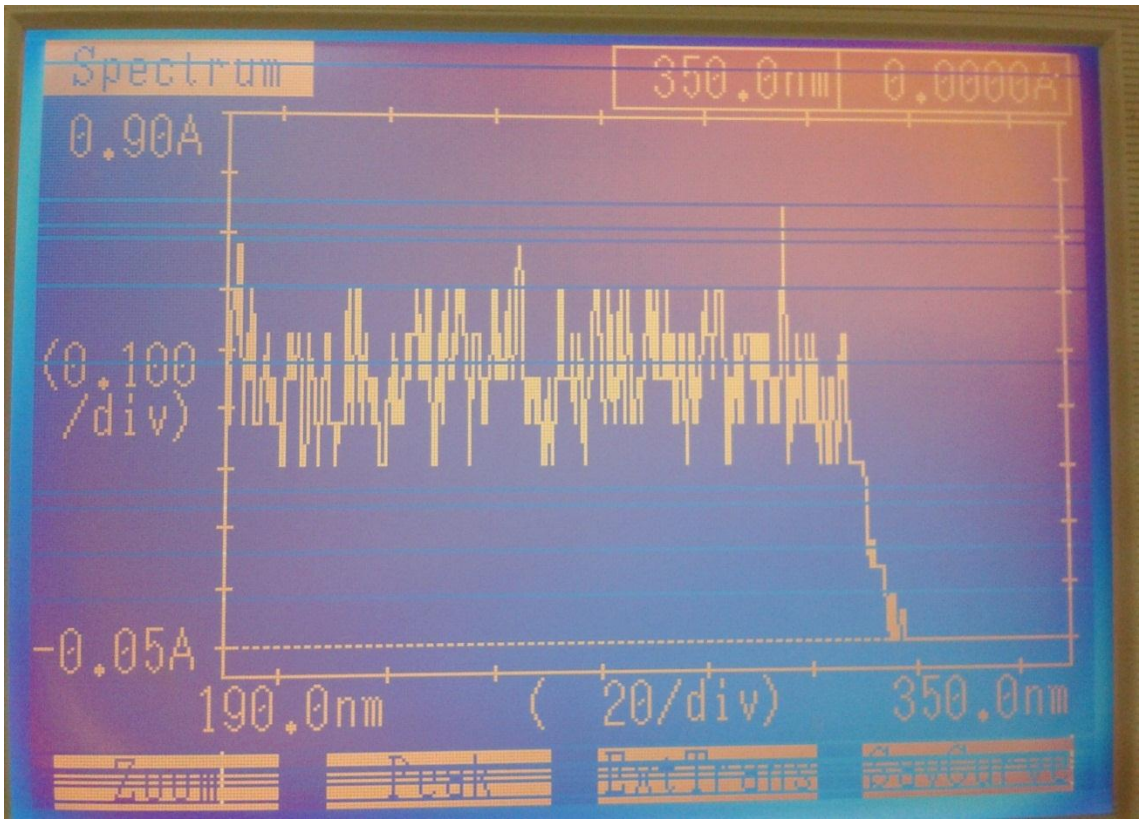

Figure 4.2: UV-Visible spectrophotometer image of 0.2 weight concentration (%) of TiO_2/R141b comparing with the pure R141b for more small range of wave length.

It is clear from the figure that, still there is noise and the image is not good for analysis. This would happen because when the light passed through the liquid, the refrigerants evaporated slightly inside the machine and for the vapor creation, the light could not pass clearly through the liquid. Therefore, there was noise and the output wave length was unreadable.

4.2.2 Sediment photograph capturing

Figure 4.3 shows the picture of 1 volume concentrations (%) of Al_2O_3/R141b nanorefrigerant prepared by 24 hours shaking with an orbital incubator shaker. Image of nanorefrigerants were taken after seven (7) days of preparation with a time interval of 1 day (24 hours). Figure 4.3 shows that, sedimentation starts after four days. The empty spaces of the last four specimens imply sedimentation. The amounts of empty space on the top of the bottle "after 4 days to 7 days" indicate that the sedimentation rate was very slow. Generally, the sedimentation of mixtures is measured from the bottom of the specimen. It could be possible when there are slurries obvious at the bottom of the sample. This happened, especially for the low concentration in the suspension. This 1 volume concentrations (%) of Al_2O_3/R141b nanorefrigerant is a moderate amount of volume fraction (neither so low nor so high concentration). There were no slurries obvious at the bottom of any of the specimens.

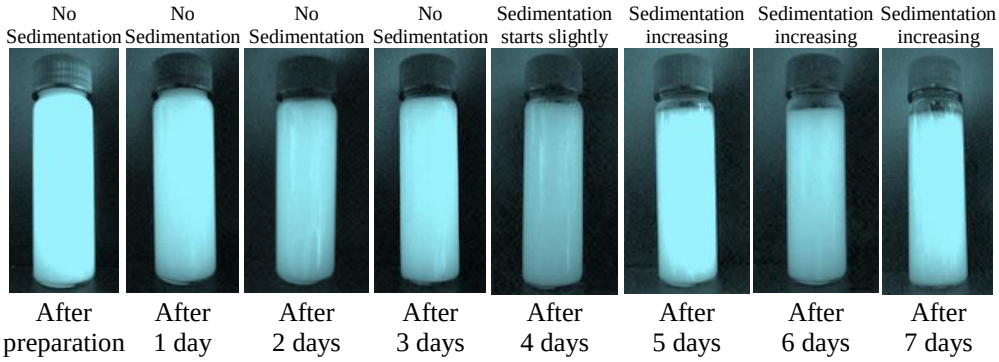

Figure 4.3: Image of 1 volume concentration (%) of Al_2O_3/R141b nanorefrigerants started from just after the preparation to after seven (7) days of preparation with a time duration of 1 day (24 hours).

Figures 4.4 and 4.5 show 1 volume concentration (%) of Al_2O_3/water and TiO_2/water nanofluids, respectively prepared by 24 hours shaking with orbital incubator shaker. The images show that, there is no sedimentation after seven days of preparation. In most cases sedimentation depends on the viscosity of base fluid as well as the preparation methods. The viscosity of water and R141b refrigerant are 0.85099 and 0.40021 mPa.s, respectively at 27°C and at atmospheric condition (Lemmon et al., 2002). For this reason during this experiment water based nanofluids found to be more stable compared to R141b based nanorefrigerants. That's why the ethylene glycol based nanofluids have more stability compared to water based nanofluids (Ghadimi et al., 2011). Figures 4.4 and 4.5 prove that, nanofluids prepared by shaking have good stability. This method is an easy procedure to prepare nanorefrigerants.

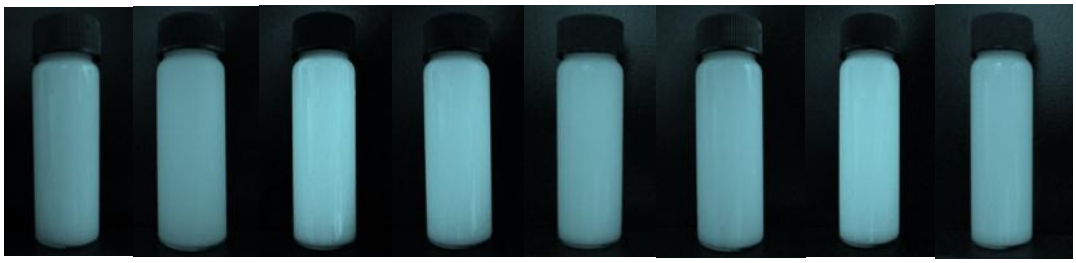

Figure 4.4: Image of 1 volume concentration (%) of Al_2O_3/water nanofluid started from just after the preparation to after seven (7) days of preparation with a time duration of 1 day (24 hours).

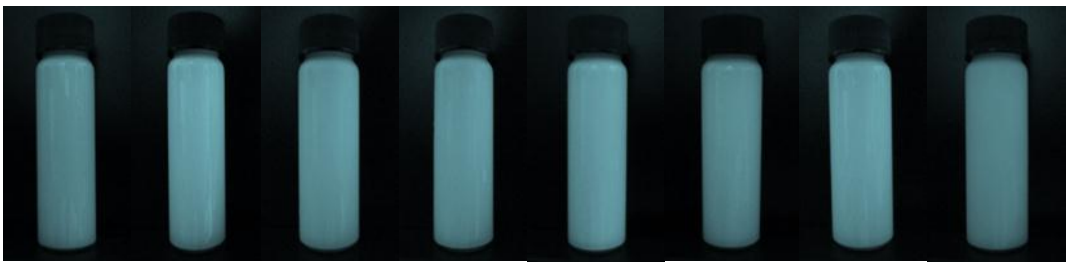

Figure 4.5: Image of 1 volume concentration (%) of TiO_2/water nanofluid started from just after the preparation to after seven (7) days of preparation with a time duration of 1 day (24 hours).

4.3 Thermophysical properties of nanorefrigerants

This section is divided into three subsections according to the results and discussions of thermal conductivity, viscosity, and density of nanorefrigerants. Each of the subsection firstly, describes the effect of volume concentrations and finally, describes the effect of temperature.

4.3.1 Thermal conductivity of nanorefrigerants

Figure 4.6 shows the thermal conductivity of Al_2O_3/R141b nanorefrigerants at 20ºC temperature for 0.5 to 3.0 volume concentrations (%) of nanoparticles. The experimental result of the present study was compared with results obtained from other models for validation. The figure shows that the thermal conductivity of Al_2O_3/R141b nanorefrigerant increases with nanoparticle volume concentration enhancement. The increment rate with the augmentation of concentration expected to be linear.

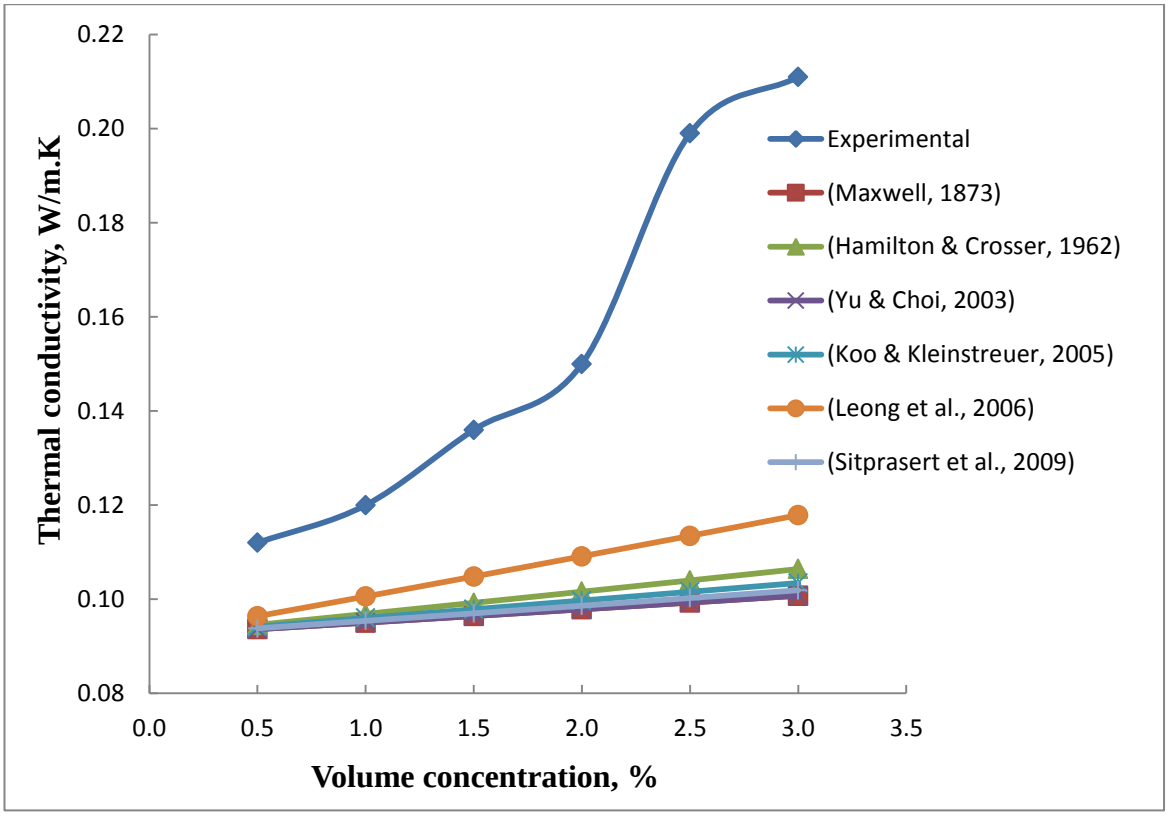

Figure 4.6: Variation of thermal conductivity of Al_2O_3/R141b as a function of particle volume fraction (at 20ºC).

However, at high concentration of nanorefrigerant, high clustering of nanoparticles have been observed which increase abnormal and nonlinear thermal conductivity tremendously. Another reason may be nanoparticle alignments that also cause abnormal increment of thermal conductivity (Zhu et al., 2006). The experimental values for this study were found to be higher than all other models such as: Leong et al. (2006) [Equation 2.14], Maxwell (1891) [Equation 2.1], Yu and Choi (2003) [Equation 2.7], and Koo and Kleinstreuer (2005) [Equation 2.13]. The mean deviation of this experimental value was 28 % and 34 % with Leong et al. (2006) and Maxwell (1891), respectively. Most of these developed models depended on water based suspensions. Peng et al. (2009a) have used Hamilton & Crosser model (1962) [Equation 2.2] to determine the thermal conductivity of CuO/R113 nanorefrigerants. Jiang et al. (2009a) measured the thermal conductivity of CNT/R113 nanorefrigerants. The authors showed that, the mean deviation of their experimental value were 15.1 % and 26.9 % with Yu & Choi (2003) and Hamilton & Crosser model (1962), respectively. However, it can be concluded that the thermal conductivity of nanorefrigerant increases with the intensification of particle volume fraction.

The experimental values of this present study were compared with some other experimental works about thermal conductivity of nanorefrigerants. Figure 4.7 shows the thermal conductivity enhancement ratio for 1 volume concentration (%) of nanorefrigerants for different nanoparticles with two base refrigerants. The increment rates varied with one another. The highest thermal conductivity increment was 204 % for No. 2 CNT-R113 nanorefrigerants (Jiang et al., 2009b). The thermal conductivity intensification for the present study was 141 % which was less than that of No. 2 CNT-R113 nanorefrigerants. These values were the relative values compared with the base

fluids thermal conductivity. Thermal conductivity of R113 and R141b at 30°C are 0.067223 and 0.089447 W/(m.K), respectively (Lemmon et al., 2002). The thermal conductivity of CNT and Al_2O_3 is about 3000 and 40 W/(m.K), respectively. Furthermore, the thermal conductivity of the nanofluids or nanorefrigerants depends on both the nanoparticles' and fluid's self-thermal conductivity. Therefore, the thermal conductivity of CNT's nanorefrigerants was higher than other nanorefrigerants and thermal conductivity of Al_2O_3/R141b was higher than Al_2O_3/R113 nanorefrigerants.

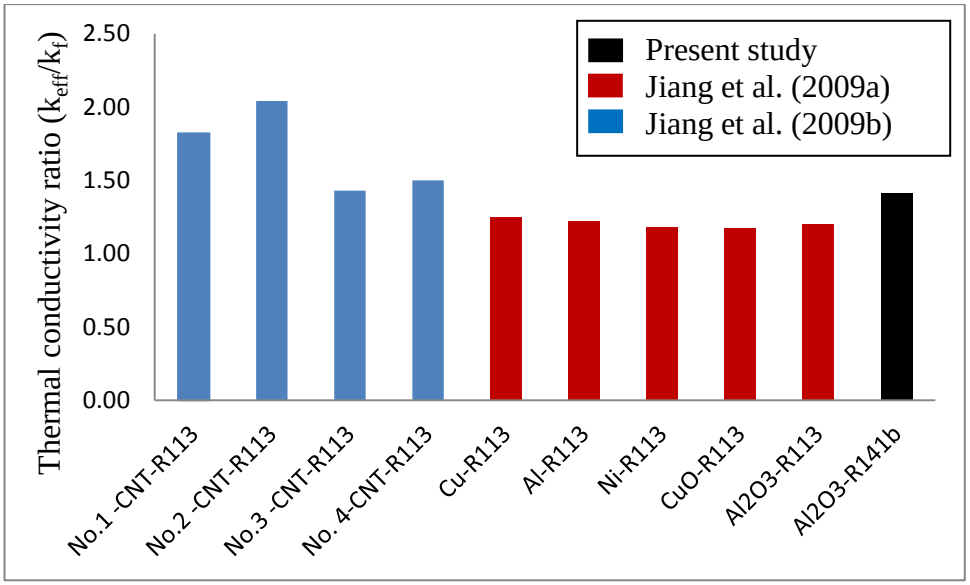

Figure 4.7: Comparison of thermal conductivity ratio of 1 volume concentration (%) of nanorefrigerants with other experimental study.

The effects of temperatures on the thermal conductivity of nanorefrigerant were investigated by changing the temperatures from 2 to 20ºC. Figure 4.8 shows the thermal conductivity enhancement of nanorefrigerants at a temperature of 2 to 20ºC for 0.5 to 3.0 volume concentration (%) of nanoparticles. At 2ºC temperature and 0.5 particle volume concentration (%), the lowest observed thermal conductivity was 1.083 times greater than that of base fluid. The highest thermal conductivity was 2.287 times greater than base fluid at 20ºC and 3 particle volume fraction (%). The figure shows that

the thermal conductivity of nanorefrigerant is proportional to temperature. High nanorefrigerant temperature intensifies the Brownian motion of nanoparticles. With intensified Brownian motion, the contribution of micro convection in heat transport can also be increased. It is evidently shown that the thermal conductivity of nanorefrigerant can be enhanced by increasing the temperature.

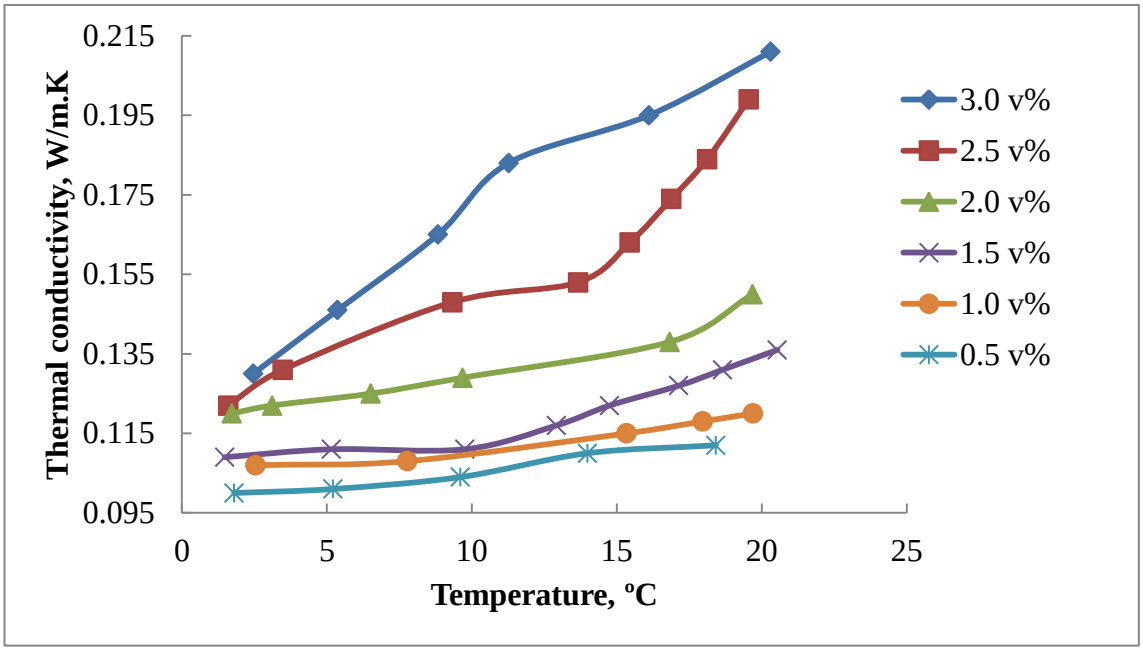

Figure 4.8: Thermal conductivity of Al_2O_3/R141b enhances accordingly with the increase of temperature.

4.3.2 Viscosity of nanorefrigerants

The viscosities of 1 volume concentration (%) of Al_2O_3/R141b nanorefrigerant for different speed of spindle are presented in Figure 4.9. It shows that, the viscosity decreases with the increase of spindle speed. The spindle speed is directly related to shear rate. Therefore, Al_2O_3/R141b nanorefrigerant is a non-Newtonian fluid.

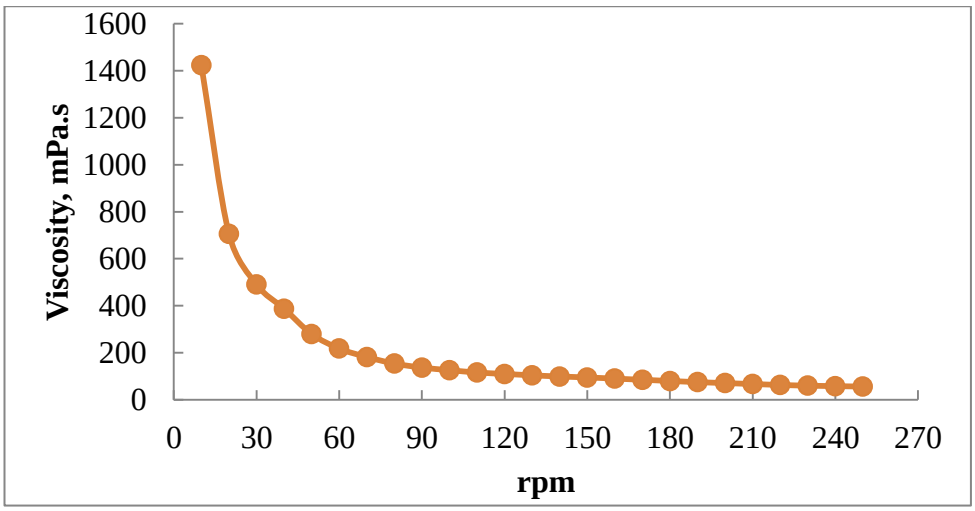

Figure 4.9: Viscosity of 1 volume concentration (%) of Al_2O_3/R141b decreases with the increase of rpm.

Viscosity of Al_2O_3/R141b nanorefrigerants for 0.5 to 2.0 of particle volume fractions at 20ºC has been plotted in Figure 4.10. Figure shows that, viscosity of nanorefrigerants increases with the increase of volume concentrations. The most widely used Brinkman model (1952) to calculate the particles suspension viscosity was compared with the measured values for different nanoparticle concentrations at 20ºC. Peng et al. (2009a) suggested Brinkman model (1952) to determine the viscosity of nanorefrigerants. Abedian and Kachanov (2010) proved that the model is better than Einstein model (1906) when high particle volume fraction is considered. However, in this experiment the measured viscosity was so high compared with this model. This model was developed for generalized suspensions viscosity. Moreover, there are many reasons for viscosity enhancement; one of which may be the large agglomeration of particles.

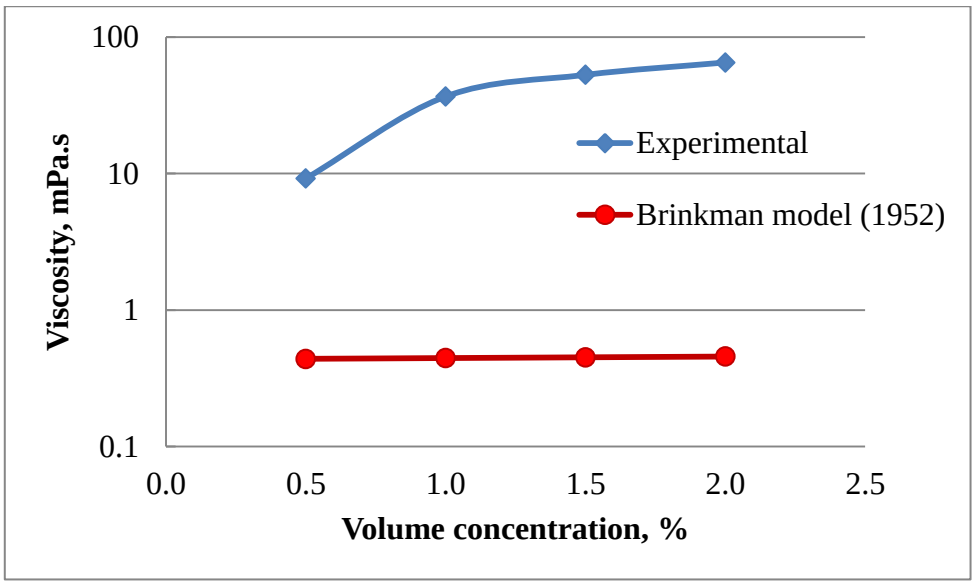

Figure 4.10: Viscosity of Al_2O_3/R141b increases with the increase of particle volume fractions (at 20ºC).

Figure 4.11 shows the effect of temperature over viscosity of nanorefrigerants. Normally viscosity of nanofluid deteriorates with the rise of temperature. The same trend for decrease of viscosity with the increase of temperature were found by some other researchers (Kulkarni et al., 2006; Namburu et al., 2007a). High nanorefrigerant temperature increases the Brownian motion of nanoparticles and reduces the viscosity of nanorefrigerant. The highest viscosity observed was 214 times greater than base fluid for 5ºC and 2 volume concentration (%) of particles. Tseng and Lin (2003) found a higher relative viscosity compared to that in this experimental value. They observed that viscosity increased up to 1200 times more than the base fluid for 12 volume concentration (%) of TiO_2 with water.

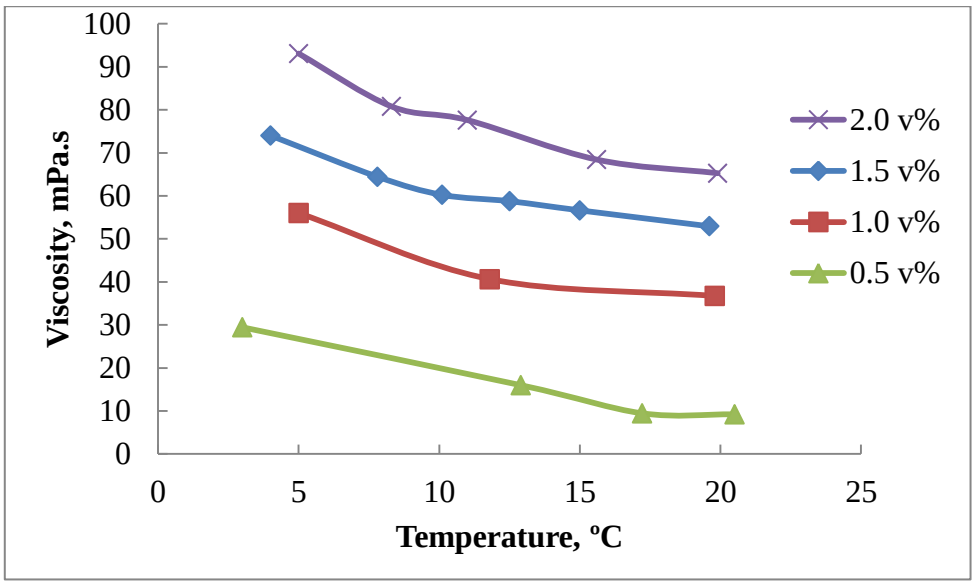

Figure 4.11: Viscosity of Al_2O_3/R141b decreases with the increase of temperature.

4.3.3 Density of nanorefrigerants

Figure 4.12 shows the measured density of Al_2O_3/R141b nanorefrigerants for 0 to 0.4 volume concentration (%) of Al_2O_3/R141b nanorefrigerant at 20ºC temperature. From the Figure 4.12, it is clear that, density increases with increase of volume concentrations. The increment trend was almost linear. Pastoriza-Gallego et al. (2011) found the same trend as density rises with the intensification of particle concentration for CuO/water nanofluid. Some other experimental results with other base fluid showed the same trend. Wasp et al. (1977) and Pak and Cho (1998) models were used to compare the obtained experimental data. Figure shows that the experimental values of this study are between the ranges of two other models. Where, the values of Pak and Cho model is higher than the experimental value and the value of Wasp model is lower than the experimental value. The Pak and Cho model was derived for water based nanofluids and the Wasp model was proposed for metal-lubricant mixture.

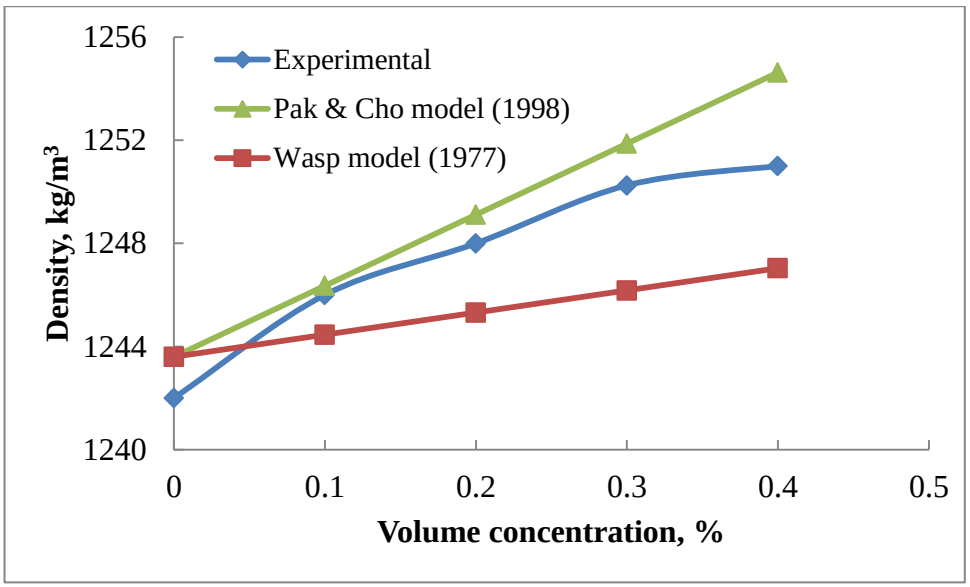

Figure 4.12: Density of Al_2O_3/R141b increases with the increase of particle volume fractions (at 20ºC).

Figure 4.13 shows the density of Al_2O_3/R141b nanorefrigerants at 5 to 20ºC with 0 to 0.4 volume concentrations (%) of nanoparticles. Figure shows that, density of nanorefrigerant deteriorates with the increase of temperature. Kedzierski (2009) found the same trend as density of suspensions decreases with the rise of temperature for CuO/lubricant. It was observed that the decrease trend was slower up to 15ºC and after 15ºC density decreased rapidly.

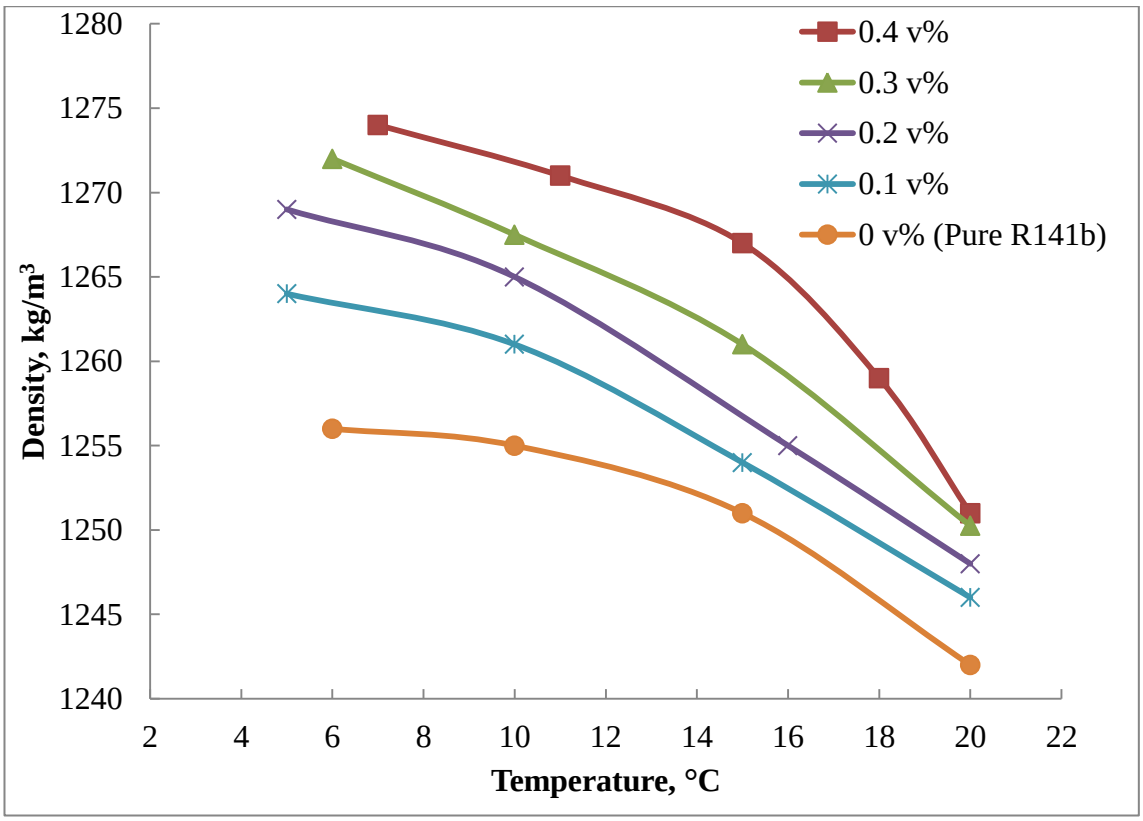

Figure 4.13: Density of nanorefrigerants at different temperature with different volume concentrations.

4.4 Migration properties of nanorefrigerants

After recording the weights, the effect of various parameters on the migration were interpreted in this section. Influence of heat flux, initial liquid level height, size of boiling vessel, insulation, nanoparticle type, particle size and finally the lubricating oil will be presented and discussed in this section.

4.4.1 Influence of heat flux on migration

Figure 4.14 shows the relationship between migrated mass of nanoparticles and the initial amount of nanoparticles for different heat fluxes. Figure shows that, migration of nanoparticles increases with the increase of initial nanoparticle mass fraction and for higher heat flux, migration of nanoparticles also increases. Besides, there is a strong relationship between migration of nanoparticles and heat flux variations. Increase in the amount of nanoparticles near the wall leads to the augmentation of superheat at a certain

heat flux. Consequently when there are more particles in the vicinity of the heated surface, there is more heat transfer to the fluid. On the other hand, existence of nanoparticles affects the bubble dynamics as well as the frequency in which bubbles depart from the surface. The bubbles are formed in larger volumes during boiling of nanofluids. Due to this phenomenon more particles would be attached to the bubbles and consequently more migration would occur. With the enhancement of heat flux the bubble departure frequency increases and as a result more volumetric bubbles would depart along with higher amount of nanoparticles. The stirring effects of bubbles might also be effective. When the speed of departure increases, the particles disperse more under the influence of buoyancy and bubble movements.

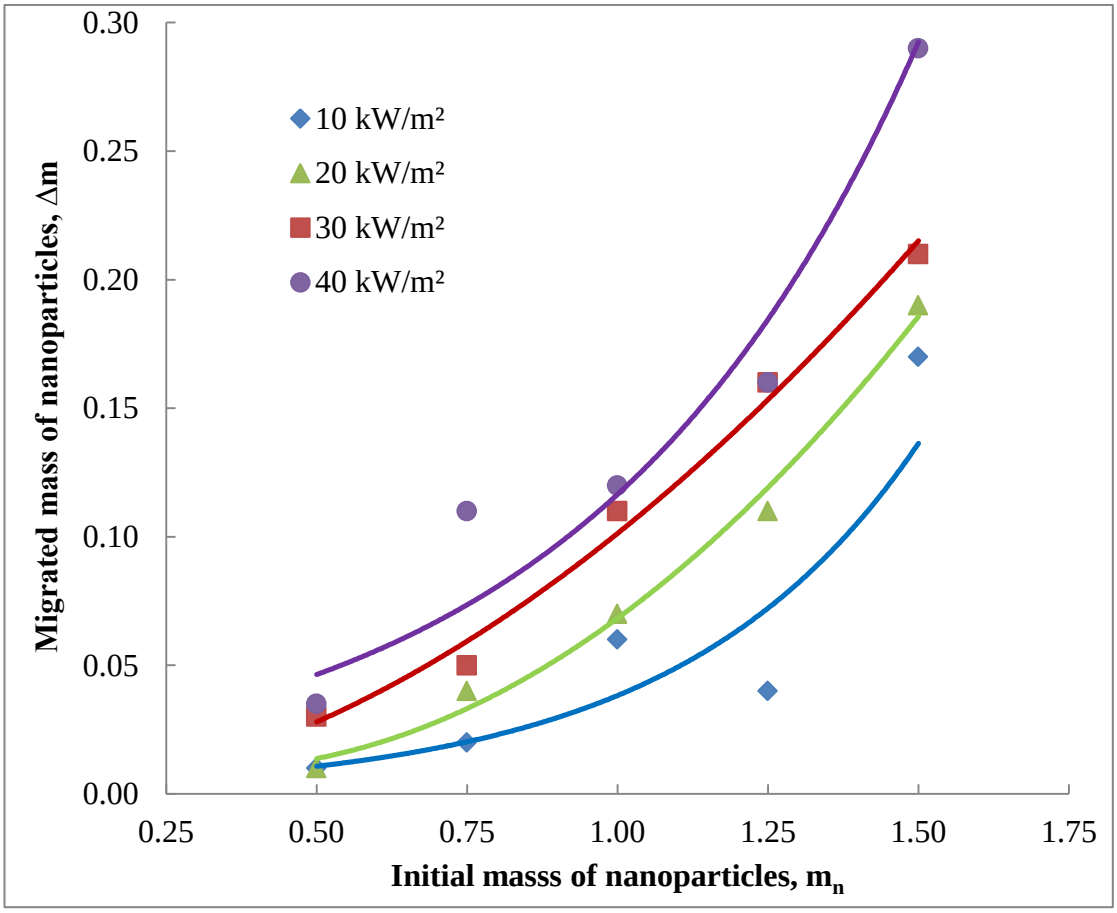

Figure 4.14: Influence of heat flux on migration of nanoparticles.

4.4.2 Influence of initial liquid level height on migration

Figure 4.15 shows the relationship between migrated nanoparticles with initial mass fraction for two different initial liquid level heights of R141b refrigerant. From the figure it is evident that, migration of nanoparticle is more for the lower liquid level of R141b refrigerant. This is because when liquid level is low for the same nanoparticle mass fraction, it takes less time to fully evaporate the refrigerants. Therefore, the nanoparticles get less time to become agglomerated and sediment.

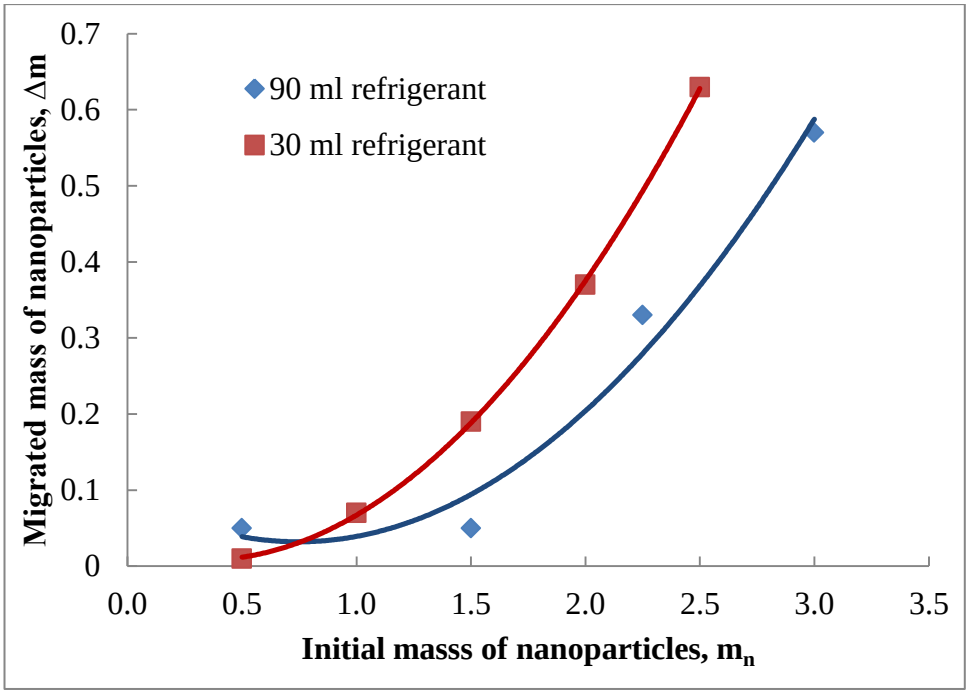

Figure 4.15: Influence of initial liquid level height on migration of nanoparticles.

4.4.3 Influence of size of boiling vessel on migration

Figure 4.16 shows the influence of size of boiling vessel on migration of nanoparticles. This figure shows that more migration of nanoparticles happens when the boiling vessel is smaller. For example, for the initial weight of 2 grams of nanoparticles, a migration mass of about 0.38 grams is observed for the 250 ml beaker compared to a value of 0.57 grams for the 100 ml beaker. This can be explained by the fact that when the

characteristic size of the heater surface increases the enhancement in critical heat flux would be reduced. The increase of boiling heat transfer for nanofluids is more pronounced for smaller heaters. This was also suggested by Haramura and Kato (1983) in their experiment. Hence, increasing the heated surface area will reduce the migration of particles for the same value of initial particle mass. It is noteworthy that to maintain the same liquid levels for two containers, more volume of refrigerant was contained in the bigger beaker. This in turn added to the evaporation time of all the mixture. More time during the boiling yielded more chance for the particles to agglomerate.

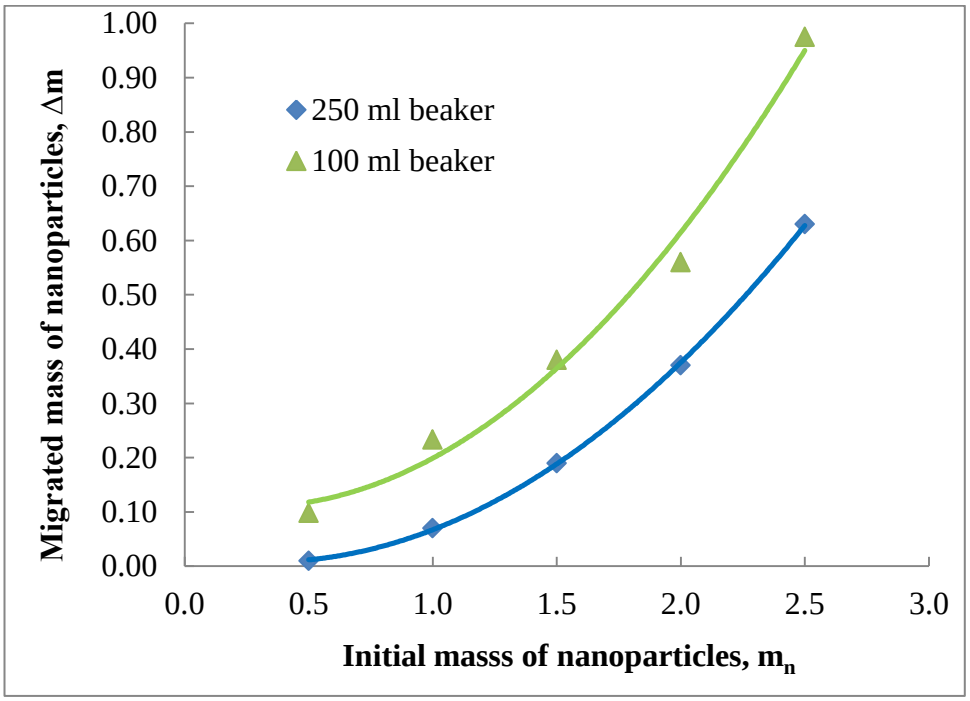

Figure 4.16: Influence of size of boiling vessel on migration of nanoparticles.

4.4.4 Influence of insulation of boiling vessel on migration

The wall can be considered as non-conducting as heat dissipation occurs mostly on the bottom of the beaker. Figure 4.17 shows the influence of insulation of boiling vessel on migration. From the figure it is clear that, when the beaker is insulated migration of nanoparticle would be more. This is because, for the insulation of the boiling vessel

there is less heat loss. Accordingly, there will be a higher wall superheat and more active nucleation site throughout the surface. With the increase in the number of nucleation sites more bubbles would be generated and consequently more particles would migrate.

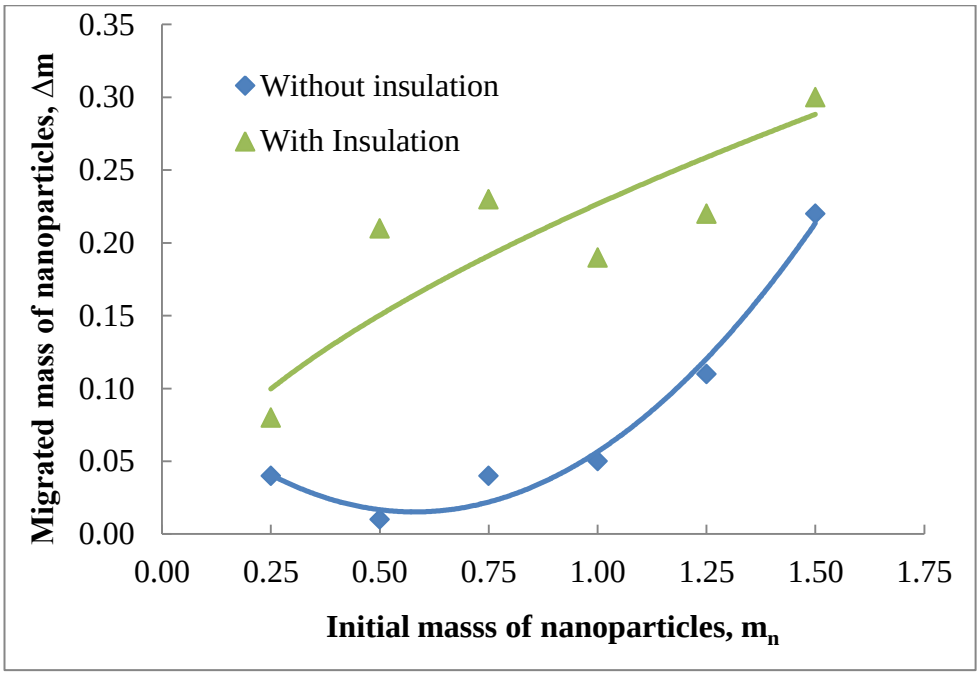

Figure 4.17: Influence of insulation of boiling vessel on migration of nanoparticles.

4.4.5 Influence of nanoparticle type on migration

Figure 4.18 shows the relationship between migrations of nanoparticles with initial mass fraction of nanoparticles for two different types of nanoparticles. Figure shows that migration of nanoparticle is highest for TiO_2 nanoparticle and migration of nanoparticle is lowest for Al_2O_3 nanoparticles. This implies the impact of self-density of various types of nanoparticles. While Al_2O_3 nanoparticles have density of 4000 kg/m^3 and TiO_2 nanoparticles have density of 4260 kg/m^3. The more density means it will sediment faster for it's self-weight. That has happened here for TiO_2 nanoparticles.

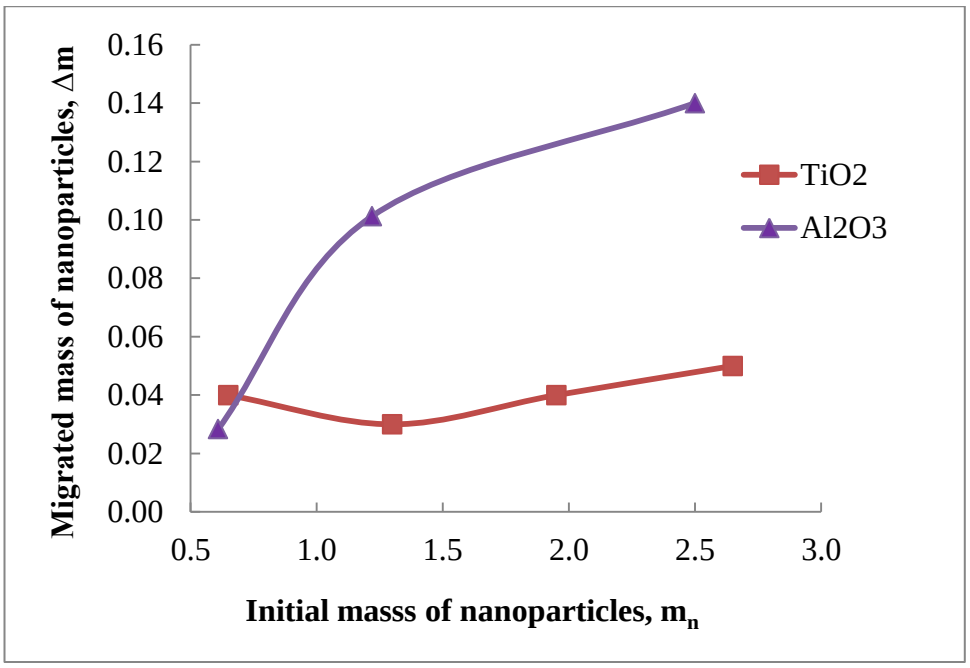

Figure 4.18: Influence of nanoparticles types on migration of nanoparticles.

4.4.6 Influence of nanoparticles sizes on migration

Figure 4.19 shows the effect of nanoparticle size for two different sizes of TiO_2 nanoparticles. Migration of nanoparticles were more for TiO_2 nanoparticles with 40 nm size compared with migration of 21 nm size of TiO_2 nanoparticles. The probable cause for this occurrence was the bubbles produced during the pool boiling that create the migration of nanoparticles. Particles bubbles depend on its capture that are related to the mechanisms of Brownian diffusion, interception, gravity and inertia impact (Edzwald et al., 1991). The intensification of external diameter is the reason of increased Stokes diameter of nanoparticles (Henn, 1996). Peng et al. (2011d) observed the same phenomenon on their experimental study. However, Peng et al. (2011b) found that, migration ratio increases with the decrease of nanoparticles size.

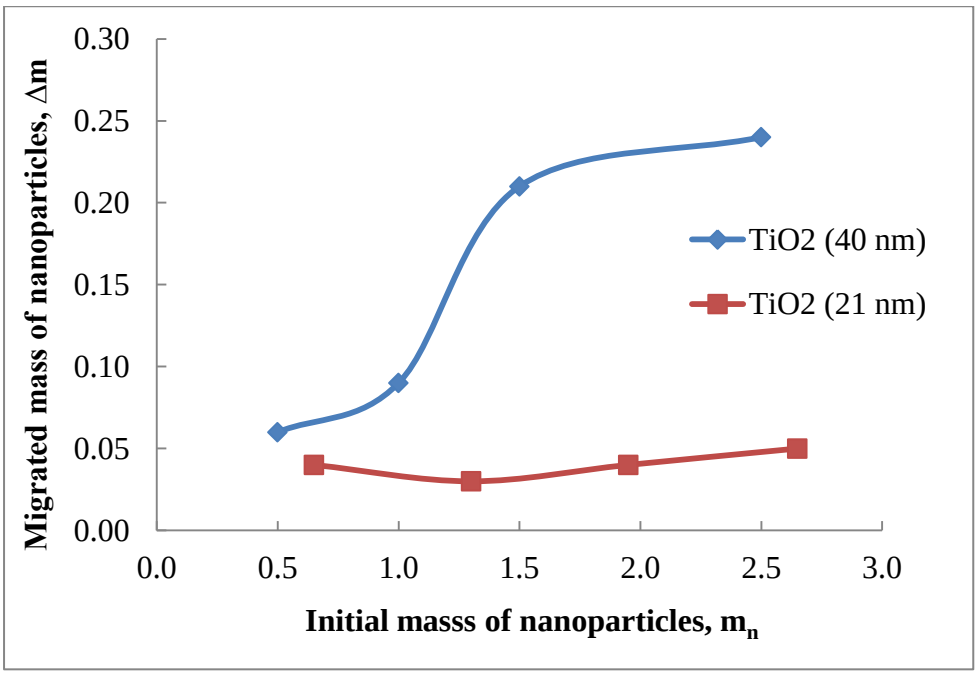

Figure 4.19: Influence of nanoparticles sizes on migration of nanoparticles.

4.4.7 Influence of mass fractions of lubricating oil on migration

Figure 4.20 shows the relationship between migrations of nanoparticles with initial mass fraction of nanoparticles for three different types of compositions. Figure shows that, nanorefrigerants without oil have less migration of nanoparticles. However, nanorefrigerants with 10 volume concentration (%) of oil have more migration of nanoparticles and nanorefrigerants with 5 volume concentration (%) of oil have less migration of nanoparticles than that with 10 volume concentration (%) of nanorefrigerant-oil but still more than the nanorefrigerant without oil. A decreasing trend for the migration is observed for 10 volume concentration (%) of nanorefrigerant-oil while it increases for 5 volume concentration (%) of nanorefrigerant-oil as well as for nanorefrigerants without oil. For the 2.5 grams of initial nanoparticle mass, the migration of nanoparticle is almost the same for 10 volume concentration (%) of nanorefrigerant-oil and 5 volume concentration (%) of nanorefrigerant-oil.

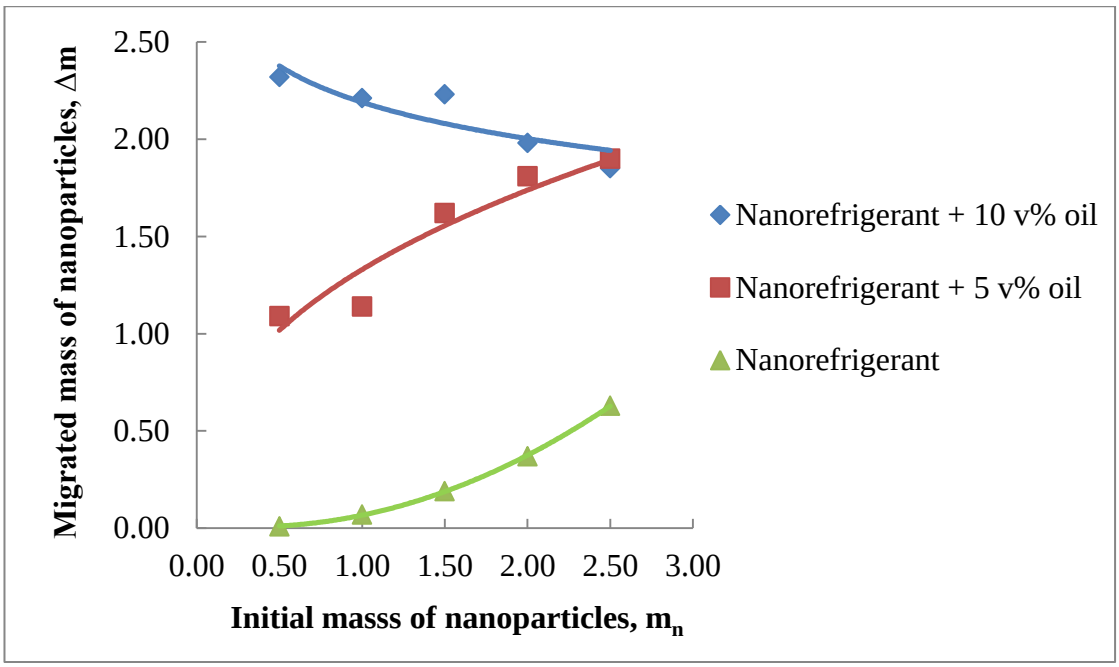

Figure 4.20: Influence of mass fractions of lubricating oil on migration of nanoparticles.

CHAPTER 5: CONCLUSIONS AND RECOMMENDATIONS

5.1 Introduction

This chapter is divided into two sections. The first section starts with some concluding remarks and the second section is about some recommendations for future work.

5.2 Conclusions

From the comparative analysis and evaluation, the conclusions can be drawn as followings:

- Preparation of refrigerants by ultrasonic processor is quite difficult and preparation by using mechanical shaker is an easier process. Moreover, nanofluids/nanorefrigerants prepared by mechanical shaking have good stability.

- Characterization of refrigerant based nanofluids with UV-Visible spectrophotometer and Zeta potential analyzer are very difficult. Sediment photograph capturing is a fundamental method to observe the sediment of suspension and it is helpful to identify the sedimentation rate.

- Like other nanofluids, thermal conductivity of the nanorefrigerants augmented with the increase of nanoparticle volume concentrations and temperatures. It increases sharply due to nanoparticle concentration compared to temperature effects.

- Al_2O_3/R141b is a non-Newtonian fluid. Volume fractions and temperature have significant effects with viscosity of nanorefrigerants. Results show that viscosity

rises with the increase of the particle volume concentrations. However, it deteriorates with the rise of temperatures.

- Like the viscosity, density of nanorefrigerants also rises with the enhancement of volume concentration. Similarly, it deteriorates with the rise of temperature.

- Migration of nanoparticles during the pool boiling of R141b refrigerant was analyzed under various situations. Different factors influence the amount of migrated mass of particles during the pool boiling of nanorefrigerants. Heat flux, insulation, initial liquid level height, initial mass of nanoparticles, nanoparticle type, and particle size as well as the vessel size can alter the amount of migration. An increase in the heat flux, initial mass and insulating the container would yield augmentation in the amount of migrated solid particles from the liquid refrigerant during boiling. Higher super heat, enhanced bubble departure frequency and the enhancement in boiling due to the smaller size of the heater are suggested to be responsible for the observations made in this experiment in terms of the migrated mass.

- From this experiment it is clear that distributions of nanoparticles have a significant effect in liquid and vapor phase of refrigerants.

5.3 Limitations of the study

Most of the refrigerants are in gaseous state at the ambient temperature and pressure. Especially, the commonly used refrigerants (e.g. R22, R410A, and R134a) evaporate at negative temperatures. Therefore it is quite difficult to mix nano powder with such refrigerants. Moreover, studies of their physical properties are also very difficult as these refrigerants could not be tested in an open environment. However, it is very difficult to do experiment in the laboratory due to several reasons:

- Some nanoparticles and the equipment to establish the experimental setup are quite expensive.
- There are not adequate funding sources for this research work.
- There are very limited experimental facilities for investigating the fundamental properties of nanorefrigerants.
- Refrigerants are not good solvents for nanoparticles to prepare nanofluids.
- Some equipment and accessories (e.g. AND Vibro Viscometer and SHIMADZU UV-Visible spectrophotometer) do not supports these types of refrigerants.

Some pictorial examples of limitation have been included in Figures 5.1 to 5.3. Figure 5.1 is the sample holder used in UV-Visible spectrophotometer, UV-1601 (made by SHIMADZU) and it is melted when filled with refrigerant R141b. Figure 5.2 (a), (b) and Figure 5.3 (a), (b) show that the internal sample holder and the external guard of the internal cup, respectively become cracked as soon as filled up with R141b refrigerants.

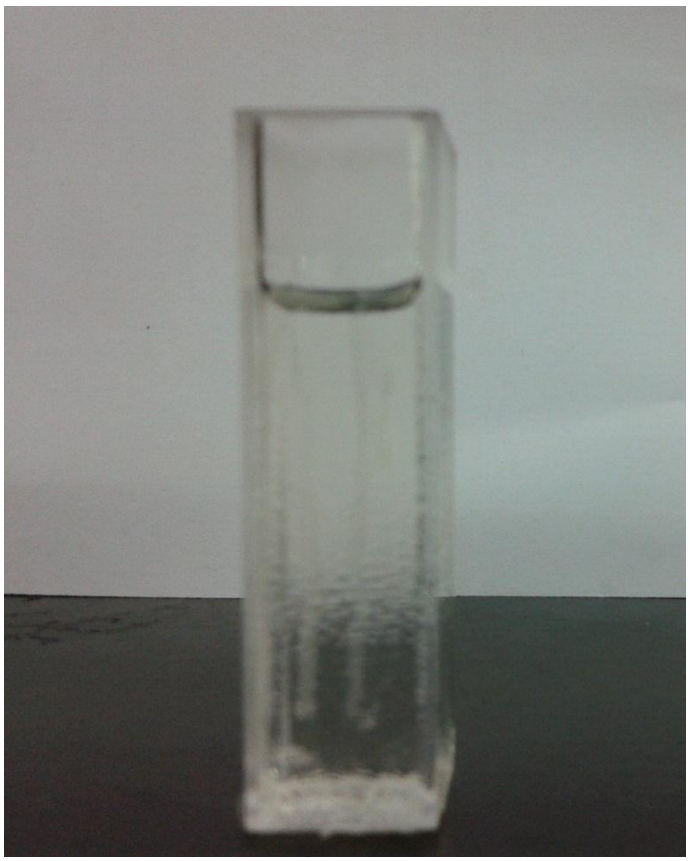

Figure 5.1: The sample holder used in UV-Visible spectrophotometer is going to be melted with R141b refrigerant.

(a)

(b)

Figure 5.2 (a), (b): The cup used to carry the sample liquid while measuring the viscosity with “AND” Vibro Viscometer is going to be cracked.

(a)

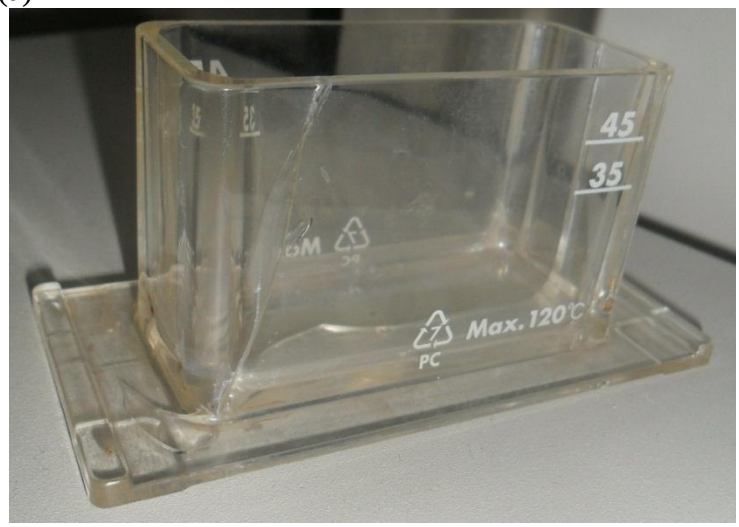

(b)

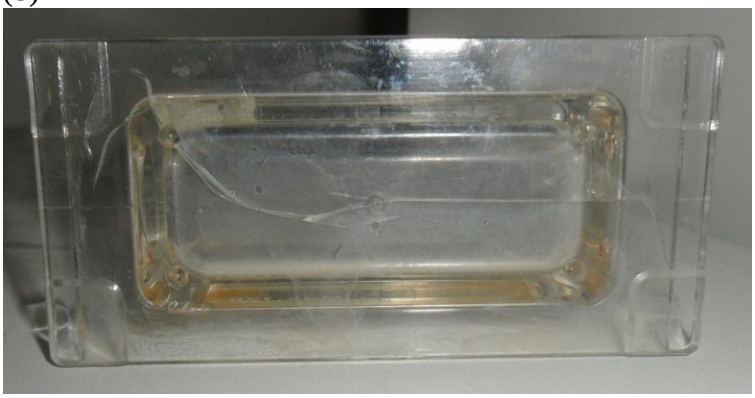

Figure 5.3 (a), (b): The external guard of the cup used to carry the sample liquid while measuring the viscosity with “AND” Vibro Viscometer is going to be cracked.

5.4 Recommendations

- More commonly used refrigerants, such as R-134a and R-410A, are in the gaseous state at room temperature and pressure. R141b is mainly used in foam insulation of transport. This refrigerant is not a good solvent and some apparatus do not support it. However, nanoparticles can be used in refrigeration to enhance heat transfer performance as well as energy performances. In most of the compressors, some refrigeration compressor oil is often used. Nanoparticles can be mixed with refrigerant oil as a good alternative solution.

- Specific heat capacity and surface tension are two important properties. These are directly related to the heat transfer performance analysis. These two parameters need to be determined experimentally for nanorefrigerants.

- Thermal conductivity increases with the enhancement of nanoparticle concentration and temperatures. However, viscosity increment simultaneously is a penalty. Viscosity is directly related to pressure drop and pumping power. An optimum quantity of nanoparticle needs to be found out considering the energy and cooling performance.

- However, an optimal particle volume fraction exists when considering thermal conductivity, viscosity, and density as well as migration properties of nanorefrigerants that need to be calculated.

APPENDIX A: SPECIFICATIONS OF SENSORS AND SPINDLES

Table A1: Specifications of the sensors of KD 2 pro thermal properties analyzer.

Sensor	No of Needle	Length, mm	Diameter, mm	Designed for (material type)	Measurement range, W/(m· K)	Accuracy
KS-1	1	60	1.3	Liquid	0.02 to 2.00	± 5% from 0.2 - 2 W/(m· K) ±0.01 W/(m· K) from 0.02 - 0.2 W/(m· K)
TR-1	1	100	2.4	Solid	0.10 to 2.00	±10% from 0.2 - 2 W/(m· K) ±0.02 W/(m· K) from 0.1 - 0.2 W/(m· K)
SH-1	2	30	1.3	Solid	0.02 to 2.00	± 5% from 0.2 - 2 W/(m· K) ±0.01 W/(m· K) from 0.02 - 0.2 W/(m· K)

Table A2: Measurement range of the spindles of Brookfield LVDV III Ultra Rheometer.

Spindle	Spindle code	Measurement range* (mPa.s)
LV-1	61	15–20,000
LV-2	62	50–100,000
LV-3	63	200–400,000
LV-4	64	1,000–2,000,000
LV-5	65	2,000–4,000,000
LV-2C		50–100,000
LV-3C		200–400,000

*This measurement range is for standard LVDV machine and for below 60 rpm.

APPENDIX B: ELEMENTAL COMPOSITION OF NANOPARTICLES BY SEM-EDAX ANALYSIS

Table B1: Elemental composition of TiO_2 (~21 nm) nanoparticles by EDAX analysis at point 1.

Element	Wt%	At%
TiL	52.29	26.80
OK	47.71	73.20
Matrix	Correction	ZAF

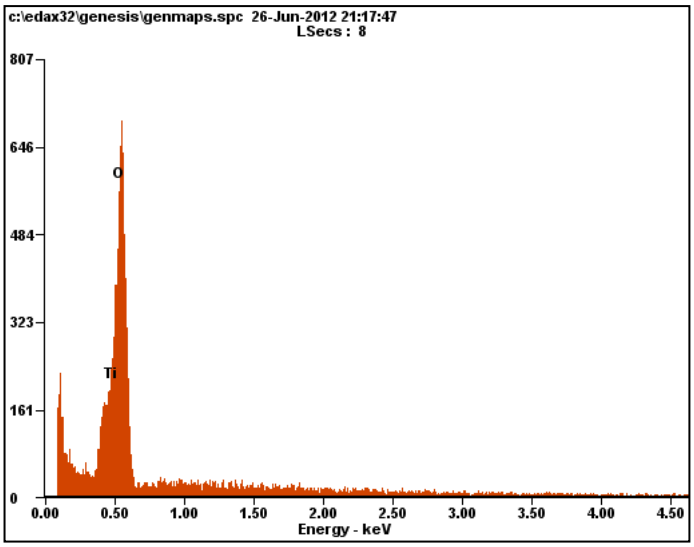

Figure B1: EDAX analysis of TiO_2 (~21 nm) nanoparticles at point 1.

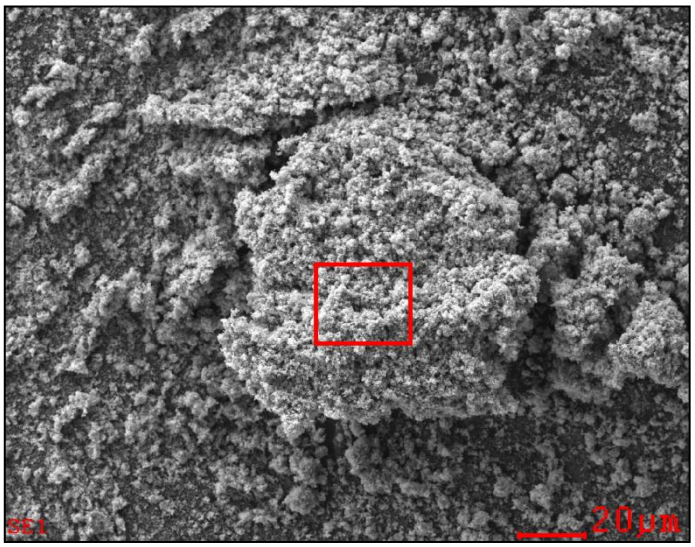

Figure B2: SEM image of TiO_2 (~21 nm) nanoparticles during EDAX analysis with the marking of point 1.

Table B2: Elemental composition of TiO_2 (~21 nm) nanoparticles by EDAX analysis at point 2.

Element	Wt%	At%
TiL	60.52	33.86
OK	39.48	66.14
Matrix	Correction	ZAF

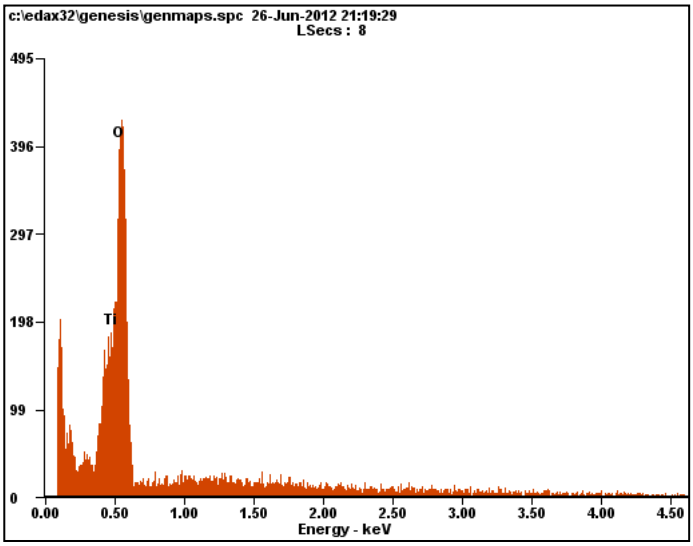

Figure B3: EDAX analysis of TiO_2 (~21 nm) nanoparticles at point 2.

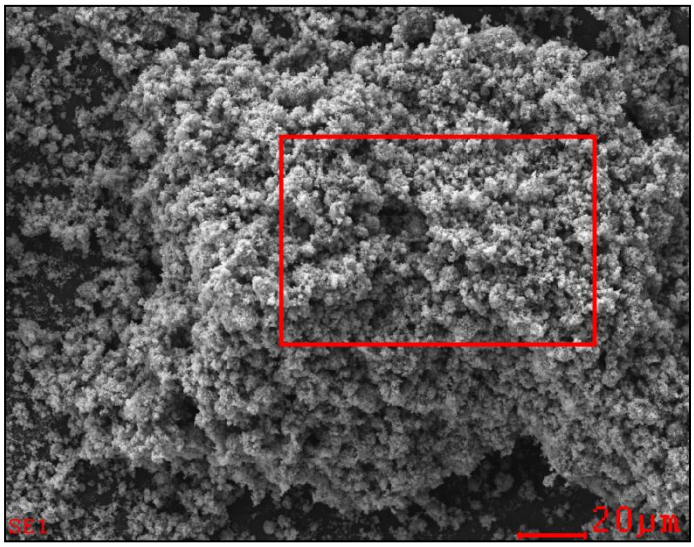

Figure B4: SEM image of TiO_2 (~21 nm) nanoparticles during EDAX analysis with the marking of point 2.

Table B3: Elemental composition of TiO_2 (40 nm) nanoparticles by EDAX analysis at point 1.

Element	Wt%	At%
TiL	53.85	28.04
OK	46.15	71.96
Matrix	Correction	ZAF

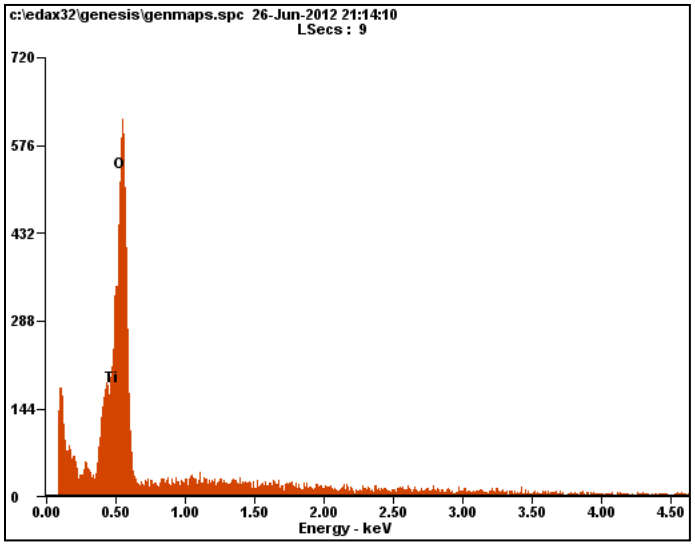

Figure B5: EDAX analysis of TiO_2 (40 nm) nanoparticles at point 1.

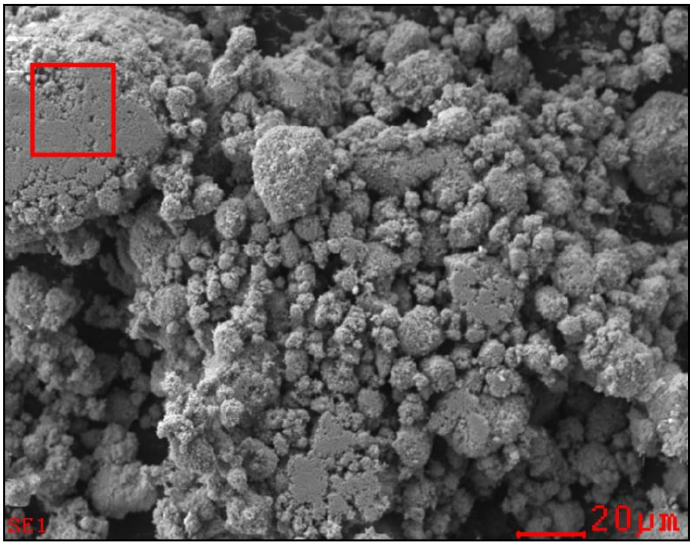

Figure B6: SEM image of TiO_2 (40 nm) nanoparticles during EDAX analysis with the marking of point 1.

Table B4: Elemental composition of TiO_2 (40 nm) nanoparticles by EDAX analysis at point 2.

Element	Wt%	At%
TiL	57.52	31.14
OK	42.48	68.86
Matrix	Correction	ZAF

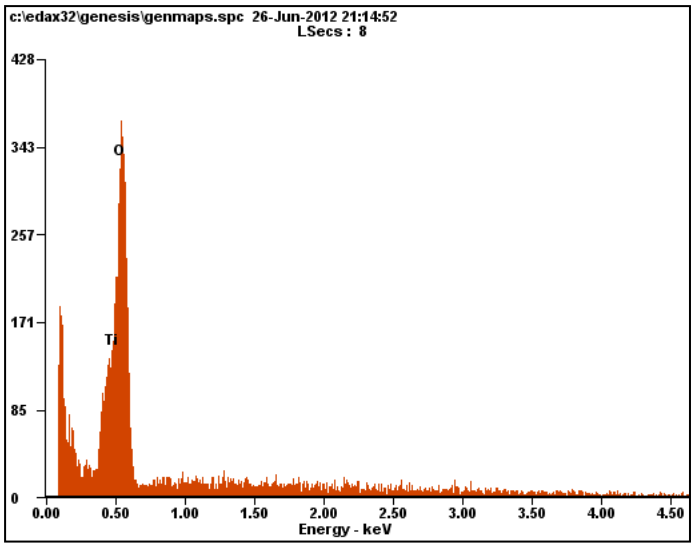

Figure B7: EDAX analysis of TiO_2 (40 nm) nanoparticles at point 2.

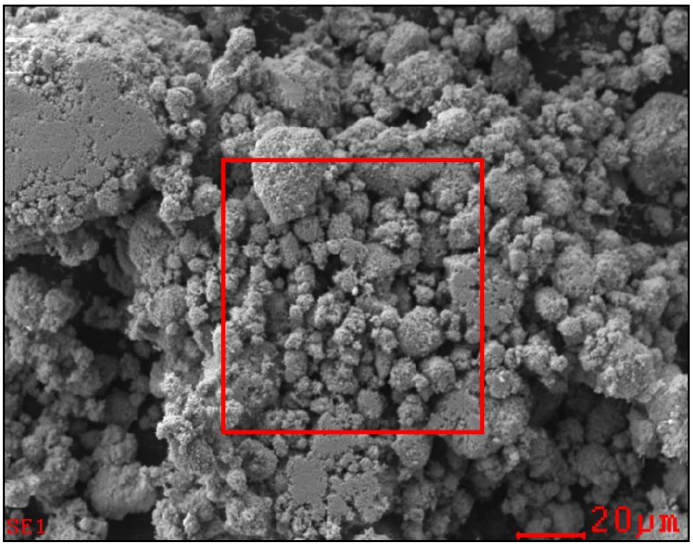

Figure B8: SEM image of TiO_2 (40 nm) nanoparticles during EDAX analysis with the marking of point 2.

Table B5: Elemental composition of Al_2O_3 (13 nm) nanoparticles by EDAX analysis at point 1.

Element	Wt%	At%
OK	44.73	57.71
AlK	55.27	42.29
Matrix	Correction	ZAF

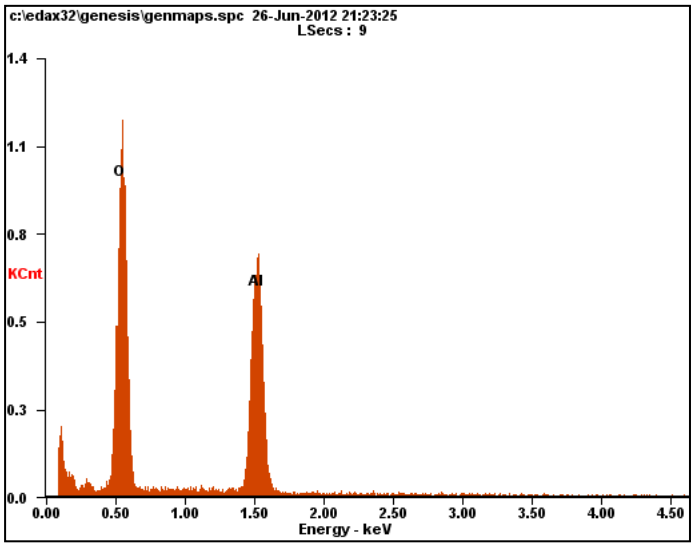

Figure B9: EDAX analysis of Al_2O_3 (13 nm) nanoparticles at point 1.

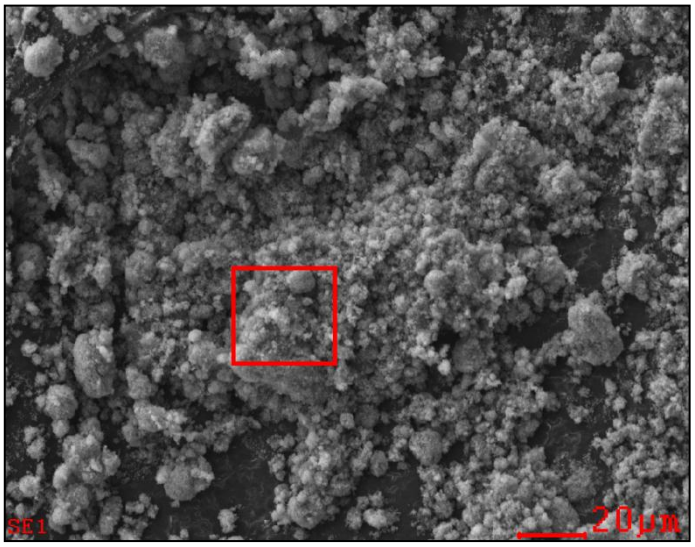

Figure B10: SEM image of Al_2O_3 (13 nm) nanoparticles during EDAX analysis with the marking of point 1.

Table B6: Elemental composition of Al_2O_3 (13 nm) nanoparticles by EDAX analysis at point 2.

Element	Wt%	At%
OK	44.72	57.71
AlK	55.28	42.29
Matrix	Correction	ZAF

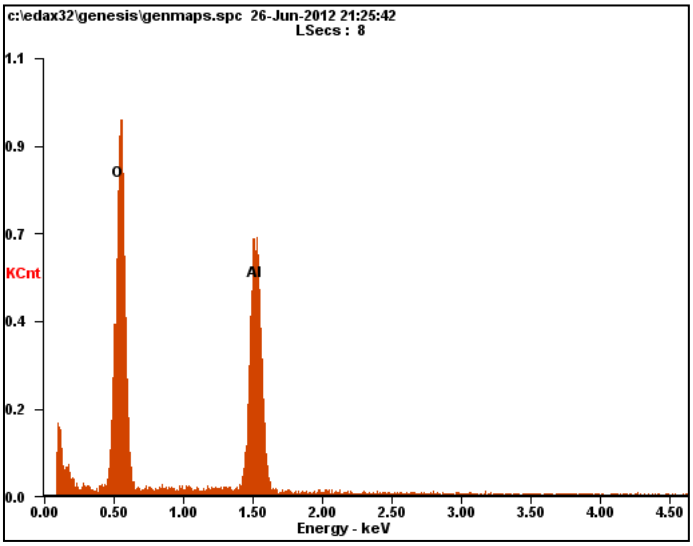

Figure B11: EDAX analysis of Al_2O_3 (13 nm) nanoparticles at point 2.

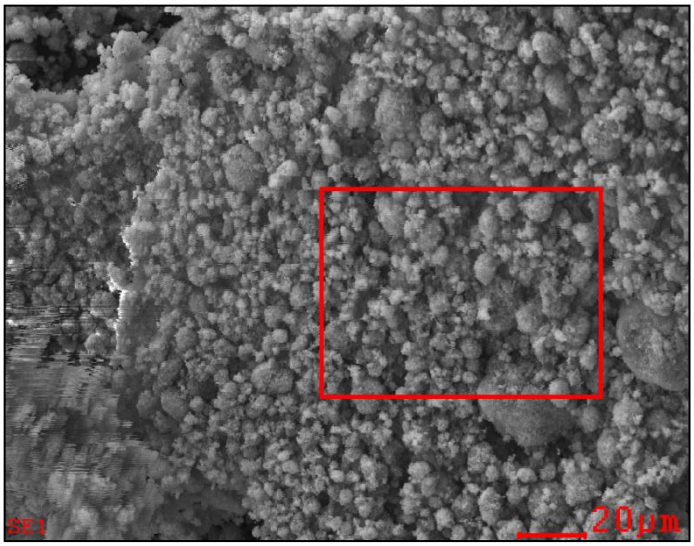

Figure B12: SEM image of Al_2O_3 (13 nm) nanoparticles during EDAX analysis with the marking of point 2.

Table B7: Elemental composition of Al_2O_3 (50 nm) nanoparticles by EDAX analysis at point 1.

Element	Wt%	At%
OK	42.42	55.40
AlK	57.58	44.60
Matrix	Correction	ZAF

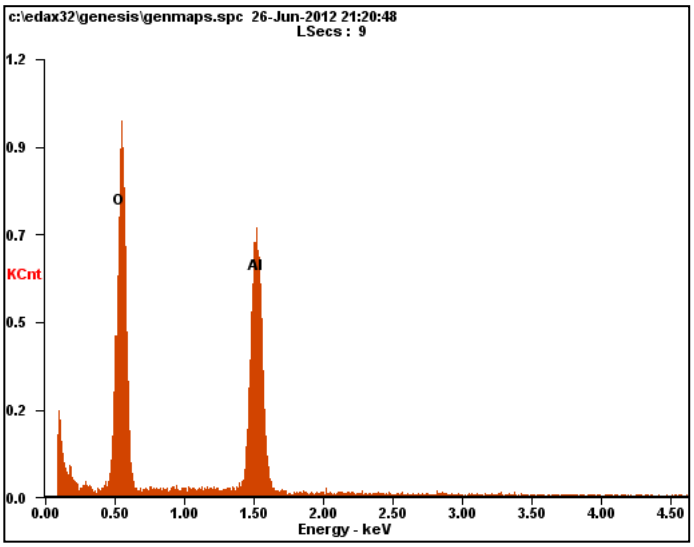

Figure B13: EDAX analysis of Al_2O_3 (50 nm) nanoparticles at point 1.

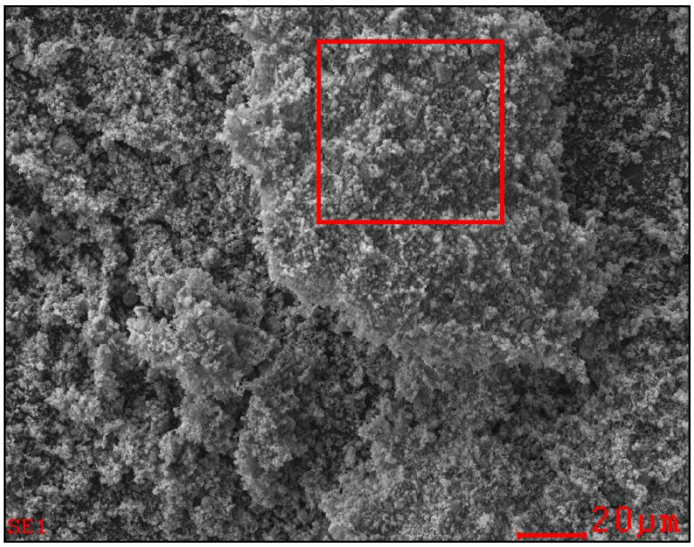

Figure B14: SEM image of Al_2O_3 (50 nm) nanoparticles during EDAX analysis with the marking of point 1.

Table B8: Elemental composition of Al_2O_3 (50 nm) nanoparticles by EDAX analysis at point 2.

Element	Wt%	At%
OK	42.96	55.95
AlK	57.04	44.05
Matrix	Correction	ZAF

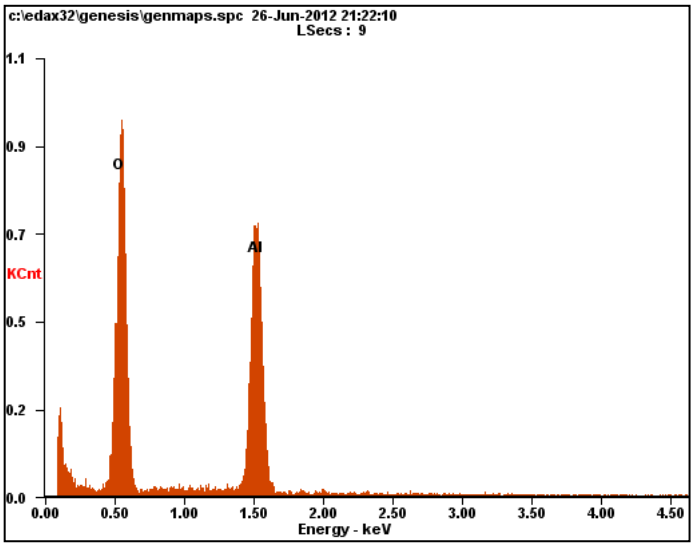

Figure B15: EDAX analysis of Al_2O_3 (50 nm) nanoparticles at point 2.

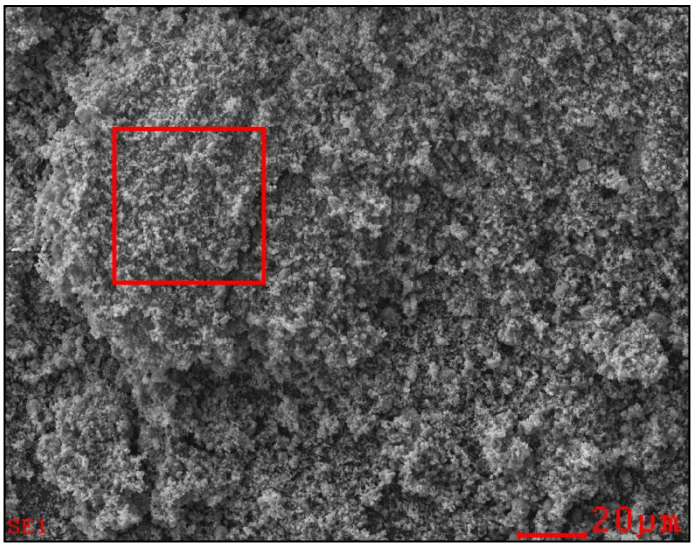

Figure B16: SEM image of Al_2O_3 (50 nm) nanoparticles during EDAX analysis with the marking of point 2.

APPENDIX C: NANOPARTICLES SIZE MEASUREMENT

Figure C1 shows the SEM image of TiO_2 (~21nm) nanoparticles. Measurements of the approximate diameter of some of the individual particle by SEM are shown in Figure C2. The elemental composition of TiO_2 (~21nm) nanoparticles by SEM-EDAX analysis is presented in Tables B1 and B2 (Appendix B).

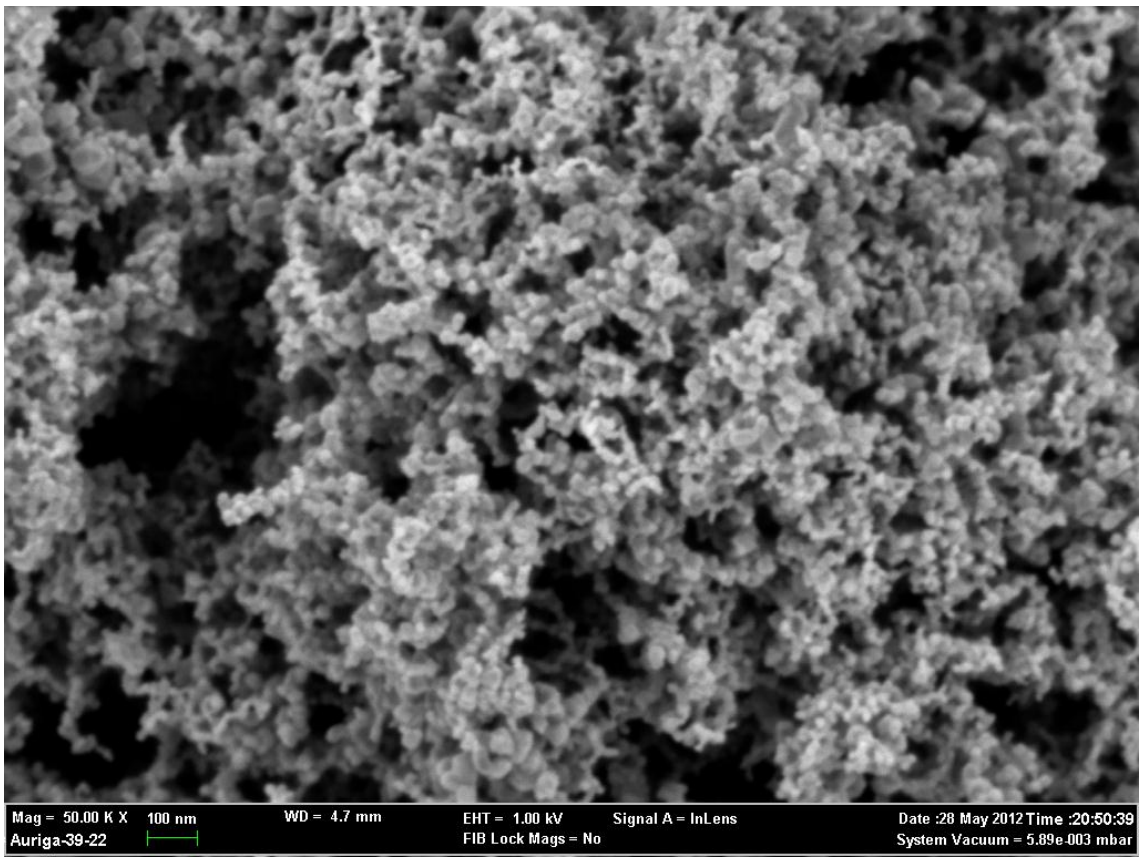

Figure C1: SEM image of TiO_2 (~21 nm) nanoparticles.

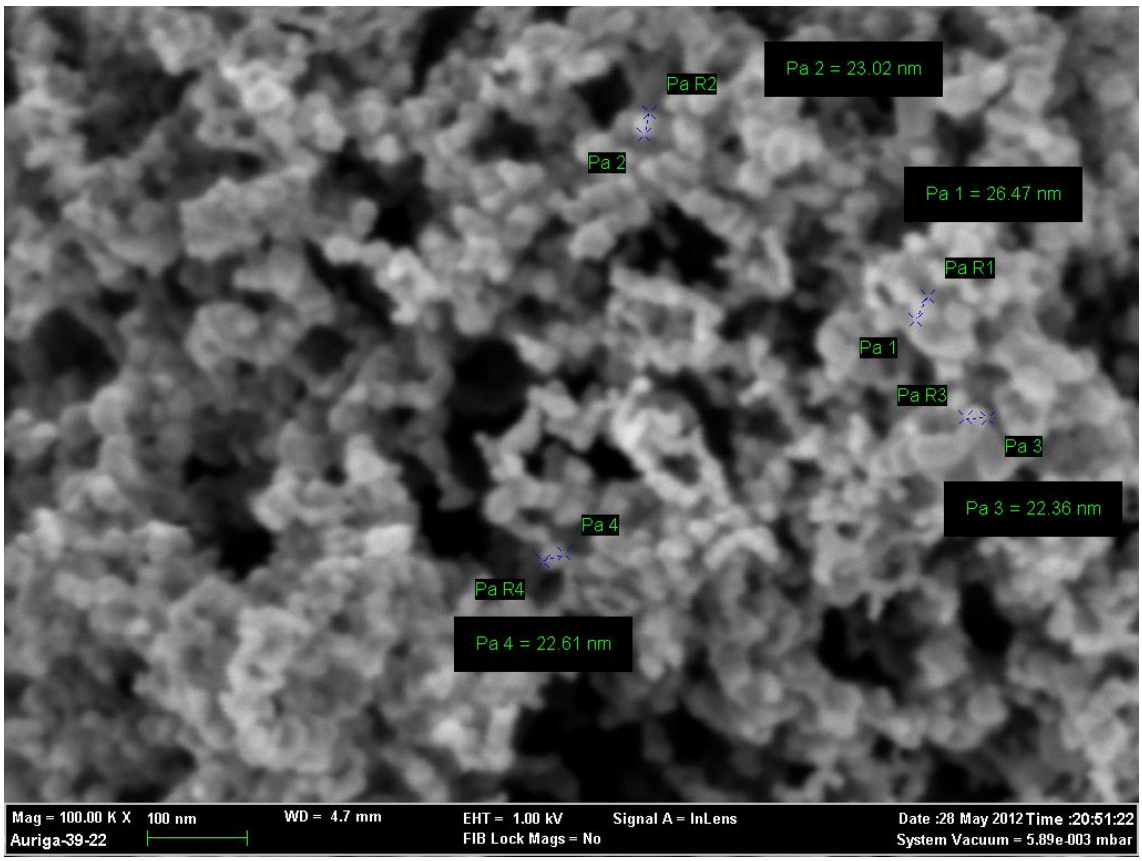

Figure C2: SEM image of TiO_2 (~21 nm) nanoparticles with the approximate measurement of some particle's diameter.

Figure C3 shows the TEM image of R141b/TiO_2 (~21nm) nanorefrigerant (with 0.5 volume concentration (%) of nanoparticles). Measurements of the approximate diameter of some of the individual particle by TEM are shown in Figure C4. From the SEM and TEM images, it was assumed that, the sizes of the particles were about 21 nm and the particle shape is almost spherical. The TEM image shows less agglomeration for this solution even after 24 hours of preparation.

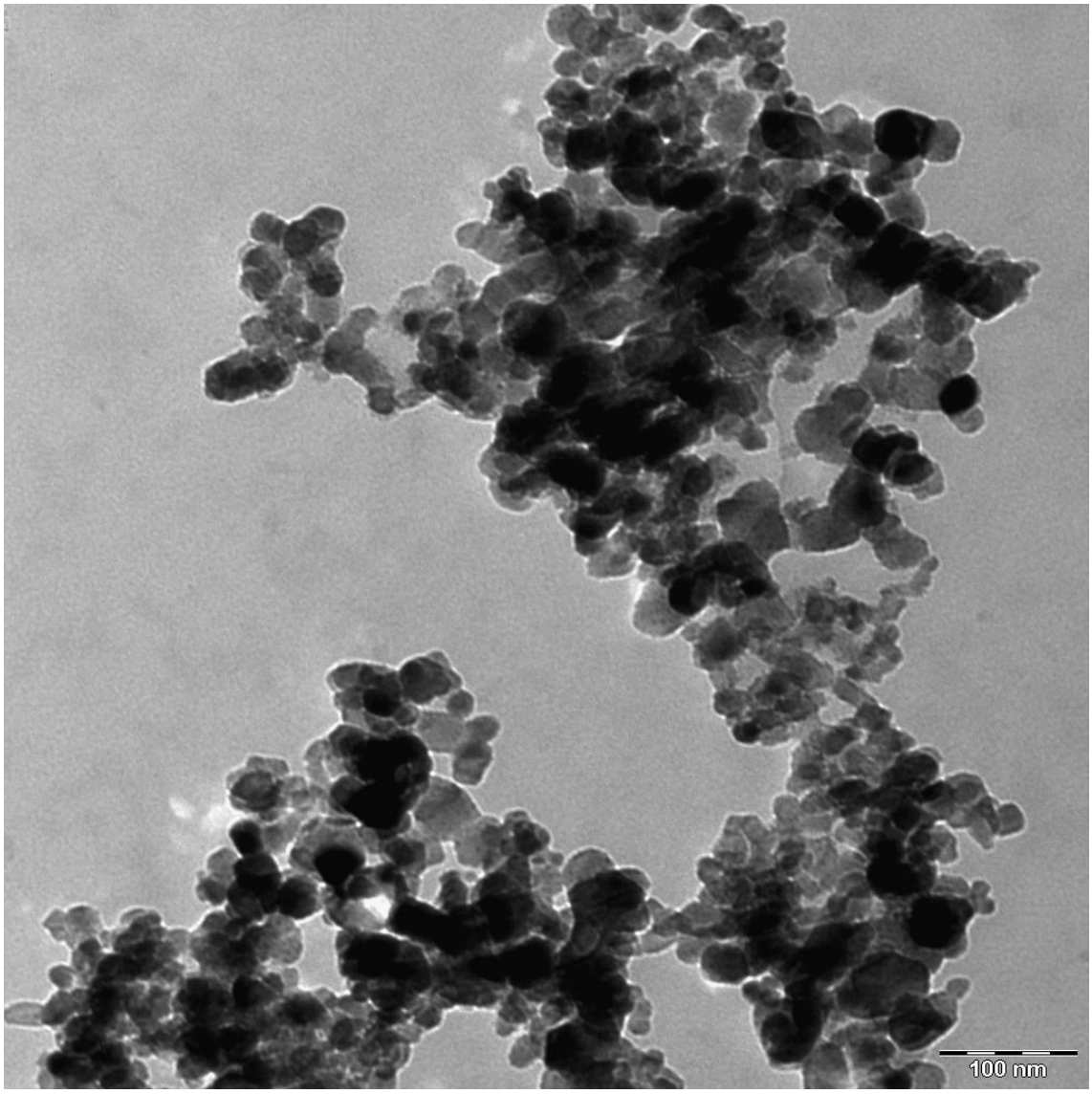

Figure C3: TEM image of R141b/TiO_2 (~21 nm) nanorefrigerants.

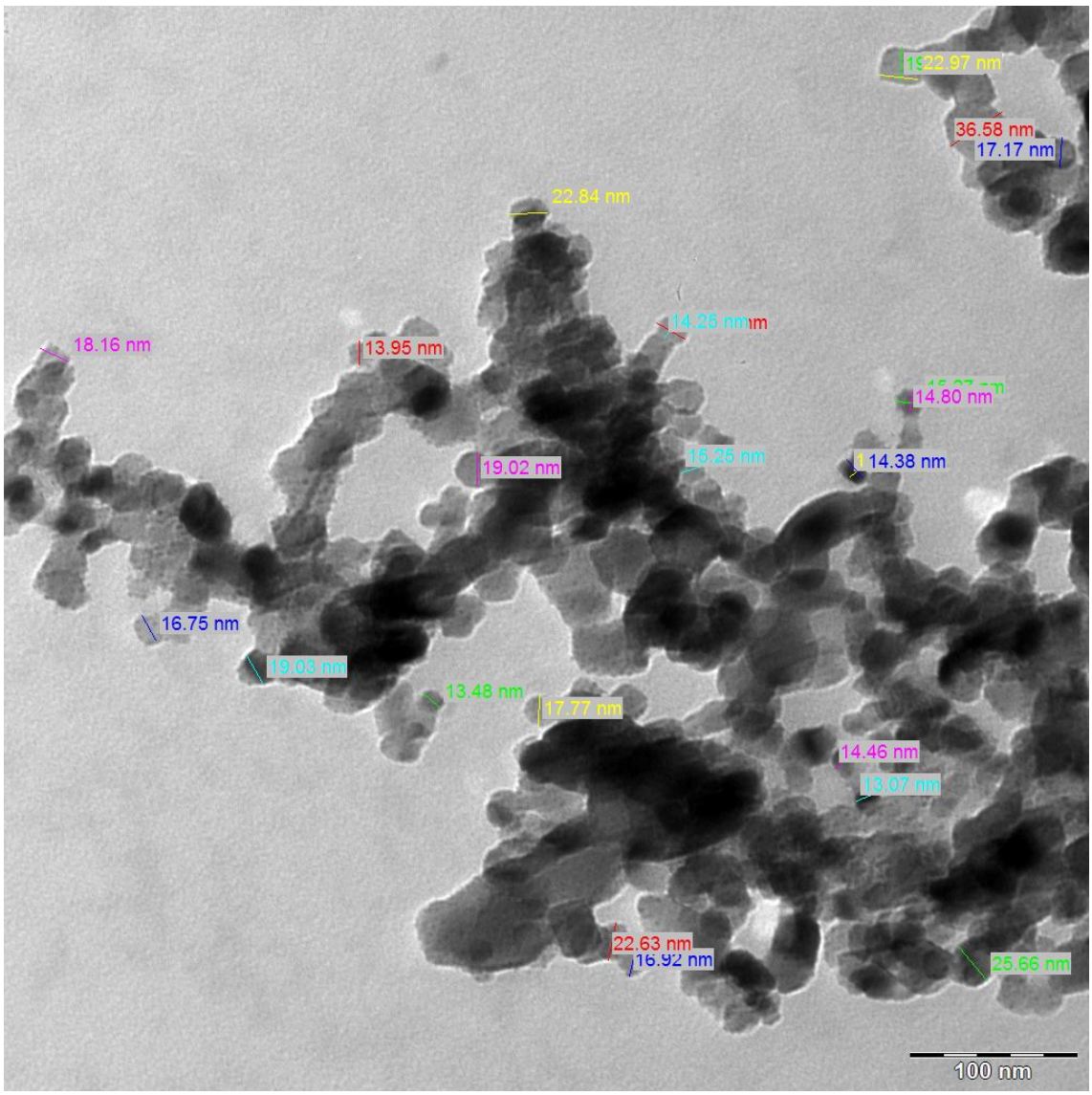

Figure C4: TEM image of R141b/TiO_2 (~21 nm) nanorefrigerants with the approximate measurement of some particle's diameter.

Figure C5 shows the SEM image of TiO_2 (40 nm) nanoparticles. Measurements of the approximate diameter of some of the individual particle by SEM are shown in Figure C6. The elemental composition of TiO_2 (40 nm) nanoparticles by SEM-EDAX analysis is presented in Tables B3 and B4 (Appendix B).

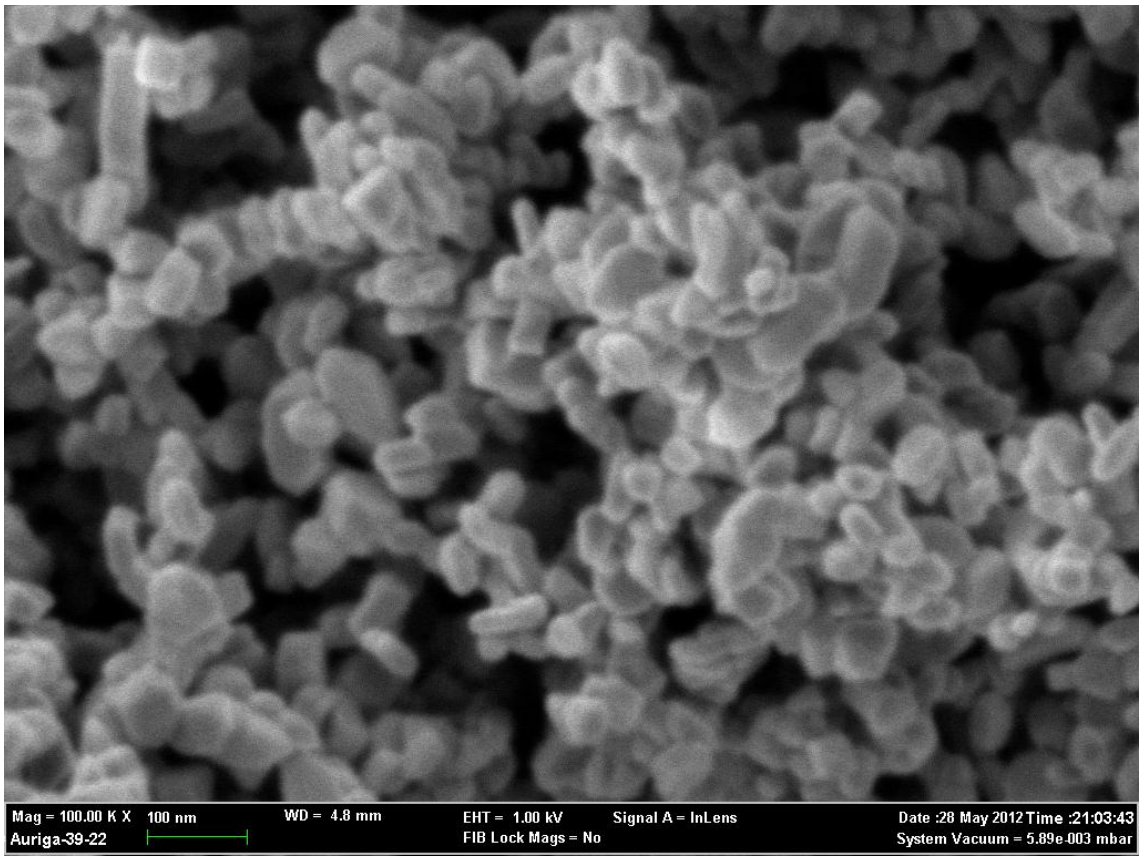

Figure C5: SEM image of TiO_2 (40 nm) nanoparticles.

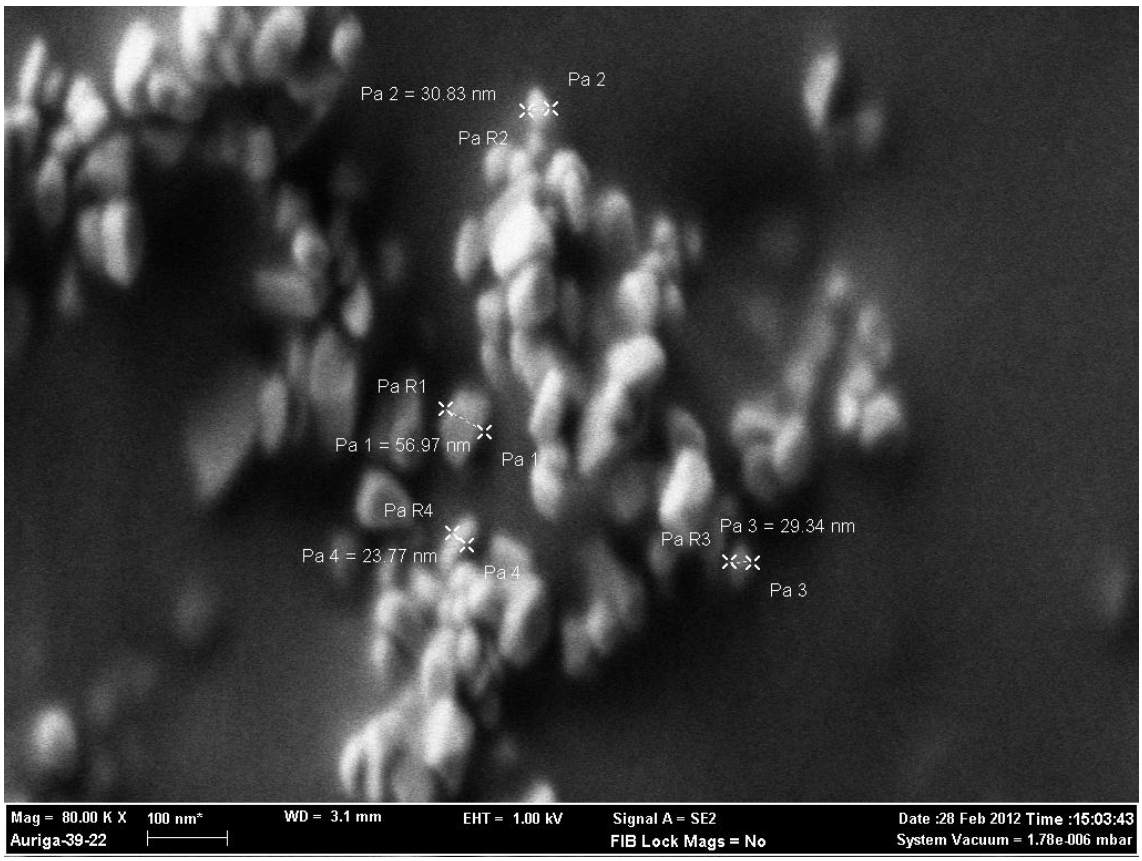

Figure C6: SEM image of TiO_2 (40 nm) nanoparticles with the approximate measurement of some particle's diameter.

Figure C7 shows the TEM image of R141b/TiO_2 (40 nm) nanorefrigerants (with 0.5 volume concentration (%) of nanoparticles). Measurements of the approximate diameter of some of the individual particle by TEM are shown in Figure C8. From the SEM and TEM images, it was assumed that, the sizes of the particles were about 40 nm and the particle shape is irregular. However, images show that, the size varies from 25 nm to 70 nm. The TEM image shows less agglomeration for this solution even after 24 hours of preparation.

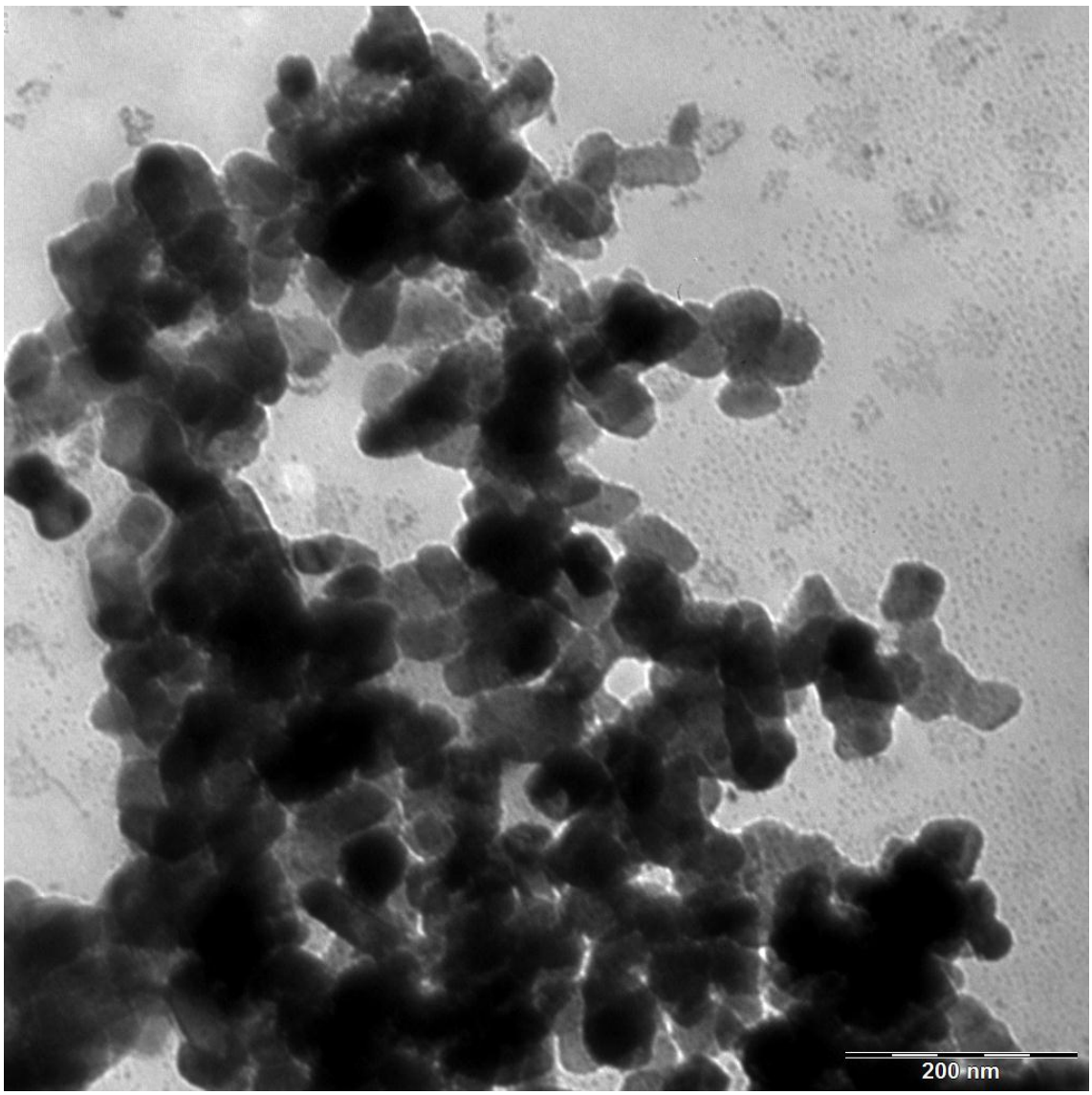

Figure C7: TEM image of R141b/TiO_2 (40 nm) nanorefrigerants.

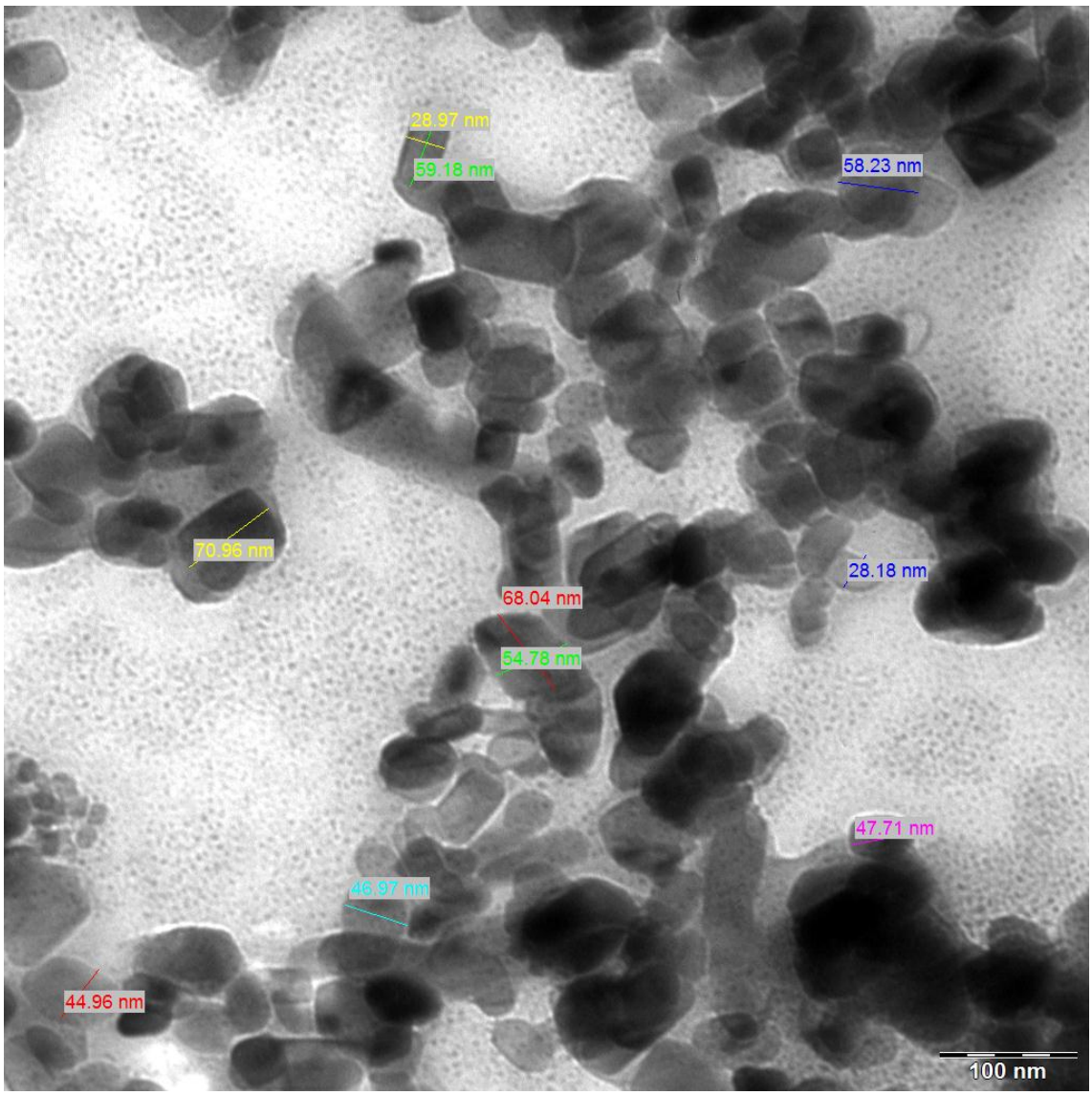

Figure C8: TEM image of R141b/TiO_2 (40 nm) nanorefrigerants with the approximate measurement of some particle's diameter.

Figure C9 shows the SEM image of Al_2O_3 (13 nm) nanoparticles. The elemental composition of Al_2O_3 (13 nm) nanoparticles by SEM-EDAX analysis is presented in Tables B5 and B6 (Appendix B).

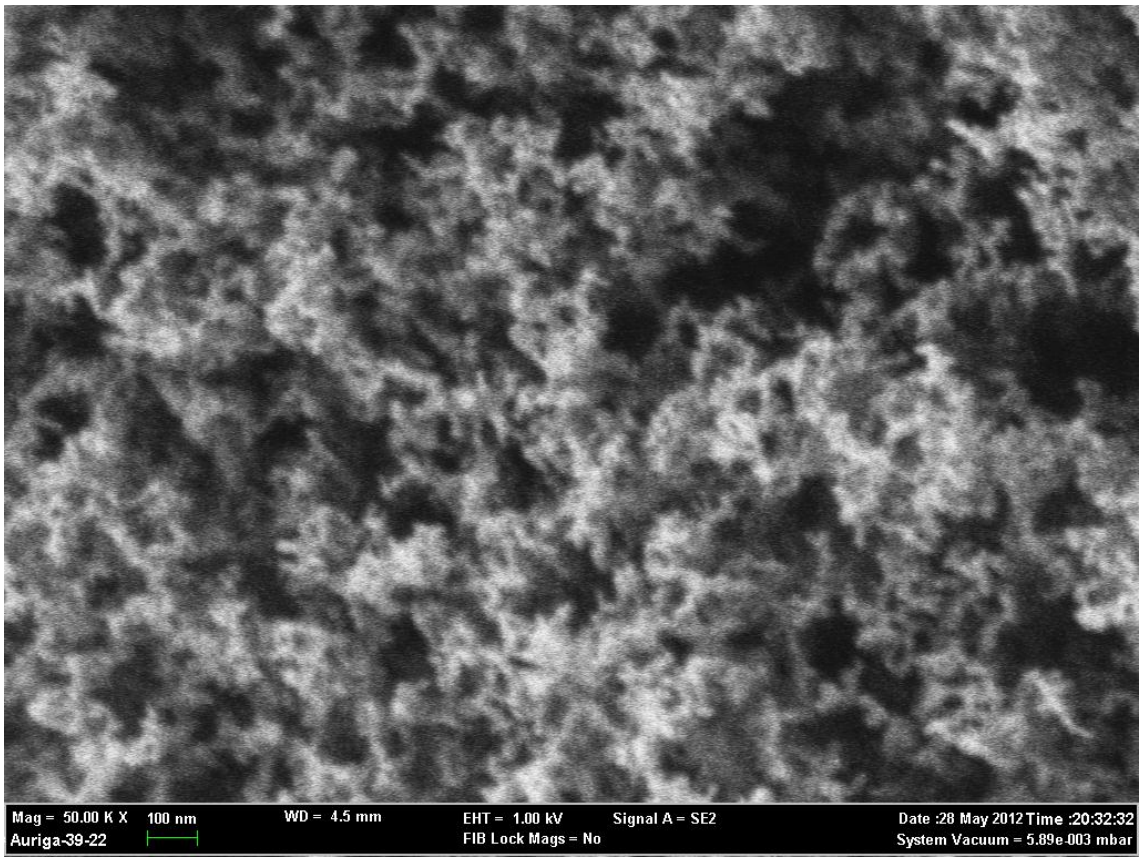

Figure C9: SEM image of Al_2O_3 (13 nm) nanoparticles.

Figure C10 shows the TEM image of R141b/Al_2O_3 (13 nm) nanorefrigerants (with 0.5 volume concentration (%) of nanoparticles). Measurements of the approximate diameter of some of the individual particle by TEM are shown in Figure C11. From the SEM and TEM images, it was assumed that, the sizes of the particles were about 13 nm and the particle shape is spherical. However, the size varies from 9 nm to 15 nm. The TEM image shows less agglomeration for this solution even after 24 hours of preparation.

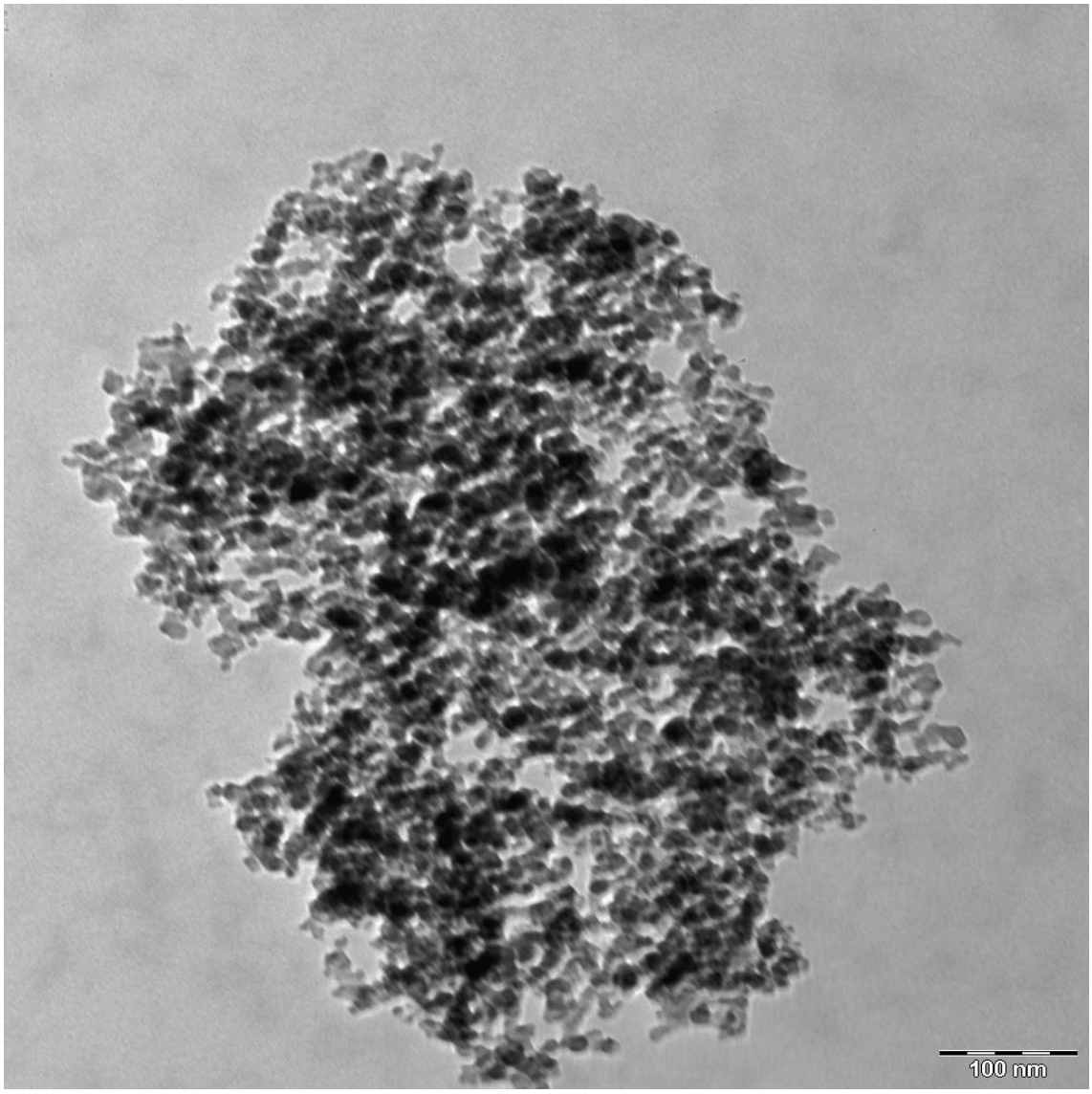

Figure C10: TEM image of R141b/Al_2O_3 (13 nm) nanorefrigerants.

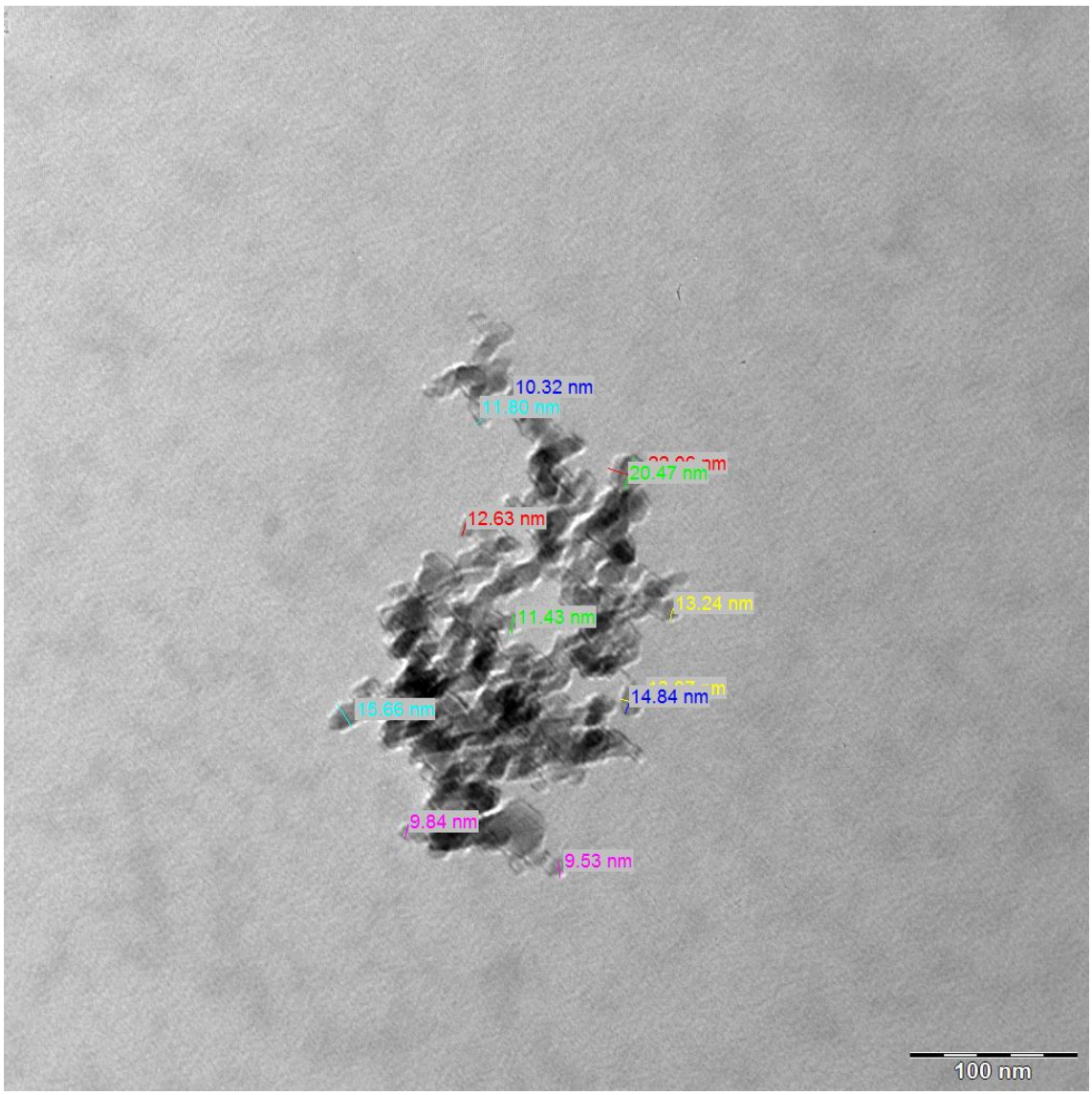

Figure C11: TEM image of R141b/Al_2O_3 (13 nm) nanorefrigerants with the approximate measurement of some particle's diameter.

Figure C12 shows the SEM image of Al_2O_3 (50 nm) nanoparticles. The elemental composition of Al_2O_3 (50 nm) nanoparticles by SEM-EDAX analysis is presented in Table B7 and B8 (Appendix B).

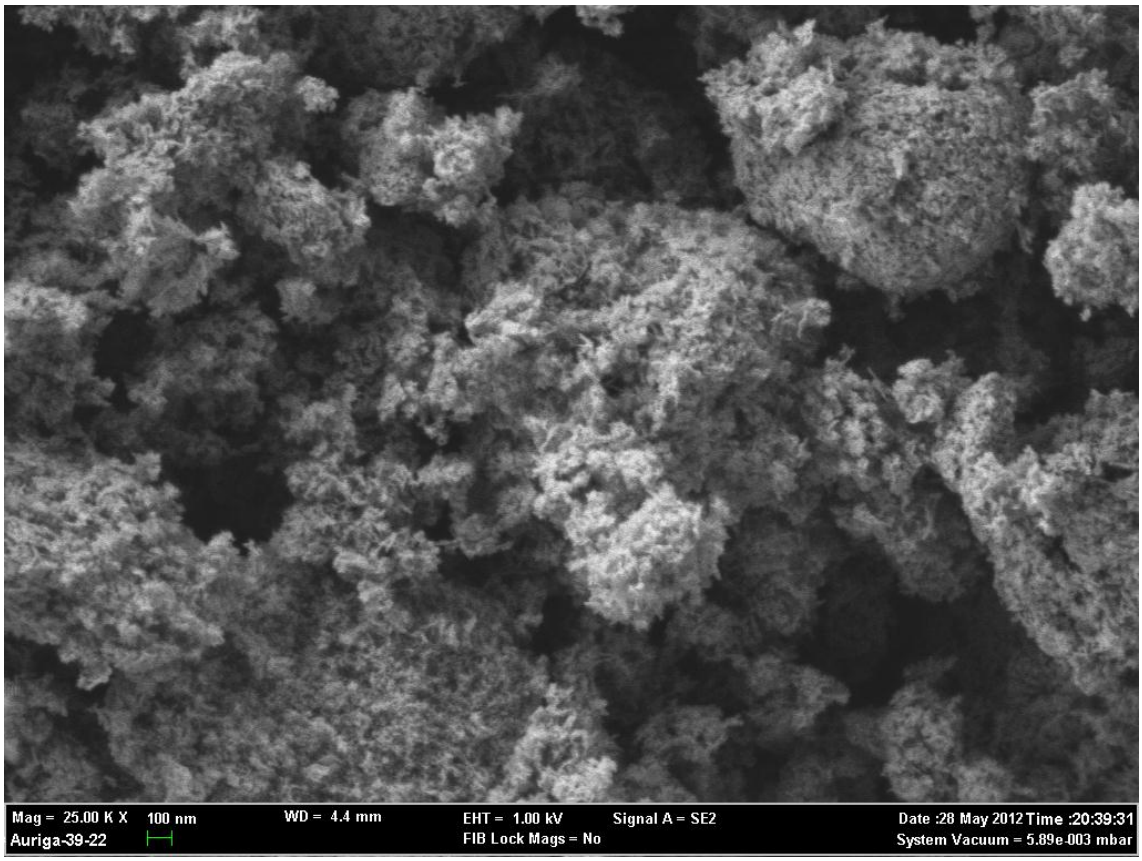

Figure C12: SEM image of Al_2O_3 (50 nm) nanoparticles.

Figure C13 shows the TEM image of R141b/ Al_2O_3 (50 nm) nanorefrigerants (with 0.5 volume concentration (%) of nanoparticles). The measurements of the approximate diameter of some of the individual particle by TEM have shown in Figure C14. From the SEM and TEM images, it was assumed that, the sizes of the particles were about 50 nm long and 8 nm diameters, and the particle had tubular shape. However, the length of the particles is approximately 50 nm but the diameter of the particle varies from 5 nm to 12 nm. Furthermore, The TEM image also shows huge agglomeration.

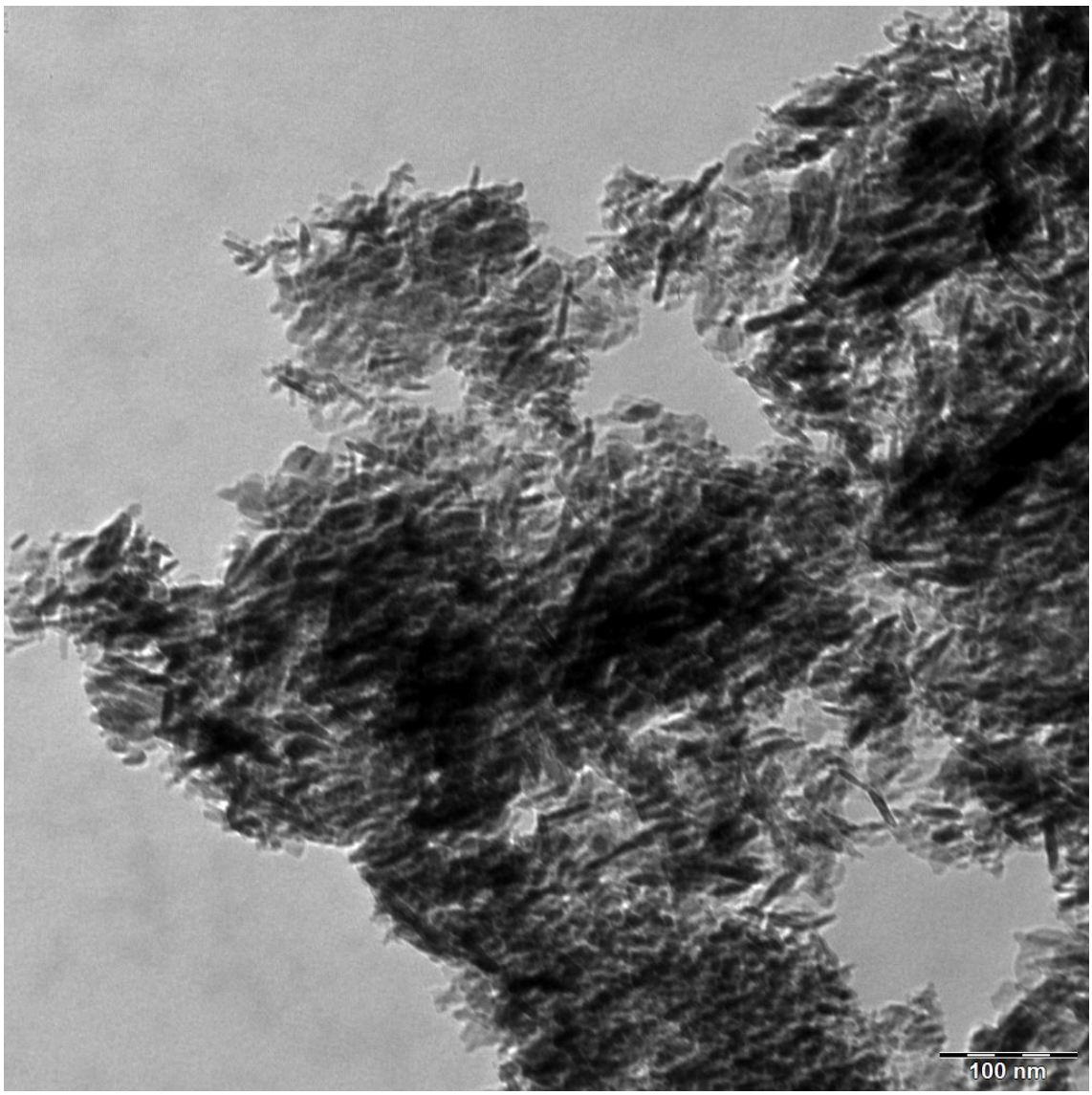

Figure C13: TEM image of R141b/Al_2O_3 (50 nm) nanorefrigerants.

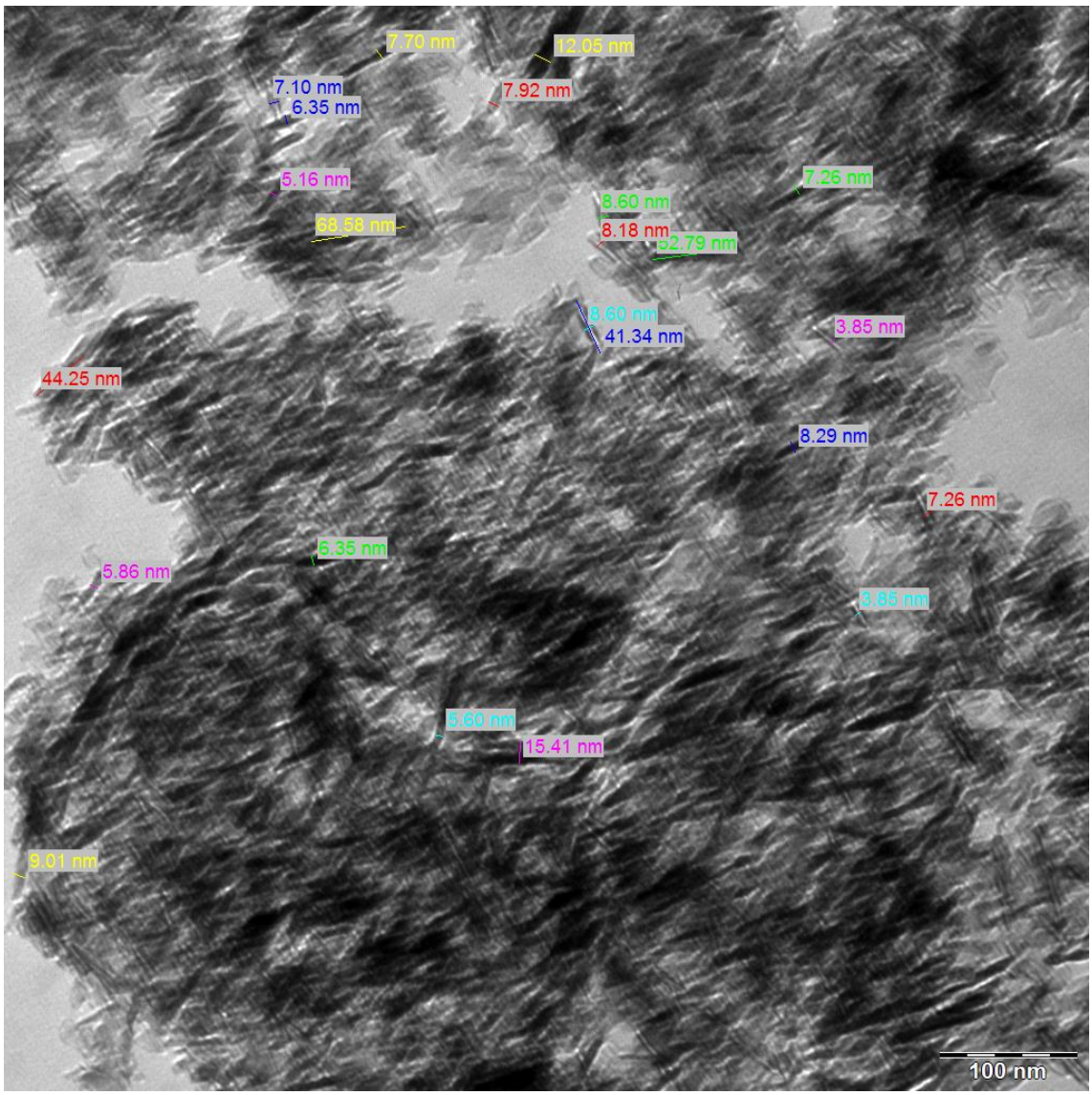

Figure C14: TEM image of R141b/Al_2O_3 (50 nm) nanorefrigerants with the approximate measurement of some particle's diameter and length.

APPENDIX D: RELATED PUBLICATIONS

Journal:

1. **I.M. Mahbubul,** R. Saidur, M.A. Amalina, Latest developments on the viscosity of nanofluids, International Journal of Heat and Mass Transfer 55 (4) (2012) 877-888. (*ISI/Scopus Cited Publication*)

2. **I.M. Mahbubul,** S.A Fadhilah, R. Saidur, K.Y. Leong, M.A. Amalina, Thermophysical properties and heat transfer performances of Al_2O_3/R134a nanorefrigerants, International Journal of Heat and Mass Transfer [Accepted: Article no: HMT9361; DOI: 10.1016/j.ijheatmasstransfer.2012.10.007] (*ISI/Scopus Cited Publication*).

3. **I.M. Mahbubul,** A. Kamyar, R. Saidur, M.A. Amalina, Migration properties of TiO_2 nanoparticles during the pool boiling of nanorefrigerants, Industrial & Engineering Chemistry Research (under review).

Conference:

1. **I.M. Mahbubul,** R.Saıdur, M.A. Amalına, 2011. Investigation of viscosity of R123-TiO_2 nanorefrigerant. Regional Tribology Conference, November 22-24, 2011, Langkawi Island, Malaysia. 1-4.

2. **I.M. Mahbubul,** R.Saıdur, M.A. Amalına. Thermal conductivity, viscosity and density of R141b refrigerant based nanofluid. 5th BSME-International Conference on Thermal Engineering 2012. December 21-23, 2012, Dhaka, Bangladesh (Accepted, Manuscript No: 112).

REFERENCES

Abedian, B., & Kachanov, M. (2010). On the effective viscosity of suspensions. *International Journal of Engineering Science, 48*, 962-965.

Anoop, K. B., Kabelac, S., Sundararajan, T., & Das, S. K. (2009a). Rheological and flow characteristics of nanofluids: Influence of electroviscous effects and particle agglomeration. *Journal of Applied Physics, 106*(3), 034909.

Anoop, K. B., Sundararajan, T., & Das, S. K. (2009b). Effect of particle size on the convective heat transfer in nanofluid in the developing region. *International Journal of Heat and Mass Transfer, 52*(9-10), 2189-2195.

Batchelor, G. (1977). The effect of Brownian motion on the bulk stress in a suspension of spherical particles. *Journal of Fluid Mechanics, 83*(01), 97-117.

Bi, S., Guo, K., Liu, Z., & Wu, J. (2011). Performance of a domestic refrigerator using TiO_2-R600a nano-refrigerant as working fluid. *Energy Conversion and Management, 52*(1), 733-737.

Bi, S., & Shi, L. (2007). Experimental investigation of a refrigerator with a nano-refrigerant. *Qinghua Daxue Xuebao/Journal of Tsinghua University, 47*(11), 2002-2005.

Bi, S., Shi, L., & Zhang, L. (2008). Application of nanoparticles in domestic refrigerators. *Applied Thermal Engineering, 28*(14-15), 1834-1843.

Brinkman, H. (1952). The viscosity of concentrated suspensions and solutions. *The Journal of Chemical Physics, 20*, 571.

Chandrasekar, M., Suresh, S., & Chandra Bose, A. (2010). Experimental investigations and theoretical determination of thermal conductivity and viscosity of Al_2O_3/water nanofluid. *Experimental Thermal and Fluid Science, 34*(2), 210-216.

Chen, H., Ding, Y., He, Y., & Tan, C. (2007a). Rheological behaviour of ethylene glycol based titania nanofluids. *Chemical Physics Letters, 444*(4-6), 333-337.

Chen, H., Ding, Y., Lapkin, A., & Fan, X. (2009a). Rheological behaviour of ethylene glycol-titanate nanotube nanofluids. *Journal of Nanoparticle Research, 11*(6), 1513-1520.

Chen, H., Ding, Y., & Tan, C. (2007b). Rheological behaviour of nanofluids. *New Journal of Physics, 9*(10), 367.

Chen, H., Witharana, S., Jin, Y., Kim, C., & Ding, Y. (2009b). Predicting thermal conductivity of liquid suspensions of nanoparticles (nanofluids) based on rheology. *Particuology, 7*(2), 151-157.

Chen, H., Yang, W., He, Y., Ding, Y., Zhang, L., Tan, C., et al. (2008a). Heat transfer and flow behaviour of aqueous suspensions of titanate nanotubes (nanofluids). *Powder Technology, 183*(1), 63-72.

Chen, L., Xie, H., Li, Y., & Yu, W. (2008b). Nanofluids containing carbon nanotubes treated by mechanochemical reaction. *Thermochimica Acta, 477*(1-2), 21-24.

Chevalier, J., Tillement, O., & Ayela, F. (2007). Rheological properties of nanofluids flowing through microchannels. *Applied Physics Letters, 91*(23), 233103.

Choi, S. (1995). Enhancing thermal conductivity of fluids with nanoparticles In: Siginer DA, Wang HP (eds) Developments applications of non-newtonian flows, FED-vol 231/MD-vol 66. *ASME, New York*, 99–105.

Choi, S. U. S., Zhang, Z. G., & Kelinski, P. (2004). Nanofluids. *Encyclopedia of nanoscience and nanotechnology, 6*, 757-773.

Das, S. K., Choi, S. U. S., & Patel, H. E. (2006). Heat transfer in nanofluids—a review. *Heat Transfer Engineering, 27*(10), 3-19.

Das, S. K., Putra, N., & Roetzel, W. (2003). Pool boiling characteristics of nano-fluids. *International Journal of Heat and Mass Transfer, 46*(5), 851-862.

Daungthongsuk, W., & Wongwises, S. (2007). A critical review of convective heat transfer of nanofluids. *Renewable and sustainable energy reviews, 11*(5), 797-817.

Ding, G., Peng, H., Jiang, W., & Gao, Y. (2009). The migration characteristics of nanoparticles in the pool boiling process of nanorefrigerant and nanorefrigerant–oil mixture. *International Journal of Refrigeration, 32*(1), 114-123.

Ding, Y., Alias, H., Wen, D., & Williams, R. (2006). Heat transfer of aqueous suspensions of carbon nanotubes (CNT nanofluids). *International Journal of Heat and Mass Transfer, 49*(1-2), 240-250.

Duangthongsuk, W., & Wongwises, S. (2009). Measurement of temperature-dependent thermal conductivity and viscosity of TiO_2-water nanofluids. *Experimental Thermal and Fluid Science, 33*(4), 706-714.

Eastman, J., Choi, S., Li, S., Yu, W., & Thompson, L. (2001). Anomalously increased effective thermal conductivities of ethylene glycol-based nanofluids containing copper nanoparticles. *Applied Physics Letters, 78*(6), 718-720.

Edzwald, J. K., Malley Jr, J. P., & Yu, C. (1991). A conceptual model for dissolved air flotation in water treatment. *Water Supply, 9*(1), 141-150.

Einstein, A. (1906). Eine neue bestimmung der moleküldimensionen. *Annalen der Physik, 324*(2), 289-306.

Garg, J., Poudel, B., Chiesa, M., Gordon, J., Ma, J., Wang, J., et al. (2008). Enhanced thermal conductivity and viscosity of copper nanoparticles in ethylene glycol nanofluid. *Journal of Applied Physics, 103*, 074301.

Garg, P., Alvarado, J. L., Marsh, C., Carlson, T. A., Kessler, D. A., & Annamalai, K. (2009). An experimental study on the effect of ultrasonication on viscosity and heat transfer performance of multi-wall carbon nanotube-based aqueous nanofluids. *International Journal of Heat and Mass Transfer, 52*(21-22), 5090-5101.

Ghadimi, A., Saidur, R., & Metselaar, H. S. C. (2011). A review of nanofluid stability properties and characterization in stationary conditions. *International Journal of Heat and Mass Transfer, 54*(17-18), 4051-4068.

Goharshadi, E., Ding, Y., Jorabchi, M., & Nancarrow, P. (2009). Ultrasound-assisted green synthesis of nanocrystalline ZnO in the ionic liquid [hmim][NTf2]. *Ultrasonics Sonochemistry, 16*(1), 120-123.

Hamilton, R., & Crosser, O. (1962). Thermal conductivity of heterogeneous two-component systems. *Industrial & Engineering chemistry fundamentals, 1*(3), 187-191.

Haramura, Y., & Katto, Y. (1983). A new hydrodynamic model of critical heat flux, applicable widely to both pool and forced convection boiling on submerged bodies in saturated liquids. *International Journal of Heat and Mass Transfer, 26*(3), 389-399.

He, Y., Jin, Y., Chen, H., Ding, Y., Cang, D., & Lu, H. (2007). Heat transfer and flow behaviour of aqueous suspensions of TiO_2 nanoparticles (nanofluids) flowing upward through a vertical pipe. *International Journal of Heat and Mass Transfer, 50*(11-12), 2272-2281.

Henderson, K., Park, Y.-G., Liu, L., & Jacobi, A. M. (2010). Flow-boiling heat transfer of R-134a-based nanofluids in a horizontal tube. *International Journal of Heat and Mass Transfer, 53*(5-6), 944-951.

Henn, A. R. (1996). Calculation of the stokes and aerodynamic equivalent diameters of a short reinforcing fiber. *Particle & particle systems characterization, 13*(4), 249-253.

Hui, P. M., Zhang, X., Markworth, A., & Stroud, D. (1999). Thermal conductivity of graded composites: Numerical simulations and an effective medium approximation. *Journal of materials science, 34*(22), 5497-5503.

Incropera, F., DeWitt, D., Bergman, T., & Lavine, A. (2007). *Fundamentals of heat and mass transfer*: John Wiley and Sons, Inc., New York.

Jang, S. P., & Choi, S. U. S. (2004). Role of Brownian motion in the enhanced thermal conductivity of nanofluids. *Applied Physics Letters, 84*, 4316.

Jiang, L., Gao, L., & Sun, J. (2003). Production of aqueous colloidal dispersions of carbon nanotubes. *Journal of Colloid and Interface Science, 260*(1), 89-94.

Jiang, W., Ding, G., & Peng, H. (2009a). Measurement and model on thermal conductivities of carbon nanotube nanorefrigerants. *International Journal of Thermal Sciences, 48*(6), 1108-1115.

Jiang, W., Ding, G., Peng, H., Gao, Y., & Wang, K. (2009b). Experimental and Model Research on Nanorefrigerant Thermal Conductivity. *HVAC&R Research, 15*(3), 651-669.

Jones, J., & Stoecker, W. (1982). Refrigeration and Air Conditioning (2nd ed.): New York: McGraw Hill.

Kedzierski, M. A. (2009). *Viscosity and density of CuO nanolubricant*. Paper presented at the Third conference on thermophysical properties and transfer processes of refrigerants.

Kedzierski, M. A. (2011). Effect of Al_2O_3 nanolubricant on R134a pool boiling heat transfer. *International Journal of Refrigeration, 34*(2), 498-508.

Kedzierski, M. A., Gong, M., Building, & Division, F. R. L. B. E. (2007). *Effect of CuO nanolubricant on R134a pool boiling heat transfer with extensive measurement and analysis details*: US Dept. of Commerce, National Institute of Standards and Technology.

Kim, S., Bang, I., Buongiorno, J., & Hu, L. (2007). Surface wettability change during pool boiling of nanofluids and its effect on critical heat flux. *International Journal of Heat and Mass Transfer, 50*(19-20), 4105-4116.

Kole, M., & Dey, T. K. (2010). Viscosity of alumina nanoparticles dispersed in car engine coolant. *Experimental Thermal and Fluid Science, 34*(6), 677-683.

Koo, J., & Kleinstreuer, C. (2005). A new thermal conductivity model for nanofluids. *Journal of Nanoparticle Research, 6*(6), 577-588.

Krieger, I. M. (1959). A mechanism for non Newtonian flow in suspensions of rigid spheres. *Trans. Soc. Rheol., 3*, 137-152.

Kulkarni, D. P., Das, D. K., & Chukwu, G. A. (2006). Temperature dependent rheological property of copper oxide nanoparticles suspension (nanofluid). *Journal of nanoscience and nanotechnology, 6*(4), 1150-1154.

Kulkarni, D. P., Das, D. K., & Vajjha, R. S. (2009). Application of nanofluids in heating buildings and reducing pollution. *Applied Energy, 86*(12), 2566-2573.

Kwak, K., & Kim, C. (2005). Viscosity and thermal conductivity of copper oxide nanofluid dispersed in ethylene glycol. *Korea-Australia Rheology Journal, 17*(2), 35-40.

Lee, K., Hwang, Y., Cheong, S., Kwon, L., Kim, S., & Lee, J. (2009). Performance evaluation of nano-lubricants of fullerene nanoparticles in refrigeration mineral oil. *Current Applied Physics, 9*(2), e128-e131.

Lee, S. W., Park, S. D., Kang, S., Bang, I. C., & Kim, J. H. (2011). Investigation of viscosity and thermal conductivity of SiC nanofluids for heat transfer applications. *International Journal of Heat and Mass Transfer, 54*(1-3), 433-438.

Lemmon, E. W., McLinden, M. O., & Huber, M. L. (2002). NIST Reference Fluid Thermodynamic and Transport Properties—Refprop 7.0, NIST Std, *Database*. Boulder.

Leong, K., Yang, C., & Murshed, S. (2006). A model for the thermal conductivity of nanofluids–the effect of interfacial layer. *Journal of Nanoparticle Research, 8*(2), 245-254.

Lu, W., & Fan, Q. (2008). Study for the particle's scale effect on some thermophysical properties of nanofluids by a simplified molecular dynamics method. *Engineering Analysis with Boundary Elements, 32*(4), 282-289.

Lundgren, T. S. (1972). Slow flow through stationary random beds and suspensions of spheres. *Journal of Fluid Mechanics, 51*(02), 273-299.

Madni, I., Hwang, C.-Y., Park, S.-D., Choa, Y.-H., & Kim, H.-T. (2010). Mixed surfactant system for stable suspension of multiwalled carbon nanotubes. *Colloids and Surfaces A: Physicochemical and Engineering Aspects, 358*(1-3), 101-107.

Mahbubul, I. M., Saidur, R., & Amalina, M. A. (2012). Latest developments on the viscosity of nanofluids. *International Journal of Heat and Mass Transfer, 55*(4), 877-888.

Masuda, H., Ebata, A., Teramae, K., & Hishinuma, N. (1993). Alteration of thermal conductivity and viscosity of liquid by dispersing ultra-fine particles (dispersion of -Al_2O_3, SiO_2 and TiO_2 ultra-fine particles). *Netsu Bussei (Japan), 4*(4), 227–233.

Maxwell, J. (1891). A Treatise on Electricity and Magnetisms, 3rd edn, Vol 1, Chap 9, Art 310-314: Clarendon Press, Oxford p435.

Murshed, S. M. S., Leong, K., & Yang, C. (2008a). Investigations of thermal conductivity and viscosity of nanofluids. *International Journal of Thermal Sciences, 47*(5), 560-568.

Murshed, S. M. S., Leong, K., & Yang, C. (2008b). Thermophysical and electrokinetic properties of nanofluids – A critical review. *Applied Thermal Engineering, 28*(17-18), 2109-2125.

Naik, M. T., Janardhana, G. R., Reddy, K. V. K., & Reddy, B. S. (2010). Experimental investigation into rheological property of copper oxide nanoparticles suspended in propylene glycol- water based fluids. *ARPN Journal of Engineering and Applied Sciences, 5*(6), 29-34.

Namburu, P., Kulkarni, D., Misra, D., & Das, D. (2007a). Viscosity of copper oxide nanoparticles dispersed in ethylene glycol and water mixture. *Experimental Thermal and Fluid Science, 32*(2), 397-402.

Namburu, P. K., Kulkarni, D. P., Dandekar, A., & Das, D. K. (2007b). Experimental investigation of viscosity and specific heat of silicon dioxide nanofluids. *Micro & Nano Letters, 2*(3), 67-71.

Nguyen, C., Desgranges, F., Galanis, N., Roy, G., Mare, T., Boucher, S., et al. (2008). Viscosity data for Al_2O_3–water nanofluid—hysteresis: is heat transfer enhancement using nanofluids reliable? *International Journal of Thermal Sciences, 47*(2), 103-111.

Nguyen, C., Desgranges, F., Roy, G., Galanis, N., Mare, T., Boucher, S., et al. (2007). Temperature and particle-size dependent viscosity data for water-based nanofluids – Hysteresis phenomenon. *International Journal of Heat and Fluid Flow, 28*(6), 1492-1506.

Nielsen, L. E. (1970). Generalized equation for the elastic moduli of composite materials. *Journal of Applied Physics, 41*(11), 4626-4627.

Pak, B. C., & Cho, Y. I. (1998). Hydrodynamic and heat transfer study of dispersed fluids with submicron metallic oxide particles. *Experimental heat transfer, 11*(2), 151-170.

Park, K., & Jung, D. (2007). Boiling heat transfer enhancement with carbon nanotubes for refrigerants used in building air-conditioning. *Energy and Buildings, 39*(9), 1061-1064.

Pastoriza-Gallego, M. J., Casanova, C., Legido, J. L., & Piñeiro, M. M. (2011). CuO in water nanofluid: Influence of particle size and polydispersity on volumetric behaviour and viscosity. *Fluid Phase Equilibria, 300*(1-2), 188-196.

Paul, G., Philip, J., Raj, B., Das, P. K., & Manna, I. (2011). Synthesis, characterization, and thermal property measurement of nano-Al95Zn05 dispersed nanofluid prepared by a two-step process. *International Journal of Heat and Mass Transfer, 54*(15-16), 3783-3788.

Peng, H., Ding, G., & Hu, H. (2011a). Effect of surfactant additives on nucleate pool boiling heat transfer of refrigerant-based nanofluid. *Experimental Thermal and Fluid Science, 35*, 960-970.

Peng, H., Ding, G., & Hu, H. (2011b). Influences of refrigerant-based nanofluid composition and heating condition on the migration of nanoparticles during pool boiling. Part I: Experimental measurement. *International Journal of Refrigeration, 34*(8), 1823-1832.

Peng, H., Ding, G., & Hu, H. (2011c). Influences of refrigerant-based nanofluid composition and heating condition on the migration of nanoparticles during pool boiling. Part II: Model development and validation. *International Journal of Refrigeration, 34*(8), 1833-1845.

Peng, H., Ding, G., & Hu, H. (2011d). Migration of carbon nanotubes from liquid phase to vapor phase in the refrigerant-based nanofluid pool boiling. *Nanoscale Research Letters, 6*(1), 219.

Peng, H., Ding, G., Hu, H., Jiang, W., Zhuang, D., & Wang, K. (2010). Nucleate pool boiling heat transfer characteristics of refrigerant/oil mixture with diamond nanoparticles. *International Journal of Refrigeration, 33*(2), 347-358.

Peng, H., Ding, G., Jiang, W., Hu, H., & Gao, Y. (2009a). Heat transfer characteristics of refrigerant-based nanofluid flow boiling inside a horizontal smooth tube. *International Journal of Refrigeration, 32*(6), 1259-1270.

Peng, H., Ding, G., Jiang, W., Hu, H., & Gao, Y. (2009b). Measurement and correlation of frictional pressure drop of refrigerant-based nanofluid flow boiling inside a horizontal smooth tube. *International Journal of Refrigeration, 32*(7), 1756-1764.

Phuoc, T. X., & Massoudi, M. (2009). Experimental observations of the effects of shear rates and particle concentration on the viscosity of Fe_2O_3–deionized water nanofluids. *International Journal of Thermal Sciences, 48*(7), 1294-1301.

Phuoc, T. X., Massoudi, M., & Chen, R.-H. (2011). Viscosity and thermal conductivity of nanofluids containing multi-walled carbon nanotubes stabilized by chitosan. *International Journal of Thermal Sciences, 50*(1), 12-18.

Prasher, R., Bhattacharya, P., & Phelan, P. E. (2005). Thermal conductivity of nanoscale colloidal solutions (nanofluids). *Physical Review Letters, 94*(2), 25901.

Prasher, R., Song, D., Wang, J., & Phelan, P. (2006). Measurements of nanofluid viscosity and its implications for thermal applications. *Applied Physics Letters, 89*(13), 133108.

Putra, N., Roetzel, W., & Das, S. K. (2003). Natural convection of nano-fluids. *Heat and Mass Transfer, 39*(8), 775-784.

Saidur, R., Kazi, S., Hossain, M., Rahman, M., & Mohammed, H. (2011). A review on the performance of nanoparticles suspended with refrigerants and lubricating oils in refrigeration systems. *Renewable and Sustainable Energy Reviews, 15*(1), 310-323.

Serrano, E., Rus, G., & García-Martínez, J. (2009). Nanotechnology for sustainable energy. *Renewable and sustainable energy reviews, 13*(9), 2373-2384.

Shengshan, B., & Lin, S. (2007). Experimental investigation of a refrigerator with a nano-refrigerant. *Journal of Tsinghua University (Science and Technology)*, 11.

Sitprasert, C., Dechaumphai, P., & Juntasaro, V. (2009). A thermal conductivity model for nanofluids including effect of the temperature-dependent interfacial layer. *Journal of Nanoparticle Research, 11*(6), 1465-1476.

Smalley, R. E. (2005). Future global energy prosperity: the terawatt challenge. *Mrs Bulletin, 30*(6), 412-417.

Trisaksri, V., & Wongwises, S. (2007). Critical review of heat transfer characteristics of nanofluids. *Renewable and sustainable energy reviews, 11*(3), 512-523.

Trisaksri, V., & Wongwises, S. (2009). Nucleate pool boiling heat transfer of TiO_2–R141b nanofluids. *International Journal of Heat and Mass Transfer, 52*(5-6), 1582-1588.

Tseng, W. J., & Chen, C. N. (2003). Effect of polymeric dispersant on rheological behavior of nickel-terpineol suspensions. *Materials Science and Engineering A, 347*(1-2), 145-153.

Tseng, W. J., & Chun, H. W. U. (2002). Aggregation, rheology and electrophoretic packing structure of aqueous Al_2O_3 nanoparticle suspensions. *Acta Materialia, 50*(15), 3757-3766.

Tseng, W. J., & Lin, K. C. (2003). Rheology and colloidal structure of aqueous TiO_2 nanoparticle suspensions. *Materials Science and Engineering A, 355*(1-2), 186-192.

Turgut, A., Tavman, I., Chirtoc, M., Schuchmann, H. P., Sauter, C., & Tavman, S. (2009). Thermal Conductivity and Viscosity Measurements of Water-Based TiO_2 Nanofluids. *International Journal of Thermophysics, 30*(4), 1213-1226.

Vasu, V., Krishna, K. R., & Kumar, A. C. S. (2008). Thermal design analysis of compact heat exchanger using nanofluids. *International Journal of Nanomanufacturing, 2*(3), 271-288.

Wang, B. (2003). A fractal model for predicting the effective thermal conductivity of liquid with suspension of nanoparticles. *International Journal of Heat and Mass Transfer, 46*(14), 2665-2672.

Wang, K., Ding, G., & Jiang, W. (2005, August 22-25). *Development of nanorefrigerant and its rudiment property.* Paper presented at the 8th International Symposium on Fluid Control, Measurement and Visualization, Chengdu, China.

Wang, R., Hao, B., Xie, G., & Li, H. (2003). *A refrigerating-system using HFC134A and mineral lubricant appended with N-TIO2 (R) as working fluids*.

Wang, X., Xu, X., & Choi, S. U. S. (1999). Thermal conductivity of nanoparticle-fluid mixture. *Journal of Thermophysics and Heat Transfer, 13*(4), 474-480.

Wang, X. Q., & Mujumdar, A. S. (2007). Heat transfer characteristics of nanofluids: a review. *International Journal of Thermal Sciences, 46*(1), 1-19.

Wasp, E., Kenny, J., & Gandhi, R. (1977). Solid-liquid flow slurry pipeline transportation. *Series on Bulk Materials Handling, 1*(4), 56-58.

Wen, D., & Ding, Y. (2005). Formulation of nanofluids for natural convective heat transfer applications. *International Journal of Heat and Fluid Flow, 26*(6), 855-864.

Wu, D., Zhu, H., Wang, L., & Liua, L. (2009). Critical Issues in Nanofluids Preparation, Characterization and Thermal Conductivity. *Current Nanoscience, 5*, 103-112.

Xuan, Y., & Li, Q. (2000). Heat transfer enhancement of nanofluids. *International Journal of Heat and Fluid Flow, 21*(1), 58-64.

Xuan, Y., & Li, Q. (2003). Investigation on Convective Heat Transfer and Flow Features of Nanofluids. *Journal of Heat Transfer, 125*(1), 151-155.

Xuan, Y., Li, Q., & Hu, W. (2003). Aggregation structure and thermal conductivity of nanofluids. *AIChE Journal, 49*(4), 1038-1043.

Yang, Y., Zhang, Z. G., Grulke, E. A., Anderson, W. B., & Wu, G. (2005). Heat transfer properties of nanoparticle-in-fluid dispersions (nanofluids) in laminar flow. *International Journal of Heat and Mass Transfer, 48*(6), 1107-1116.

Yu, W., & Choi, S. (2003). The role of interfacial layers in the enhanced thermal conductivity of nanofluids: a renovated Maxwell model. *Journal of Nanoparticle Research, 5*(1), 167-171.

Yu, W., & Choi, S. (2004). The role of interfacial layers in the enhanced thermal conductivity of nanofluids: a renovated Hamilton–Crosser model. *Journal of Nanoparticle Research, 6*(4), 355-361.

Yu, W., Xie, H., Li, Y., & Chen, L. (2011). Experimental investigation on thermal conductivity and viscosity of aluminum nitride nanofluid. *Particuology, 9*(2), 187-191.

Zhu, H.-t., Lin, Y.-s., & Yin, Y.-s. (2004). A novel one-step chemical method for preparation of copper nanofluids. *Journal of Colloid and Interface Science, 277*(1), 100-103.

Zhu, H., Li, C., Wu, D., Zhang, C., & Yin, Y. (2010). Preparation, characterization, viscosity and thermal conductivity of $CaCO_3$ aqueous nanofluids. *Science China Technological Sciences*, *53*(2), 360-368.

Zhu, H., Zhang, C., Liu, S., Tang, Y., & Yin, Y. (2006). Effects of nanoparticle clustering and alignment on thermal conductivities of Fe_3O_4 aqueous nanofluids. *Applied Physics Letters, 89*(2), 023123.